UNIVERSITI TEKNOLOGI MARA

CHARACTERIZATION OF POST-OVEROXIDIZED PEDOT: PSS/PEO/ PVDF/ LITFSI COMPOSITE AS A SOLID POLYMER ELECTROLYTE FOR LITHIUM- ION SEPARATOR

AWATIF BINTI HASSIM

MSc

July 2026

UNIVERSITI TEKNOLOGI MARA

CHARACTERIZATION OF POST-OVEROXIDIZED PEDOT: PSS/PEO/ PVDF/ LITFSI COMPOSITE AS A SOLID POLYMER ELECTROLYTE FOR LITHIUM- ION SEPARATOR

AWATIF BINTI HASSIM

Thesis submitted in fulfilment
of the requirements for the degree of
Master of Science
(Material Science and Technology)

Faculty of Applied Sciences

July 2026

CONFIRMATION BY PANEL OF EXAMINERS

I certify that a Panel of Examiners has met on 23 February 2026 to conduct the final examination of Awatif Binti Hassim on her Masters of Science thesis entitled "Characterization of Post- Overoxidized PEDOT: PSS/PEO/ PVDF/ LiTFSI Composite as a Solid Polymer Electrolyte For Lithium- Ion Separator" in accordance with Universiti Teknologi MARA Act 1976 (Akta 173). The Panel of Examiners recommends that the student be awarded the relevant degree. The Panel of Examiners was as follows:

Wan Izhan Nawawi Wan Ismail, PhD
Associate Professor
Faculty of Applied Sciences
Universiti Teknologi MARA
(Chairman)

Radin Siti Fazlina Nazrah Hirzin, PhD
Senior Lecturer
Faculty of Applied Sciences
Universiti Teknologi MARA
(Internal Examiner)

Ernie Suzana Ali, PhD
Associate Professor
Faculty of Science and Technology
Universiti Sains Islam Malaysia
(External Examiner)

PROF DR. HJH ZURAEDA BINTI IBRAHIM
Dean
Institute of Postgraduates Studies
Universiti Teknologi MARA
Date: 13 July 2026

AUTHOR'S DECLARATION

I declare that the work in this thesis was carried out in accordance with the regulations of Universiti Teknologi MARA. It is original and is the results of my own work, unless otherwise indicated or acknowledged as referenced work. This thesis has not been submitted to any other academic institution or non-academic institution for any degree or qualification.

I, hereby, acknowledge that I have been supplied with the Academic Rules and Regulations for Postgraduate, Universiti Teknologi MARA, regulating the conduct of my study and research.

Name of Student	:	Awatif Binti Hassim
Student ID. No.	:	2023715523
Programme	:	Master of Science (Material Science and Technology-AS762)
Faculty	:	Applied Sciences
Thesis Title	:	Characterization of Post- Overoxidized PEDOT: PSS/PEO/ PVDF/ LiTFSI Composite as a Solid Polymer Electrolyte for Lithium-Ion Separator
Signature of Student	:	
Date	:	July 2026

ABSTRACT

The increasing demand for lithium-ion batteries (LIBs) presents challenges for efficient and sustainable recycling processes due to the depletion of the resource, as well as associated environmental challenges. This study explored the use of PEDOT: PSS as a conductive polymer in PEO/PVDF/LiTFSI composite membranes for lithium-ion separators in electrochemical recycling. The study focused on determining the optimum PEO formulation in PVDF/LiTFSI solutions, evaluating the effect of PEDOT: PSS on ionic conductivity and analysing the specific chemical, crystallinity, and morphology of the composite membranes. The membranes were developed by solvent casting with varying content (0 - 1.0 wt%) of PEDOT: PSS and were characterized using field emission scanning electron microscopy (FESEM), fourier transform infrared spectroscopy (FTIR), x-ray diffraction (XRD), electrochemical impedance spectroscopy (EIS), and transference number (TN) study. The maximum amount of 1.0 wt% PEDOT: PSS resulted in the highest degree of morphological development with a completely formed IPN structure, which is highly fibrous in nature. Peaks were found to be very prominent using FTIR Spectroscopy which includes stretching of C-O-C ether group of PEO at approximately 1100 cm^{-1}, stretching of C=C thiophene ring of PEDOT at 1510 cm^{-1}, stretching of S=O of PSS in 1050–1180 cm^{-1} range, bending of CF_2 groups of PVDF at 1180 cm^{-1} and 840 cm^{-1}, stretching of SO_2 group at about 1350 cm^{-1}, and bending of CF_3 group of $TFSI^-$ at 740 cm^{-1} with considerable broadening and shift in peaks due to increasing concentration of PEDOT:PSS. XRD spectra showed a clear non-linear pattern in which sample (a) 0 wt% and sample (d) 0.7 wt% belong to one group that includes all the peaks for crystals, such as PEO (19.24°) and PVDF (23.49°), while sample (b) 0.1 wt%, sample (c) 0.4 wt%, and sample (e) 1.0 wt% belong to another group that has few peaks only at 38.44° and 44.68° but does not contain the PEO peak of 19.24° or any other high angle structure was maintained. The EIS results indicated that the peak ionic conductivity of 6.16×10^{-4} S/cm was at the 1.0 wt% of PEDOT: PSS due to the presence of conductive pathways induced and dissociation of salt. The TN analysis revealed dominant Li^+ conduction ($t_+ \approx 0.98–0.99$) at lower PEDOT: PSS loadings (0.4–0.7 wt%), but there were slight deviations at 1.0 wt% indicating small electronic contributions associated with PEDOT: PSS aggregation. This study provided confirmation of a clear enhancement of performance of PEO/PVDF/LiTFSI membranes with the addition of PEDOT: PSS into the system. This indicates a compromise in which 1.0 wt% optimizes conductivity for efficient charge transfer and 0.4-0.7 wt% optimizes ionic selectivity for purity of lithium extraction, whereas 0 wt% represents the control condition. Overall, these results are significant towards achieving a sustainable technique for membrane separator fabrication for LIBs recycling purposes. Future research should target the issue of long-term stability of such membranes as well as the possibility of large-scale PEDOT:PSS application in the process of fabrication.

ACKNOWLEDGEMENT

First and foremost, praises and thanks to Allah SWT, the Almighty, for showering His blessings throughout this semester to finish my lab work and thesis writing successfully. I would like to express my deepest and sincere gratitude to my supervisor, Dr Suzana Ratim, and co- supervisor Ts. Dr. Nur Aimi Jani for allowing me to do my research and lab work and providing me with indispensable guidance throughout this journey. It was such a great honour to work and study under their guidance. I am extremely grateful for what they have offered me.

Words can never adequately express the depth of gratitude I owe my loving parents, Mr. Hassim Awang and , who provided me with encouragement and inspiration all along this journey. Your love, prayers, and sacrifices are the unseen pillars of my dreams that helped shape my destiny. Every breath you take, every atom of your being, is cherished within me as though it were my own.

I am deeply thankful to my siblings throughout this academic journey. To Afaf, Munsif, Amni, Alyaa', Arija, and Aifah, to whom I will forever owe my gratitude. They hear my challenges and offer me solace whenever I'm feeling low. I will always be thankful to my cousins, Haidhar and Afitriah, for all that they have done. I cherish my entire family and all those who have stood by me and supported me in navigating through everything.

I would like to thank my friends and colleagues at the laboratory, Nur Najiha, Mohd Arif, Fatin Nurazmina, and Azra Umairah. For all the help and support to go to the laboratory regularly, I am indebted to all of you. I would like to thank you for the discussions, for sharing the laughter and above all for giving me invaluable support.

For my dear friends Sarah Nadiah and Asilah Fasihah, your company and support meant a lot throughout this ordeal. I would like to thank you especially for the conversations we had together, as they made this entire process much easier and enjoyable.

Finally, to my dear mamatok (, you will always be in my thoughts, and my love for you is immense!

TABLE OF CONTENTS

		Page
CONFIRMATION BY PANEL OF EXAMINERS		**ii**
AUTHOR'S DECLARATION		**iii**
ABSTRACT		**iv**
ACKNOWLEDGEMENT		**v**
TABLE OF CONTENTS		**vi**
LIST OF TABLES		**ix**
LIST OF FIGURES		**x**
LIST OF SYMBOLS		**xiv**
LIST OF ABBREVIATIONS		**xv**
LIST OF NOMENCLATURE		**xviii**
CHAPTER 1 INTRODUCTION		**1**
1.1	Research Background	1
1.2	Problem Statement	2
1.3	Research Objectives	3
1.4	Research Question	3
1.5	Significance of the Study	4
CHAPTER 2 LITERATURE REVIEW		**6**
2.1	Lithium- Ion Batteries (LIBs)	6
2.2	Lithium- Ion Batteries (LIBs) Recycling	9
2.3	Extraction of LIBs Components	10
2.4	Method for LIBs Recycling	12
	2.4.1 Hydrometallurgy	13
	2.4.2 Pyrometallurgy	14
	2.4.3 Electrochemical	18
2.5	Polymer Electrolyte	23
2.6	Solid Polymer Electrolyte (SPE)	25
	2.6.1 Polyethylene Oxide (PEO)	26

2.6.2 Polyvinyl Fluoride (PVDF) 28
2.7 Lithium Bis (Trifluoromethanesulfonyl) Imide (LiTFSI) Salt 29
2.8 Interpenetrating Network (IPN) 31
2.9 Conducting Polymer (CP) 33
2.9.1 Polypyrrole 36
2.9.2 Polyaniline (PANI) 37
2.9.3 Poly (3,4- ethylenedioxythiophene) (PEDOT) 38
2.9.4 Poly (3,4- Ethylenedioxythiophene): Poly (Styrene Sulfonate) (PEDOT: PSS) 39
2.10 Compatibility of Two Different Mix of Polymer 42
2.11 Overoxidation of Conducting Polymer (CP) 43
2.12 Properties or Characteristics of Conducting Polymer (CP) 45
2.12.1 X-Ray Diffraction (XRD) 45
2.12.2 Fourier Transform Infrared Spectroscopy (FTIR) 47
2.12.3 Field Emission Scanning Electron Microscopy (FESEM) 49
2.12.4 Electrochemical Impedance Spectroscopy (EIS) 50
2.12.5 Transference Number (TN) 52

CHAPTER 3 RESEARCH METHODOLOGY 55
3.1 Materials 55
3.2 Sample Preparation 56
3.2.1 Flow of Synthesis Works 56
3.2.2 EDOT: PSS Polymerization 56
3.2.3 Synthesis of PEO/ PVDF/ LiTFSI Solution 57
3.2.4 PEDOT: PSS/ PEO/ PVDF/ LiTFSI Blend 58
3.2.5 Fabricated PEDOT: PSS/PEO/PVDF/LiTFSI Membrane 59
3.2.6 Overoxidation Treatment on PEDOT: PSS/ PEO/ PVDF/ LiTFSI Membrane 60
3.3 Characterization Methods for The Samples 62
3.3.1 X- Ray Diffraction (XRD) 62
3.3.2 Fourier Transform Infrared Spectroscopy (FTIR) 63
3.3.3 Field Emission Scanning Electron Microscopy (FESEM) 63
3.3.4 Electrochemical Impedance Spectroscopy (EIS) 64
3.3.5 Transference Number (TN) 64

CHAPTER 4 RESULTS AND DISCUSSION **68**
4.1 Morphological Characterization of Membrane 68
4.2 Structural Confirmation and Elemental Identification of Membrane 71
4.3 Phase Study of the Membrane 75
4.4 Electrochemical Impedance Spectroscopy (EIS) Analysis 81
4.5 Transference Number (TN) Analysis 85

CHAPTER 5 CONCLUSION AND RECOMMENDATIONS **89**
5.1 Conclusion 89
5.2 Recommendations 91

REFERENCES **93**

APPENDICES **106**

AUTHOR'S PROFILE **111**

LIST OF TABLES

Tables	Title	Page
Table 2. 1	A Summary For Reviewed Hydrometallurgy And Pyrometallurgy Methods	17
Table 2. 2	A Summary of The Reviewed Electrochemical Process For LIBs Recycling.	22
Table 2. 3	The Maximum Requirements For All Solid- State Polymer Electrolytes In LIBs.	26
Table 3. 1	Concentration Table of PEO/ PVDF/ LiTFSI	57
Table 3. 2	Formulation of Solution Mixing.	58
Table 4. 1	Ionic Conductivity of PEO/PVDF/LiTFSI Composite Membranes at Varying PEDOT: PSS Loadings (0 wt%, 0.1 wt%, 0.4 wt%, 0.7 wt%, and 1.0 wt%). Five Independent Measurements (a–e) are Shown, Demonstrating A Progressive Increase In Conductivity With Higher PEDOT: PSS Content. The Minimum Conductivity Of 4.76×10^{-4} S/Cm is Recorded At 0 Wt%, While The Maximum Conductivity Of 6.16×10^{-4} S/Cm Is Achieved At 1.0 Wt% PEDOT: PSS.	85

LIST OF FIGURES

Figures	Title	Page
Figure 2. 1	The Global Scenario Of Lithium Reserves And Their Potential Depletion In 30 Years Under An 18% Annual Increase In Lithium Consumption (Bae & Kim, 2021).	6
Figure 2. 2	Schematic Diagram Of Cylindrical LIBs (Bankole et al., 2013)	8
Figure 2. 3	Global Concern And Focus From Main Publications Related To Spent LIBs (Taylor et al., 2013).	9
Figure 2. 4	Typical Hydrometallurgy And Pyrometallurgy Recycling Methods For The Recovery Of LIBs Active Materials (Baum et al., 2022).	16
Figure 2. 5	Electrochemical Setup For Lithium-Ion Battery Recycling.	18
Figure 2. 6	The Incorporation Of An Electrochemical Technique To Recover Wasted LIBs (Li et al., 2023).	20
Figure 2. 7	A Brief Chronology of the Development of Typical Polymer Electrolytes for Non-aqueous Li-Based Batteries (D. Zhou et al., 2019)	26
Figure 2. 8	Chemical Structure of LiTFSI Salt	30
Figure 2. 9	Schematic Diagram of IPN For PEDOT/ PEO (Fong et al., 2017).	33
Figure 2. 10	Applications of Conducting Polymers And Their Composites Are Shown Schematically (Namsheer et al., 2021).	35
Figure 2. 11	Chemical Structure of Polypyrrole.	37
Figure 2. 12	Chemical Structure of PANI	38
Figure 2. 13	Chemical Structure of Polymerized PEDOT: PSS	41
Figure 2. 14	Illustrated Mechanism Of PEDOT: PSS Formation Via Oxidative Polymerization (Sakunpongpitiporn et al., 2019).	42
Figure 2. 15	AFM Images Of PEDOT: PSS Films: a) Pristine PEDOT: PSS; b) PEDOT: PSS/PEO.	43

Figure 2. 16	Example Of XRD Spectra a) PEO, b) PEO/ PPy, c) PEO/ PEDOT: PSS, And d) PEO/ PPy/ PEDOT: PSS (Balaji et al., 2022).	46
Figure 2. 17	Example of The FTIR Spectrum of a) PEO, b) PEO/PPY, c) PEO/ PEDOT: PSS And d) PEO/PPY/ PEDOT: PSS (Balaji et al., 2022).	48
Figure 2. 18	Example Illustration Of a) PEDOT: PSS, b) ZnO and c) PEDOT: PSS/ ZnO (H. Wang et al., 2015).	50
Figure 2. 19	Schematic Representation of The EIS Measurement System Used To Analyze The Impedance Response of The Thin-Film Solid Polymer Electrolyte (Asri et al., 2022).	51
Figure 2. 20	Electrochemical Impedance Spectroscopy (EIS) Nyquist Plots Comparing Ionic Conductivity of Chitosan-LiTRIF-PC Electrolytes With And Without PEDOT:PSS (Eren, 2018).	52
Figure 2. 21	Li^+ Transference Number (t_+) Determination by Bruce-Vincent Method (Xu, 2022).	54
Figure 3. 1	The Overall Synthesis Workflow Was Illustrated	56
Figure 3. 2	PEDOT: PSS/ PEO Film Membrane.	59
Figure 3. 3	Illustration Of Overoxidation Treatment On Membrane	60
Figure 3. 4	PANanalytical X-Pert Pro XRD Instrument	62
Figure 3. 5	Perkin Elmer 100 Infrared Spectrum Analyzer	63
Figure 3. 6	FESEM Apreo 2 Instrument	63
Figure 3. 7	HIOKI 3520 LCR Hi- Ester Electrochemical Impedance Spectroscopy (EIS)	64
Figure 3. 8	Flowchart Of The Methodology	66
Figure 4. 1	FESEM Micrographs Of Membranes With 0–1.0 Wt% PEDOT:PSS. The Morphology Evolves From Rough, Phase-Segregated Surfaces At 0 Wt% To A Fibrous, Porous, And Interconnected Microstructure At 1.0 Wt%, Indicative Of An Interpenetrating Network (IPN). Comparable IPN Morphologies Have Been Shown To Improve Charge	

Transport Efficiency In Conductive Polymer Composites (Fong et al., 2017). 70

Figure 4. 2 Fourier Transform Infrared (FTIR) Spectra Of Pure PEO, PVDF, LiTFSi, And PEDOT: PSS 71

Figure 4. 3 Fourier Transform Infrared (FTIR) Transmittance Spectra Of Pure Poly(3,4-Ethylenedioxythiophene):Poly(Styrenesulfonate) (PEDOT:PSS) And PEO/PVDF/LiTFSI Salt Composite Polymer Electrolytes With Different PEDOT:PSS Loadings (0.1 Wt% To 1.0 Wt%). 73

Figure 4. 4 XRD Patterns Of The Pure Components: Lithium Bis(Trifluoromethanesulfonyl)Imide (LiTFSi), Poly(Ethylene Oxide) (PEO), Poly(Vinylidene Fluoride) (PVDF), And Poly(3,4-Ethylenedioxythiophene):Poly(Styrenesulfonate) (PEDOT:PSS). 76

Figure 4. 5 XRD Patterns Of PEO/PVDF/LiTFSi Composite Polymer Electrolytes With Varying Poly(3,4-Ethylenedioxythiophene):Poly(Styrenesulfonate) (Pedot:Pss) Loadings: (A) 0.0 Wt%, (B) 0.1 Wt%, (C) 0.4 Wt%, (D) 0.7 Wt%, And (E) 1.0 Wt%. 78

Figure 4. 6 PEO/PVDF/LiTFSI Composite Membranes Ionic Conductivity with Various Weight Percentages of PEDOT: PSS (0%, 0.1%, 0.4%, 0.7%, and 1.0%). The Maximum Ionic Conductivity Value Of 6.16×10^{-4} S/Cm Was Recorded For The Sample With The Maximum Weight Percentage Of PEDOT: PSS of 1.0%. This Indicates A Positive Relationship Between The Concentration Of PEDOT: PSS And The Ionic Conductivity Studied Range. 84

Figure 4. 7 Current–Time Polarization Curves For PEO/PVDF/LiTFSI Membranes With Different Levels Of PEDOT: PSS Doping (0.0–1.0 Wt%). All The Membranes Display A Decline In Current Before Stabilizing, Which Demonstrates That Ionic Transport Is The Primary Transport Mechanism In These Membranes. The Membranes Doped With 0.0–0.7 Wt%

Demonstrate Consistent Current Decay To Zero, Which Corresponds To High Values Of Ionic Transference Number. 88

LIST OF SYMBOLS

Symbols

σ	Ionic conductivity
t_+	Lithium-Ion Transference Number
i_0	Total current
i_{ss}	Steady-state current
λ	Wavelength
θ	Bragg's diffraction angle (Theta)
Al_2O_3	Aluminium Oxide
CO_2	Carbon dioxide
H_2SO_4	Sulfuric acid
HNO_3	Nitric acid
$LiCoO_2$	Lithium Cobalt Oxide
Na_2SO_4	Sodium Persulfate
SiO2	Silica
SO_2	Sulfur dioxide
TiO_2	Titanium Dioxide
ZnO	Zinc Oxide
ZrO_2	Zircanium Dioxide

LIST OF ABBREVIATIONS

Abbreviations

AC	Alternating Current
APS	Ammonium Persulfate
Au	Gold
Cd	Cadmium
Co	Cobalt
CE	Counter Electrode
CPs	Conducting Polymers
CV	Cyclic Voltammetry
DI	Deionised
DC	Direct Current
DMC	Dimethyl Carbonate
DMSO	Dimethyl Sulfoxide
DMF	Dimethylformamide
EB	Emeraldine base
EC	Ethylene Carbonate
ECDs	Electrochromic Devices
EDOT	3,4- ethylenedioxythiophene
EIS	Electrochemical Impedance Spectroscopy
EU	European Union

EV	Electric Vehicle
FESEM	Field Emission Scanning Electron Microscopy
FTIR	Fourier Transform Infrared Spectroscopy
HCl	Hydrochloric acid
HF	Hydrogen Fluoride
Hg	Mercury
IPN	Interpenetrating Network
LATP	Lithium Aluminium Titanium Phosphate
LIBs	Lithium- ion batteries
Li	Lithium
LiTFSI	Lithium bis(trifluoromethanesulfonyl)imide
NMP	N-methyl-2-pyrrolidone
NMR	Nuclear Magnetic Resonance
Pb	Lead
PAN	Polyacrylonitrile
PANI	Polyaniline
PC	Polycarbonate
PEDOT	Poly(3,4-ethylenedioxythiophene)
PEDOT: PSS	Poly (3,4-ethylenedioxythiophene): polystyrene sulfonate
PEG	Polyethylene glycol
PEO	Polyethylene Oxide
pfg- NMR	Pulsed Field Gradient Nuclear Magnetic Resonance

PMMA	Polymethyl methacrylate
PPy	Polypyrrole
PSS	Poly styrene sulfonate
PTh	Polthiophene
PVDF	Polyvinylidene fluoride
PVDF- HFP	Poly (vinylidene fluoride-co-hexafluoropropylene)
Rb	Bulk Resistance
RE	Reference Electrode
SEM	Scanning Electron Microscopy
s-IPN	Sem-interpenetrating Network
SPE	Solid Polymer Electrolyte
SSICc	Solid-state ionic Conductors
THF	Tetrahydrofuran
TN	Transference number
WE	Working Electrode
XRD	X- ray diffraction

LIST OF NOMENCLATURE

Nomenclatures

~	Approximately
$^{-}$	Superscript Minus (Negative Charge)
$^{+}$	Superscript Plus (Positive Charge)
%	Percent
^{o}C	Degree Celsius
w/v	Weight/volume, the concentration of a solution.
wt%	Weight percent

CHAPTER 1
INTRODUCTION

1.1 Research Background

In 1991, Sony became the first company to commercialise lithium-ion batteries (LIBs). As one of the important metals of the 21st century, lithium has been increasingly used in the electricity production, and its demand is developing rapidly due to the increasing use of lithium-ion batteries (Zhang et al., 2020). The development of high-performance LIBs has drawn more and more attention as interest in the commercialization of portable devices for everyday use, hybrid and electric cars for the automotive sector, and power tools grows (Xue et al., 2015). Due to its numerous benefits, including their high energy density, high cell voltage, low self-discharge rate, and wide operating temperature range, LIBs are frequently utilised in electronic equipment (Jha et al., 2013).

Among the many energy storage devices, LIBs stand out the most. The electrochemical cells of LIBs transform electrical energy from chemical energy (Martins et al., 2020). There are approximately 0.54 million tonnes of lithium in underground brines in China, with the bulk of them having a high Mg2+/ Li+ ratio. The extraction of lithium from these liquid lithium deposits remains a challenging process, especially to the equivalent physical and chemical characteristics of these two elements (Zhang et al., 2020).

The European Union has developed a Battery Regulation policy that prioritizes sustainability and circularity in the battery business. The policy requires new batteries entering the EU market to have minimum recycled content levels by 2030; new batteries may be required to contain minimum levels of recycled materials, such as 12% cobalt (Co), 4% lithium (Li), and 4% nickel (Ni), promoting the reuse of materials from end-of-life batteries and reducing dependability on raw materials. The strategy also establishes recycling objectives, strengthens Extended Producer Responsibility initiatives, enforces environmental and social standards, and promotes battery technology innovation. The EU intends to accelerate the transition to a more sustainable and resource-efficient battery ecosystem, while upholding high environmental and social standards throughout the battery's life cycle.

Hydrometallurgical processes dissolve metals by leaching LIB components with solvents, whereas pyrometallurgical methods utilize LIBs to high temperatures to recover metals in their molten state. Electrochemical extraction involves the selective dissolving or deposition of metals using calibrated voltage and current. Each approach has benefits and disadvantages, but when combined, they provide feasible alternatives for recovering valuable materials from wasted LIBs while encouraging resource conservation and environmental preservation.

1.2 Problem Statement

The surge in lithium-ion battery (LIB) production has led to an escalating demand for lithium (Li). Electronic devices contain valuable and finite resources, including metals like gold, silver, copper, and rare earth elements. When e-waste is not properly recycled, these resources are lost and must be replaced with newly mined materials, contributing to resource depletion and environmental degradation associated with mining and extraction processes. A future pressing problem may arise as a shortage of lithium resources is expected to happen in Malaysia for the next 5 years and there would not be enough raw materials of lithium to meet the demand (Kasri et al., 2024).

The current methods of recycling that were introduced are very toxic and not environmentally friendly. The pyrometallurgy process relies on high temperatures to separate different elements, which are separated by their melting or boiling points and/or their temperature-dependent solubility. It used a high temperature, which occasionally exceeded 1000 °C, resulting in pollution from volatile chemical tar, ash, and compounds. For hydrometallurgy, the oxidation of metallic components in electronic scrap is crucial. This oxidation is necessary for efficient leaching, or it enhances the technological feasibility of the leaching process. The leaching process consumed a large amount of either acid or alkaline solution, which is not good for the environment (Bae & Kim, 2021). Electrochemical will be the right method to recycle the lithium in a greener way (Bae et al., 2016). However, to increase efficiency, we need to improve the membrane separator. That is why the purpose of this study is to contribute to the development of novel and sustainable techniques for LIBs recycling using a conductive membrane, which will be integrated into an electrochemical setup.

Previous studies show that lithium-ion-conducting glass-ceramic lithium aluminium titanium phosphate (LATP) solid membranes were used specifically for

electrochemical lithium recycling. LATP was not conventionally an environmentally friendly material thus, it can be harmful to people and hurts the environment. This material required a high amount of heat energy thus, the synthesis might be complicated. LATP has low flexibility and high brittleness which do not meet the membrane separator's requirement (Bae et al., 2016). Hence, conducting polymer (CP) will be used to tackle this problem as it is greener and more flexible than LATP.

CP has a high electronic conductivity thus, it will constrain the movement of Li-ion while SPE has a high ionic conductivity. CP will be composited with a solid polymer electrolyte (SPE) to develop a membrane separator (Kaneto, 2014). It is essential for overoxidation treatment to be conducted on the membrane separator as it can manifest its ionic conductivity. However, the conductivity of CP composite SPE as a membrane separator for overoxidation treatment is still unknown. To overcome these difficulties, authorities, research organisations, and society must work together in a multidisciplinary and cooperative manner. To find long-term solutions for the recycling and appropriate management of LIBs is critical not just for reducing environmental and resource problems, but also for advancing the field of electric

1.3 Research Objectives

The main objective of this study is to develop modified polymer membrane for lithium- ion separation. Besides that, the other objectives of this study are:

a) To investigate the optimum composition of PEO on PVDF/ LiTFSI solution.
b) To evaluate the effect of PEDOT: PSS composition on ionic conductivity PEO/ PVDF/ LiTFSI membrane.
c) To analyse the chemical properties, crystallinity, and morphological structure of the different PEDOT: PSS/ PEO/ PVDF/ LiTFSI composite membrane.

1.4 Research Question

a) How does PEO composition play a role as a host polymer in PVDF/ LiTFSI solution?
b) How does the presence of the PEDOT: PSS affect the ionic conductivity of the PEDOT: PSS based membrane separator?

c) What are the chemical properties, crystallinity and morphological structure of a conductive membrane composed of PEDOT: PSS as a conducting polymer?

1.5 Significance of the Study

This research is significant, as it proposes a new approach to lithium-ion battery recycling that changes the conventional method into a more environmentally-friendly option, which is based on membrane-based technologies. Conventional methods for recycling lithium-ion batteries rely on toxic chemicals that lead to toxic sludge and acidic wastewater, which pose other inherent risks to the health and safety of the environment. Using solid polymer electrolyte membranes, the research demonstrates a more environmentally friendly approach to recycling that results in much less hazardous waste and environmental impact. The membrane method also has lower operating and maintenance costs when compared to alternative methods, as it eliminates complicated chemical processes. This produces an overall improved cost-benefit analysis for the recycling stream utilized, while also promoting a more widespread acceptance of lithium-ion recycling. Furthermore, the membrane system can be modified, configured, and upgraded to be either small or large. However, since no stability and durability studies involving cyclic performance, ion conduction under sustained conditions, and chemical stability under acidic and basic conditions were done, there is a possibility that the expected lifetime of the membrane was left unexplored.

Moreover, it promotes membrane-based technologies for lithium-ion battery recycling as a sustainable, cost-effective, and commercially viable alternative to conventional techniques. As membrane solutions are adaptable and scalable, they are suitable to a direct operational scale, from trial projects to large-scale industrial processes, safeguarding their relevance as international recycling needs grow. Membrane systems simplify recycling operations, reducing process complexity, lead times, and resource use, which allows more efficient recovery of valuable materials, as well as sustainability and throughput benefits. Enhanced efficiency carries operational cost savings and improved economic feasibility, encouraging broader adoption within the industry. Additionally, membrane-based recycling can seamlessly integrate into current infrastructures, reducing barriers to implementation while facilitating timely adoption of more sustainable, safer, and efficient recycling processes. However, there are certain important limitations that should be considered. This work was conducted

only in laboratory settings through solvent casting methods of small batches, and if large-scale manufacturing of such membranes is intended, additional development will be required to address problems of uniformity, defects, and productivity.

The transformative potential of advanced membrane technology in sustainable lithium-ion battery recycling by enabling the efficient recovery of important metals and reducing global mining demand by up to 90%, protecting resources and minimizing environmental impact. Unlike conventional chemical processes, membrane-based recycling does not produce toxic waste, reducing significant environmental and health risks. It produces ultra-pure metals of higher quality than natural ores, thus facilitating the production of batteries with exceptionally high performance. It also decreases carbon emissions by up to 50% over conventional processes and contributes to the necessary decarbonisation that must occur to address climate change while catalysing more sustainable practices in responsible industries. In conclusion, the research presents a practical and future-proof way of promoting membrane science with sustainable resource use, green technology development, and a circular economy for energy storage.

CHAPTER 2
LITERATURE REVIEW

2.1 Lithium- Ion Batteries (LIBs)

LIBs are a prominent advancing trend. Small LIBs are found in portable electronic devices, and a few large LIBs have been created. They are now the most prominent mobile power sources for portable technology, such as cell phones and laptop computers (Deng, 2015). and also, for hybrid and electric vehicles (Meshram et al., 2015). Depends on the usage of the batteries, the life span of LIBs can be used up to 2-3 years (Contestabile et al., 2001). With the increasing rate of expansion, there is substantial pressure on the supply side of cobalt and lithium. It is expected that Co and Li will be in low supply in the near future (Lv et al., 2018).

Based on Figure 2.1, the amount of lithium used increased by 18% from 49,100 tonnes in 2018 to 57,700 tonnes in 2019. The latest global lithium reserve estimate is roughly 17 billion tonnes. If yearly demand increases of 18% continues, worldwide lithium reserves are expected to be consumed. The demand for lithium is expected to reach 63 million tonnes during the next 30 years, surpassing the remaining reserves by 40 million tonnes. While new lithium reserves are possible, the increasing demand is projected to intensify due to the developing market for lithium-ion batteries. Numerous global authorities foresee lithium shortages, spurring significant research interest in recent years (Bae et al., 2021).

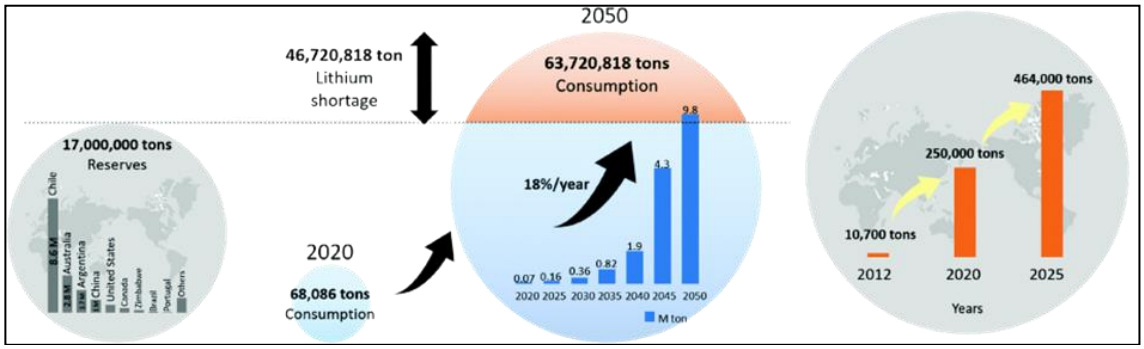

Figure 2. 1 The Global Scenario Of Lithium Reserves And Their Potential Depletion In 30 Years Under An 18% Annual Increase In Lithium Consumption (Bae & Kim, 2021).

Following on their advantageous characteristics, LIBs were chosen as a system in the consumer electronics market. Increasing in the number of consumer products happened in a very fast pace. As a consequence, the amounts of batteries introduced in the market is also growing and because of that, the issues on the correct way of recycling it become a bigger problem (Contestabile et al., 2001). Toxic components inside of the LIBs prevented it from being disposed as it can be very harmful and dangerous to the environment especially when it is exposed to the water, unless if it was treated or handled properly. Moreover, it can seep into the soil to ground water which is extremely non- environmentally friendly which can affect human, animals and environment.

While the U.S. government categorizes spent LIBs as non-environmentally hazardous or "green batteries," making them suitable for disposal in regular municipal waste streams, there are still potential challenges associated with their safe disposal. This is because even though LIBs don't contain hazardous elements like cadmium (Cd), lead (Pb), or mercury (Hg), they do contain flammable and toxic substances that can complicate their proper disposal. For instance, the solvent mixture of dimethyl carbonate (DMC) and ethylene carbonate (EC) used in LIBs is flammable. Additionally, the presence of polyvinylidene fluoride (PVDF) in the battery formulation, regardless of its proportion, can be hazardous when it burns, releasing toxic gaseous hydrogen fluoride (HF). Moreover, the commonly used solvent N-methyl-2-pyrrolidone (NMP) for preparing the electrode active materials (cathode and anode) has been identified as toxic and incompatible with environmental standards (Alfonso et al., 2004; Castillo et al., 2002; Mitchell, 2006; Robert, 2000; Roth and Orendorff, 2012; Wang et al., 2011). Given the well-known adage that "health is wealth" and the parallel notion that a "healthy environment is a wealthy environment," it becomes apparent that a polluted environment is detrimental both to health and overall well-being. Consequently, recycling is of paramount importance to safeguard our immediate surroundings and ensure the sustainability of waste management practices (Bankole et al., 2013).

It is important to look into the reserve amount, potential security challenges, and lifecycle financial aspects associated with the resource for a successful modern innovation to last into the future. The first step in evaluating the invention is to construct an overall framework within which the technology and resources reside. In a resource-constrained climate, especially when resources are not evenly geologically dispersed, it is critical to be able to assess how the possible accessibility of rare input resources may impact the technology's long-term applicability. Recycling techniques for any limited

resource may relieve pressure on the natural ecosystem while improving the financial side of the technology that consumes the resource. As a result, an extensive complete knowledge of the environment in which the resource and technology reside is required to establish resource security, evaluate the benefits of resource reuse, and assess the future practicability of the innovation.(Sisodia et al., 2018).

The current research is based on conducting systematic scientific investigations in order to develop an environmentally friendly recycling technique for recovering lithium as value added products from used LIBs.

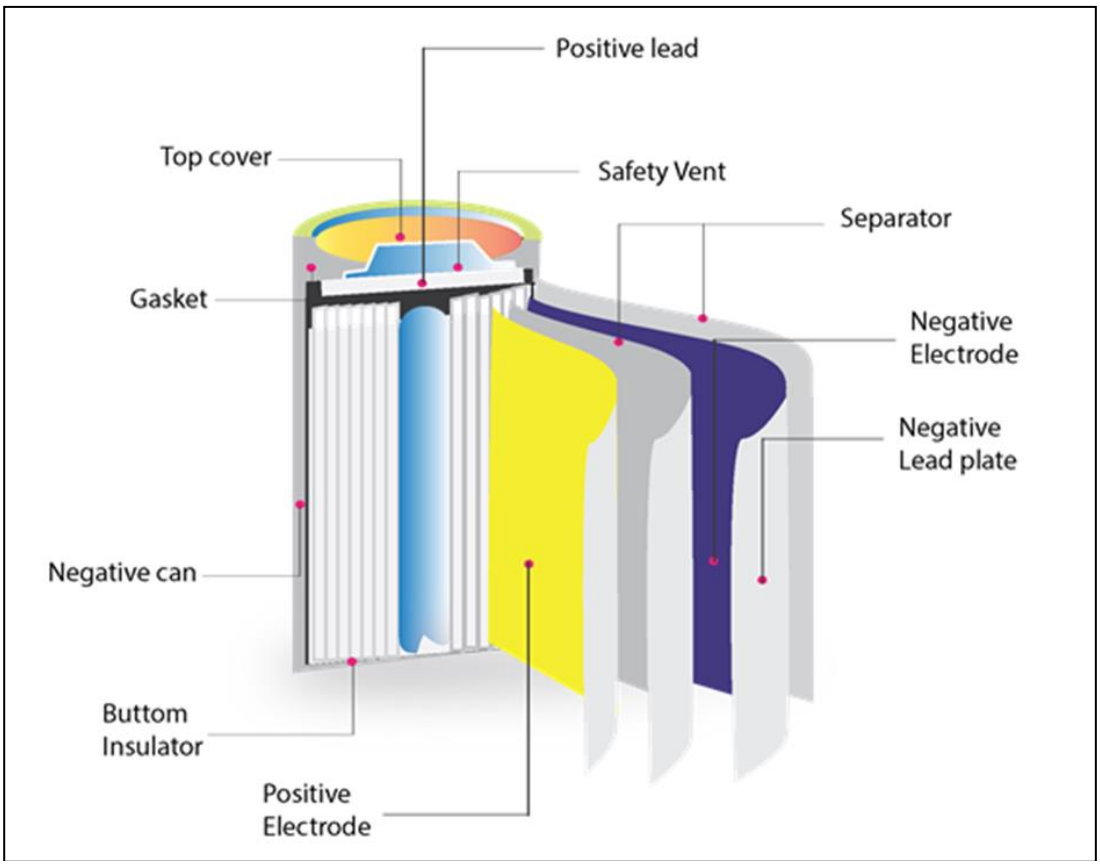

Figure 2. 2 Schematic Diagram Of Cylindrical Libs (Bankole et al., 2013)

Cylindrical lithium-ion batteries (LIBs), as seen in Figure 2.2, is a popular form of lithium-ion battery. Cylindrical cells are frequently found in a hard casing composed of aluminium or stainless steel. Cylindrical battery cells are gaining popularity in the automobile field. Not just Tesla, but several other automobile manufacturers have announced their intentions to employ them extensively.

2.2 Lithium- Ion Batteries (LIBs) Recycling

The quantities of used lithium-ion batteries have significantly increased in recent years, making the development of a recycling method for spent LIBs both essential and urgent in terms of environmental preservation and resource conservation savings (Yao et al., 2018). LIBs recycling reduces energy consumption and carbon dioxide ($CO_{2)}$ emissions, preserves natural resources by minimizing virgin material mining and imports, reduces environmental toxicity, generates economic benefits, reduces waste, and manages safety concerns (Bankole et al., 2013).

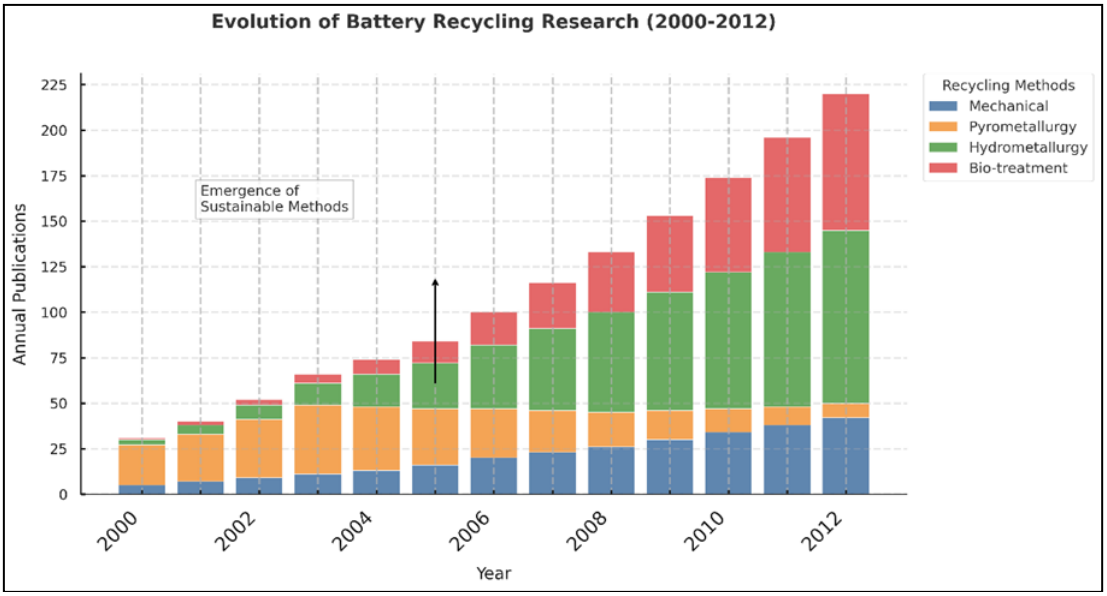

Figure 2. 3 Global Concern And Focus From Main Publications Related To Spent LIBs (Taylor et al., 2013).

The review of existing literature indicates that the recycling of spent LIBs primarily employs mechanical methods, pyrometallurgy and hydrometallurgy. Among these approaches that was stated in Figure 2.3, hydrometallurgy stands out as the most prevalent, accounting for a significant portion at 57.25%. Mechanical treatment plays a crucial role as it not only targets the recycling of elemental Cu, Al, and Fe but also serves as a preliminary step for subsequent processes like hydrometallurgy and pyrometallurgy. Pyrometallurgy represents approximately 16.79% of the overall treatment methods and is known for its ability to swiftly eliminate organic compounds found in spent LIBs, such as carbon powder, PVDF, and plastics. Additionally, there is a growing interest in biotreatment for selectively recovering certain metals from spent LIBs (Taylor et al., 2013).

2.3 Extraction of LIBs Components

Recycling of lithium-ion batteries has been steadily researched since the 1990s and has recently gained traction. Spent lithium-ion batteries (LIBs), contain considerable amounts of important metals such as lithium, cobalt, nickel, manganese, copper, aluminium, and iron. These wasted batteries typically include 5-20 wt.% cobalt, 5-7 wt.% lithium, 5-7 wt.% nickel, 15 wt.% organics, and 7 wt.% polymers. While these proportions may vary significantly amongst producers, the metal concentration is often higher than that of natural ores. Cobalt and lithium, in particular, are rare metals that are strategically essential. As a result, recycling spent LIBs is both necessary and urgent, motivated by concerns about environmental preservation and resource conservation (Yao et al., 2018).

Lithium extraction generally occurs from two primary sources which comes from mineral ore deposits (spodumene located in "hard rock" formations) and brine deposits containing lithium. This leads to variations in the extraction process, challenges, and environmental ramifications. Hard rock mining, primarily occurring in Australia, involves the physical extraction of spodumene ore and higher temperature processing, ultimately making lithium usable in chemical forms like lithium carbonate or lithium hydroxide. Mining provides consistent and reasonably high-quality feedstock; however, it also results in ecological upheaval, energy-intensive processing, and associated carbon emissions (Flexer et al., 2018).

In contrast with regions such as South America's "Lithium Triangle," which is notable for brine extraction from Chile, Argentina, and Bolivia's high-altitude salt flats, Malaysia does not host significant lithium-rich brine deposits. However, brine extraction, involving pumping lithium-containing brines into evaporation ponds for solar evaporation to concentrate lithium salts over 12 to 18 months, demonstrates challenges associated with global sourcing of lithium. While this method has advantages with fewer capital and energy demands than hard rock mining processes, it still faces significant challenges, including slow extraction rates, high water requirements, and potential ecological impacts on local water sources and ecosystems. Moreover, separation of lithium can be difficult due to ions which are chemically similar, such as magnesium (Mg^{2+}), particularly when dealing with brine that has high magnesium to lithium ratios, such as northern China's Qinghai-Tibet plateau (Huang et al., 2018). Since Malaysia does not contain such deposits, alternate viable ways to

source lithium such as imports and recycling technologies, will be necessary to strengthen its emerging battery and energy storage sector.

As there are no lithium brine or mineral resources found in Malaysia, measures such as recycling lithium from spent lithium-ion batteries are essential to meet the demand in the country. Recycling processes include hydrometallurgy where components of the battery are chemically leached with acids to dissolve the metals lithium, cobalt and nickel into solution for separation and recovery. Hydrometallurgy is the most preferable recovery process due to its high recovery rates and its ability to selectively recover lithium, often yielding better separation rates than primary or original extraction. Pyrometallurgy is the other process used for recovery, involving high temperature smelting of the spent batteries to all the metals to alloy (and solidify) metals like cobalt and nickel into metal only. However, lithium is often lost in the smelting process as the slag, just as with the case of most pyrometallurgy processes. Both Recovery techniques separately or in conjunction work to lessen the reliance on new sources of lithium and lessen the environmental impact of raw material extraction and form an essential part of sustainable lithium supply strategies (Harper et al., 2019).

Due to increasing demand challenges, geopolitical uncertainty, and environmental constraints, there is widespread consensus around the need to diversify lithium supply options beyond traditional mining and brine approaches. Potential alternative sources include unconventional lithium resources, such as geothermal brines, oilfield brines, and recycling lithium from used LIBs. Recycling has viable routes for lithium recovery, which can complement primary extraction, reduce supply risks, and reduce environmental impact by recovering lithium and other metals from used batteries (Harper et al., 2019).

The overall success of any hydrometallurgical or pyrometallurgical process is very much dependent on separation. This is where this study can make its most important contribution. Conventional methods usually involve processes that require substantial energy or considerable amounts of chemicals. To sum up, lithium extraction is still a complicated process that requires substantial resources and technology, along with important environmental and economic factors. Improvements in selective separation methods and the incorporation of recycling into the supply chain are essential for achieving sustainable growth in lithium-ion battery markets and facilitating a low-carbon energy future. Thus, the development of a solid polymer electrolyte (SPE) membrane, particularly if coupled with a conducting polymer such as PEDOT: PSS,

presents a new paradigm.

2.4 Method for LIBs Recycling

The fast-paced global uptake of lithium-ion batteries (LIB) applications, particularly for portable electronics, electric vehicles, and grid storage, has simultaneously created an enormous new end-of-life battery waste problem. Recycling LIB batteries helps reduce harmful environmental impacts, retrieve strategic metals (lithium, cobalt, and nickel), and maintain materials supply for continued technical and product growth. A broad set of LIB recycling technologies has been widely evaluated and developed to answer these concerns.

The recycling of LIBs is critical for environmental sustainability and the recovery of important minerals. There are two primary methods for extracting lithium from a lithium-ion battery. Because it is difficult to isolate lithium from the battery's compact structure, a preparatory treatment procedure is used to separate the lithium-containing active materials (cathode, anode) from the surrounding components (plastic, polymer).

Primary LIB recycling techniques can be divided into two major categories which are pyrometallurgical, and hydrometallurgical techniques. For pyrometallurgical recycling, spent batteries undergo pyrometallurgy at high temperature, recovering valuable metals (cobalt, nickel, and copper) at the same time as the form of alloys or with the slag. While widely used in an industrial context for spent LIB recycling because of its proven robustness, the process is energy-intensive, creates large combustion emissions, and has low lithium recovery efficiencies, because lithium often ends up lost in the slag (Hanna et al., 2025).

Hydrometallurgical recycling, on the other hand, uses aqueous chemical leaching with acids or bases to selectively dissolve and separate metals from electrode materials, usually at moderate conditions. Hydrometallurgy gives high recovery rates (>90%) and lithium can be recovered selectively, leading to reduced environmental costs in comparison to the pyrometallurgical method. Hydrometallurgical recycling also tends to generate more chemical waste streams that may require further treatment, as they are usually more complex separation and purification methods (Baum et al., 2022).

However, the electrochemical extraction has recently evolved as a promising technique for lithium recovery from spent lithium-ion batteries (LIBs) in addition to the

traditional methods, which are pyrometallurgical and hydrometallurgical. This method utilizes electrochemical principles to specifically extract lithium ions from electrode materials or leachates via controlled potential. These definable parameters allow for extracting lithium in a selective, energy-efficient and environmentally friendly way (Bae et al., 2016).

Following that, lithium is chemically extracted from the active minerals using processes such as pyrometallurgy, hydrometallurgy, and electrochemical extraction (Bae et al., 2021).

2.4.1 Hydrometallurgy

Hydrometallurgy is a process of extracting metals from their ores using aqueous solutions. It also involves multiple steps of leaching and separation are involved in the separation of different elements. Broadly speaking, the hydrometallurgy process typically involves disassembling, crushing, leaching, purifying, separating, and preparing the final product. Among these steps, the leaching process tends to be the focal point of attention (Maroufi et al., 2020). Most of the recycling processes use hydrometallurgy as a major approach to recycle LIBs. For instances, over 99% of cobalt and lithium were leached through this hydrometallurgy process (Huang et al., 2018). Hydrometallurgy is an important process for lithium recycling because it allows for the recovery of valuable materials from waste streams, reducing the environmental impact of disposing of these materials in landfills.

Hydrometallurgical recycling offers many considerable advantages. It achieves very high metal recoveries which is often above 90% and it can recover lithium effectively which is poorly recovered through pyrometallurgical methods. It requires significantly less energy than smelting, operates at much lower temperatures, generates less greenhouse gas emissions and air pollutants. Many hydrometallurgical methods purport to minimize or recycle waste streams, in the context of acid and water reuse in closed-loop systems, which improves their environmental benefit. This brings hydrometallurgy and circular economy closer together, since recovered materials can be directly reused in cathode manufacturing, reducing reliance on virgin raw material extraction (Huang et al., 2018).

Hydrometallurgy allows for the selective recovery of metals from ores or waste streams, which means that only the desired metals are extracted. This can result in

higher purity of the final product, which can be important for applications that require high quality metals. Besides that, hydrometallurgy usually considered to be a more environmentally friendly process than pyrometallurgy, as it produces less air pollution and generate less waste. By using this method of recycling, it can help to reduce the need for new mining which can have a significant environmental impact.

Despite the benefits, hydrometallurgy has operational challenges. Careful handling and disposal of strong acids and solvents must be done properly to reduce environmental contamination potential, and the production of affected waters raises issues in the absence of remediation technology. The processes sometimes can be chemically burdensome, with multiple process steps, making selecting for a purity of metals more difficult - adding to direct operating costs and complexity. Also, hydrometallurgy operations often require larger infrastructure and process control. The continued development of technology remains focused on increasing reagent efficiencies to allow more selective separations, and developing direct recycling methods which maintain the structure of the cathode material to reduce the cost of reprocessing.

Hydrometallurgy process typically used acid leaching of a chemically stable material. Generally, hydrometallurgy process uses strong acids to leach materials such as sulfuric acid (H_2SO_4), hydrochloric acid (HCl) or nitric acid (HNO_3). Different concentrations and temperature are needed for these acids. Besides, operational variables like the solid to liquid ratio (around 2-20% (w/v)) and the leaching time are studied in order to size the recovery processes (Joulié et al., 2014).

2.4.2 Pyrometallurgy

The rapid shift to an alternate energy system has resulted in an increase in the consumption for LIBs. According to European Union (EU) estimates, the number of electric vehicles will increase from 4 million in 2018 to 50-200 million in 2028. Electric vehicle production is estimated to reach 900 million units by 2048. As a result of this exceptional expansion, a large number of wasted LIBs are thrown. Because of technological disadvantages related to cycle, increased temperature, and rate performance, the LIBs cell has a limited life period of roughly 1-3 years, which worsens the huge output of used LIBs (Makuza et al., 2021). According to projections, around 11 million metric tons of used LIBs will be disposed by 2030. The recovery rate in the

European Union is astonishing, with barely 5% recycled in 2010, despite the anticipated growth in battery usage. Because of the intricate nature of battery chemistry, LIBs recovery has been a major key technology since its inception, and it is always altering in an effort to optimize battery storage sustainability.

Several studies have found the familiar ways for the recovery and recycling of lithium, which one of them is pyrometallurgy. This pyrometallurgical process was developed by Umicore Group by which spent LIBs were treated like natural ores (Huang et al., 2018). Pyrometallurgy is the extension alternative of metallurgy that involves high temperature processes, such as smelting, roasting, and calcining, to extract metals from their ores. The organic electrolyte, acetylene black, and binder found in destroyed LIBs are often incinerated in pyrometallurgical procedures, resulting in significant energy consumption and the production of hazardous gases (Yao et al., 2018).

This recycling method offers several benefits, including its capability for high-capacity chemical reactions, flexibility in processing various feed materials, straightforward operation, and minimal environmental impact from the resulting waste (Contestabile et al., 2001). This method is compatible with existing industry configurations and it can achieve high recovery of these metals, and it takes the organic materials and aluminum from the battery and converts it to stable oxides through high-temperature oxidation. Pyrometallurgical recycling contributes to sustainable resource use by reducing the demand for new raw materials and mitigating the impacts of mining. Furthermore, recent developments such as lithium volatilization methods and subsequent chemical processing potentially improve lithium recovery, that often gets lost in the slag. However, pyrometallurgy is associated with significant damages to the environment. The technology is energy-intensive, operating at temperatures above 1200 °C, hence generating significant carbon dioxide and associated costs due to the energy used. Smelting operations also emit toxic gases such as sulfur dioxide, nitrogen oxides, fluorine gases, and fine particulate material due to the combustion and decomposition of battery materials, which raises air quality worst case scenarios, and often which requires costly exhaust gas capturing and control systems. Further, lithium may considerably leach to the slag which is the waste material from the smelting process on the order of (12-40 % lithium) which compromises primary recycling processes. The impurities in the alloys also require costly refining processes, which complicate processes, increase costs and further elevate environmental stressors. The process also

consumes considerable resources, including air, cooling water, and slagging agents. Economic recycling plants depend on the quality of the recovered products and on the flexibility of the implemented process. Typical hydrometallurgy and pyrometallurgy recycling methods for recovery of LIBs active materials can be seen in figure 2.4.

Pyrometallurgy tends to have higher greenhouse gas emissions and cumulative energy consumption compared to hydrometallurgical recycling, but it is still preferred for some battery types (which was specifically the case for lead-acid batteries) and for larger processing goals. Efforts to improve the slag composition, lessen consumption of the coke and use alternatives fuels or heating methods are meant to minimize the environmental impacts. As it has limits, pyrometallurgy provides a solid and scalable pathway for recycling LIB metals and ongoing improvements have sought to address its sustainability issues.

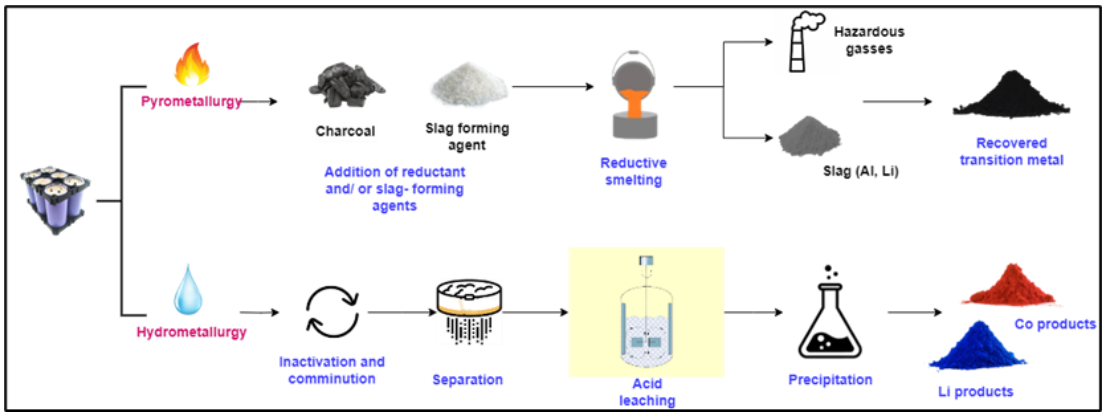

Figure 2. 4 Typical Hydrometallurgy And Pyrometallurgy Recycling Methods For The Recovery Of LIBs Active Materials (Baum et al., 2022).

Table 2. 1
A Summary For Reviewed Hydrometallurgy And Pyrometallurgy Methods

No	Author/ Year	Method of recycling	Study	
1.	(Makuza et al., 2021)	Hydrometallurgy	-	Involves pre-treatment for cathode material recovery, leaching, and purification techniques like selective precipitation, ion exchange, and solvent extraction to extract valuable metals.
		Pyrometallurgy	-	Pyrolysis, incineration, roasting, and smelting are the main pyrometallurgical options for recycling spent lithium-ion batteries.
			-	This process is dominant and mature due to its short reaction time, high productivity, and ease of scaling up.
2.	(Li et al., 2023)	Hydrometallurgy	-	Commonly used worldwide to recover each element selectively from wasted cathode powder by leaching.
			-	This technique can produce high-purity goods and is widely utilized.
		Pyrometallurgy	-	Involves high-temperature calcination. This process consumes a significant amount of energy and produces waste gas and slag. The process is relatively simple.
3.	(Bae et al., 2021)	Hydrometallurgy	-	Chemical leaching dissolves metals efficiently. Allows high-purity lithium recovery with lower energy than pyrometallurgy.
		Pyrometallurgy	-	High-temperature smelting recovers metals like Co, Ni, Cu, but loses lithium in slag. Energy-intensive with emissions challenges.
4.	(Sojka et al., 2020)	Hydrometallurgy	-	Achieves high metal recovery and purity from leaching and separation. Potential for industrial scale.
		Pyrometallurgy	-	Demonstrates that pyrometallurgy recovers valuable metals but loses lithium; suitable for mixed battery feedstocks.
5.	(Hanna et al., 2025)	Hydrometallurgy	-	Lower environmental impact and energy use compared to pyrometallurgy; better suited for lithium recovery.
		Pyrometallurgy	-	Life cycle assessment shows high energy consumption and emissions, poor lithium recovery efficiency.

2.4.3 Electrochemical

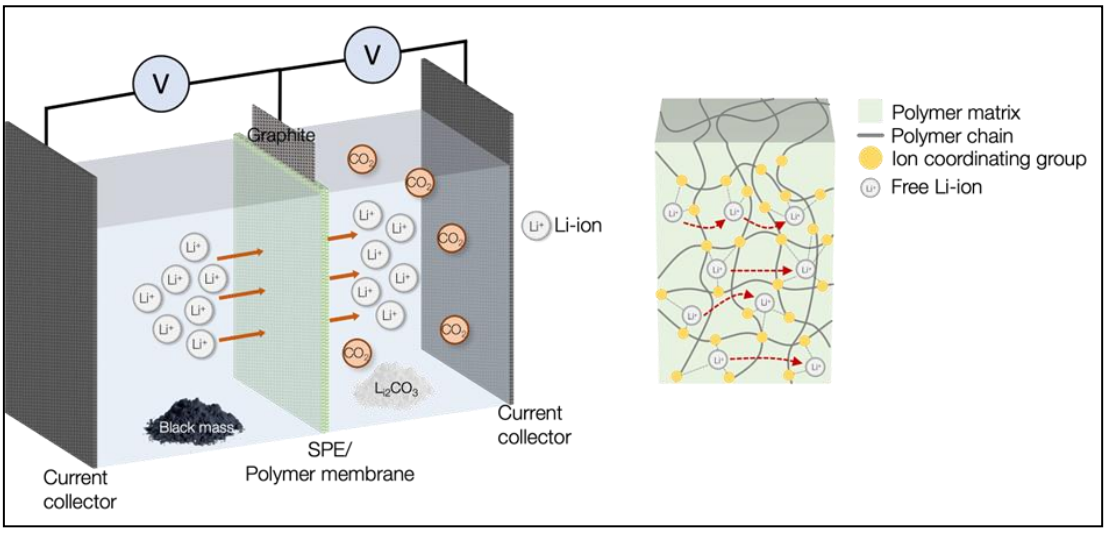

Figure 2. 5 Electrochemical Setup For Lithium-Ion Battery Recycling.

The electrochemical technique is a commonly employed technique for recovering metal elements from wastewater from industry, valuable elements from tailings, minor metals from waste materials, and lithium from lake brine. This preference stems from the electrochemical method's great selectivity for distinct ions, which allows for the dissolution or deposition of certain components. This selectivity is achieved by carefully managing voltage, current, and electrolyte conditions to efficiently separate distinct components. The electrochemical approach is not only efficient but also ecologically beneficial, and it has a lot of growth potential.

Electrochemical techniques present a useful path forward for enhancing the recycling efficiency of spent lithium-ion batteries (LIBs), offering compelling advantages over conventional pyrometallurgical and hydrometallurgical processes. Electrochemical techniques are exceptionally selective (figure 2.5), by controlling the applied voltage (the driving force for the dissolution or deposition of the desired metal ions (e.g., Li^{+}, Co^{2+}, Ni^{2+})), current density (inversely related to the polarization of the working electrode), and composition of the electrolyte, it is possible to minimize the cross-contamination of recovered materials and dramatically reduce the consumption of chemical reagents, thereby addressing two significant constraints of traditional acid-leaching methods (Xia et al., 2019) (Fakui et al., 2019).

On an environmental scale, electrochemical processes have greater amounts of sustainability through a reduction in chemical waste generation. Through the

application of electric current as the energy driving reactions, such procedures eliminate the need for high amounts of acids or oxidizing agents. As a case in point, electrochemical leaching has efficiencies of >90% metal extraction at room temperatures using dilute electrolytes and generates up to 50% less wastewater than conventional hydrometallurgy (Manthiram, 2020) (Goodenough et al., 2013). Energy efficiency is another hallmark, with the intrinsic electrochemical-thermal processes consuming only 1.59 kWh per kilogram of treated material—tiny in comparison to the energy consumed by high-temperature pyrometallurgical smelting (Goodenough et al., 2013).

Electrochemical processes are flexible throughout the recycling chain. In the pre-treatment step of the recycled battery materials, pulsed electrochemical stripping could selectively delaminate the cathode materials from aluminium current collectors without damage to the foil so they can be reused. In subsequent steps, electrodeposition allows for the separation of high-purity metals, electrodialysis allows for the separation of low-medium-purity metals, and electrochemical lithiation allows for lithium-deficient cathodes, that is lithium cobalt oxide ($LiCoO_2$), to be regenerated, or lithium brought back into the crystalline structure as Li^+ to restore greater than 95% of capacity (Thackeray et al., 2012).

As shown in Figure 2.6, there are several applications of the electrochemical approach in recycling spent lithium-ion batteries (LIBs). These applications include current collector separation, electrochemical leaching, element separation, regeneration, and synthesis. When compared to pyrometallurgical processes, electrochemical methods consume less energy and use less solution than hydrometallurgical methods.

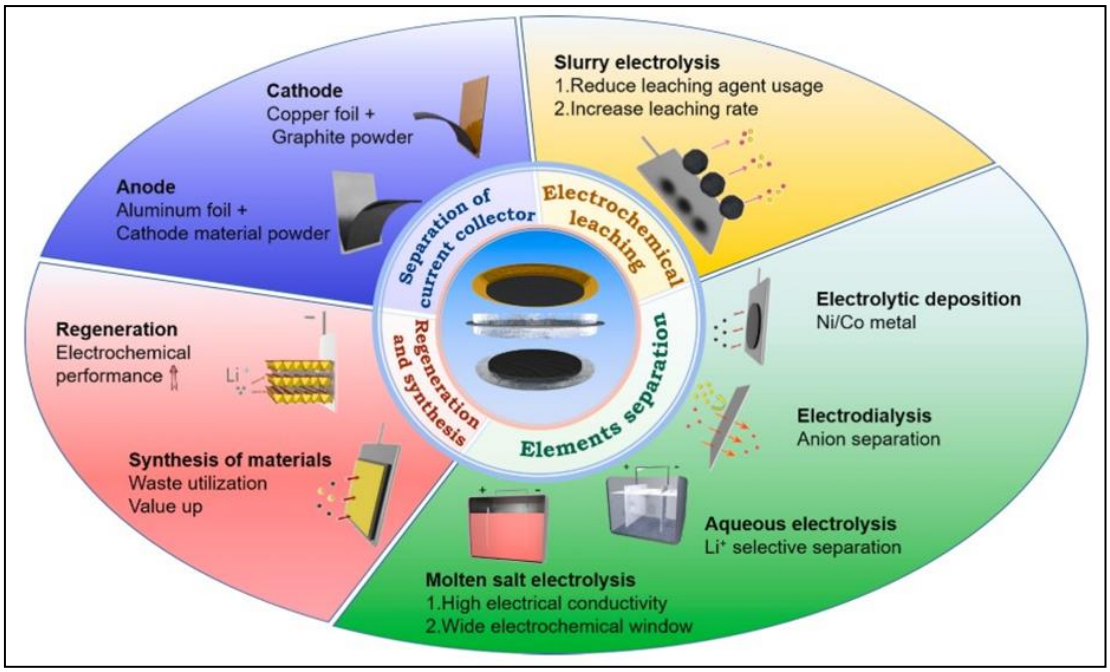

Figure 2. 6 The Incorporation Of An Electrochemical Technique To Recover Wasted LIBs (Li et al., 2023).

Electrochemical techniques are used in the pre-treatment process to separate the current collector from the active material/graphite. Working electrodes are made from spent electrodes, and the active material/graphite is removed from the current collector by the action of applied current, generating bubbles. The applied current substitutes standard chemical reagents as the driving power for the reaction in the leaching step of the used cathode material, considerably lowering reagent usage and wastewater production. Electrochemical leaching not only improves leaching efficiency but is also environmentally friendly (Li et al., 2023).

The significant selection of electrochemical techniques towards specific metal ions is beneficial for sorting distinct metal ions in the wasted cathode material leachate. Furthermore, electrochemical technologies make it easier to regenerate cathode materials and synthesise valuable compounds. Overall, the electrochemical technique appears as a flexible and long-term strategy for different stages of wasted LIB recycling (Li et al., 2023).

LIBs are a type of high-tech battery in which lithium ions play a key role in the electrochemistry. University of Washington's Clean Energy Institute, in a 2020 article, revealed that during discharge, lithium in the anode undergoes oxidation, losing electrons and becoming Li^+ ions. These small ions readily migrate through the micro-

permeable separator to the cathode, where they undergo reduction and recombine with electrons. This lithium-ion shuttle generates the battery's electrical current.

An electrochemical process happens when there is an electrical current movement involved. It also involves a matter associated with the passage of an electric current depends on the characteristics of the negatively charged electron. Electrochemical processes have transcended traditional boundaries, leaving an indelible mark on diverse industries and applications. From energy storage and generation to materials synthesis and environmental remediation, the realm of electrochemistry continues to evolve, presenting exciting opportunities for future scientific breakthroughs and sustainable solutions.

Table 2. 2
A Summary of The Reviewed Electrochemical Process For LIBs Recycling.

No	Author/ Year	Study
1	(Li et al., 2023)	Utilized to extract metals from industrial wastewater, as well as from waste solids, and salt-lake brine. Enables the dissolution or deposition of specific elements by adjusting voltage, current, and electrolyte conditions.
2	(Mcdonald et al. 2018)	This study measured the ionic conductivity of PEDOT: PSS and discovered that it is equivalent to known Li^+ conductors. When PEO is introduced, the conductivity continuously improves until it reaches a 20:1 PEO: PEDOT monomer ratio, after which the conductivity decreases with larger PEO loadings. The 300:1 PEO: PEDOT composite exhibits higher ionic conductivity than almost pure PEO due to the high concentration of PEDOT: PSS.
3	(Aannir et al., 2023)	The study effectively regenerated the cathodic component of portable phone batteries through the utilization of both different leaching acids, nitric and sulfuric. The recycled LiCoO2 cathodes have the same structural features as commercial ones, but their morphological traits resulted in altered electrochemical performance. Aluminium and salt were also retrieved for environmental and economic purposes. The findings show that recycling end-of-life lithium-ion batteries using a circular economy strategy is both feasible and effective.

2.5 Polymer Electrolyte

Polymer electrolytes are a type of electrolyte used in lithium-ion batteries. They have a polymer matrix instead of a solvent in a solution of lithium-salt, which is used to transport ions between the anode and cathode. Unlike conventional liquid electrolytes, polymer electrolytes are solid or gel-like polymers that contain lithium-salt to enable ionic transport. The structure of the polymer electrolytes allows for many advantageous properties and many unique benefits that improve battery safety, performance and design flexibility (Poinsignon, 1989). There are mainly two types of polymer electrolytes that are solid polymer electrolytes (SPE) and gel polymer electrolytes (GPE).

Polymer electrolytes first appeared as a potential option for ion-conducting materials in energy storage and conversion devices in the 1970s. They outperform organic liquid electrolytes in terms of stability and safety. Although liquid electrolytes, usually composed of dissolved salts in a solvent, often exhibit higher ionic conductivities than polymer electrolytes, leading to faster ion transport within the electrolyte and consequently quicker charge and discharge rates in batteries, they come with safety concerns (Chattopadhyay et al., 2023).

In contrast, polymer electrolytes, comprising solid or gel-like polymers infused with ionic salts, tend to have lower ionic conductivities (Chattopadhyay et al., 2023). However, recent advancements in polymer electrolyte technology have resulted in the development of highly conductive materials, particularly crucial for solid-state batteries. These polymer electrolytes combine the safety benefits of solid electrolytes with increased ionic conductivity, giving a practical performance and safety alternative to common liquid electrolytes. This family of polymer materials has gained scientific attention as a new category of solid-state ionic conductors (SSICs). While rapid ionic conductors formed of inorganic materials have good transport capabilities, their use as electrolytes and electrode separators is limited due to low electrolyte stability (Chattopadhyay et al., 2023).

In solid polymer electrolytes (SPEs), ionic conduction occurs through interactions between lithium ions and polymer chains that allows lithium-ion migration through the amorphous (non-crystalline) regions of the polymer matrix. However, high crystallinity in the polymer will limit the ionic channels and restrict ion mobility; hence, in order to limit crystallinity and increase conductivity, methods such as

copolymerization and the use of inorganic fillers are employed. SPEs usually provide good safety with no flammable solvents and good thermal and electrochemical stability; however, they usually have lower ionic conductivity than liquid electrolytes at room temperature (Xiao et al., 2009).

Gel polymer electrolytes have a small number of liquid electrolytes or plasticizers dispersed in a polymer structure to gain mechanical stability with a high ionic conductivity similar to liquid electrolytes. Commonly, polymers like PVDF-HFP or PAN are used in GPEs that hold carbonate-based solvents to move lithium ions in a safer and sealed way. GPEs have been shown to increase battery cycle life, minimize the chance of lithium dendrite growth and resist mechanical stress making them attractive for safer and flexible lithium-ion batteries.

Polymer electrolytes improve the interface between electrodes and electrolytes, reducing resistance and improving performance for the battery. Their flexibility makes them supportive of many geometries, including thin and lightweight varieties advantageous for portable electronics and electric vehicles. The improved safety benefits, due to the lack or reduction of volatile organic solvents, address two major concerns of flammability and leakage typically associated with liquid electrolyte batteries. Polymer electrolytes are a crucial aspect in the development of lithium battery technology because they provide an increase in safety, flexibility, and thermal stability, yet challenges remain in getting ionic conductivity and mechanical properties to be compatible.

A membrane is an interface that acts as a selective barrier between two adjoining phases, controlling the transport of substances between them (Ulbricht, 2006). The major benefits of membrane technology in bio- chemical engineering originate from the membrane's unique separation process, which is its capacity to selectively transport molecules. Membrane-based separations, unlike other thermal separation techniques, do not require additional substances, can be performed at constant temperatures with minimal energy consumption, and provide easy expansion, both vertically and horizontally, as well as integration with other separation or reaction techniques (Ulbricht, 2006). Membrane processes have emerged as a promising approach for effective separation due to inherent advantages such as a small footprint, a customizable separation process, and energy efficiency, while a highly permeable/selective membrane material is essential for achieving excellent molecule capture performance of membrane processes (B. Zhu et al., 2020). Current work is being done to enhance

polymer chemistries, salt compatibilities, and composite structures to better develop polymer electrolytes in advanced energy storage.

2.6 Solid Polymer Electrolyte (SPE)

A solid polymer electrolyte (SPE) is an electrolyte material that is solid as opposed to liquid or gel. It is intended to allow ions (usually cations such as lithium ions) to travel between the electrodes of a battery or electrochemical cell while retaining solid. Because of their beneficial features, solid polymer electrolytes have attracted substantial interest in modern energy storage systems such as solid-state lithium-ion batteries. Solid polymer electrolytes (SPEs) have numerous advantages compared to traditional, liquid electrolytes, particularly the absence of electrolyte leakage, reduced potential for flammability, greater mechanical flexibility, enhanced safety, and the potential to achieve stable interfacial contact with the electrodes. Because SPEs generally provide more controllable, processable, and mechanically flexible structures compared to inorganic solid electrolytes, the adhesive interactions derive from physical or chemical interactions with the electrode surfaces to help maintain stability and minimize interfacial resistance. Besides meeting the performance expectations for lithium-ion batteries, in particular, high mechanical strength, a high safety standard, better flame-retardant potentials, high thermal stability, high ionic conductivity under ambient conditions, and a broad electrochemical stability window, commercial SPE applications will have minimum accepted ranges for their distinct properties, which are summarized in Table 2.3.

The advanced SPE applications stem from the need to develop safe, efficacious, safe batteries with high energy density and high charge and discharge rates used for applications including portable electronics, energy storage units, supercapacitors, and electric vehicles. Solid-state lithium-ion batteries with solid polymer electrolytes are an intriguing potential energy storage technology. However, issues such as optimising ionic conductivity, addressing production complexities, and ensuring long-term reliability and consistency persist. Recently, a variety of SPE systems have been synthesized and studied, including polyethylene oxide (PEO), polycarbonates, polysiloxanes, and plastic crystal type electrolytes.

Table 2. 3
The Maximum Requirements For All Solid- State Polymer Electrolytes In LIBs.

Parameter	Requirement
Li^+ ion conductivity	≥ 10-5 S/cm at 25 °C
Stable potential window	≥ 4.0 V vs. Li^+ /Li
Mechanical property	≥ 30 MPa
Thermal stability	> 150 °C
Limit oxygen index (LOI)	> 27%

Polyethylene oxide (PEO), polyethylene glycol (PEG), and different polymer mixes doped with lithium ions are common materials used in solid polymer electrolytes. Researchers are continuing to investigate novel materials and formulations in order to improve the ionic conductivity and overall performance of SPEs (Teo et al., 2021).

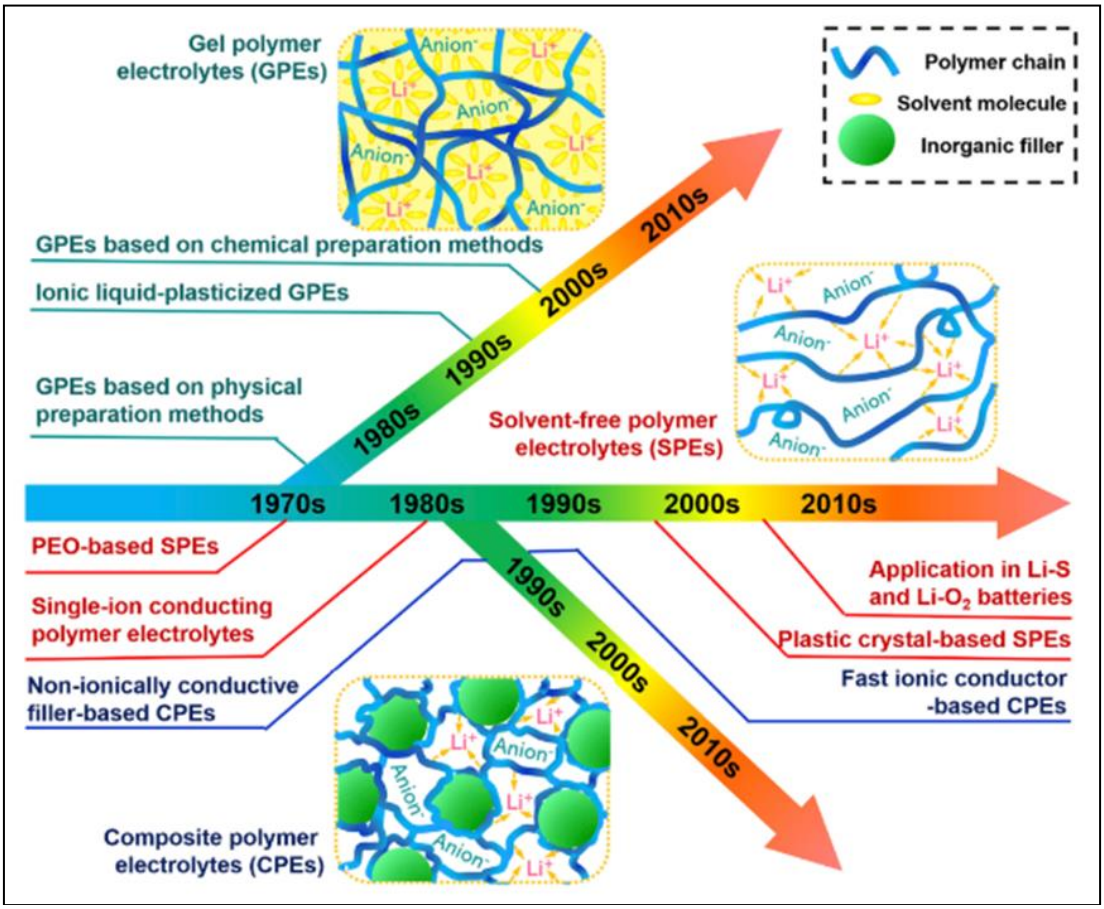

Figure 2. 7 A Brief Chronology of the Development of Typical Polymer Electrolytes for Non-aqueous Li-Based Batteries (D. Zhou et al., 2019)

2.6.1 Polyethylene Oxide (PEO)

Polyethylene oxide (PEO) has recently been the most widely used polymer matrix, owing to its strong capacity to dissolve lithium ions and display good

conductivity, particularly at high temperatures. Polyethylene oxide (PEO) stands out as an outstanding membrane material due to its inherent strong attraction to CO_2 molecules, driven by the dipole-quadrupole interaction between ethylene oxide units and CO_2. This property makes it highly versatile and enables its integration with various substances, making it suitable for use as selective layers in thin film composite membranes (B. Zhu et al., 2020). Given its low weight, high lithium salt solubility, and film-forming properties, PEO polymer electrolyte was the first and most frequently researched solid polymer electrolyte system (Ye et al., 2022). The intrinsically high crystallinity of PEO, however, exhibits a difficulty since lithium ions preferentially conduct in the amorphous zone, resulting in a very poor ionic conductivity of only 10^{-7} S/cm at ambient temperature. Furthermore, the mechanical strength of pure PEO is insufficient to prevent the production of lithium dendrites.

To overcome these difficulties, researchers have concentrated on reducing PEO crystallisation to increase the flexibility of the polymer chain. Blending, copolymerization, grafting, and the introduction of various fillers have all been commonly used modification procedures. Common nano-fillers such as aluminium oxide ($Al_2O_{3)}$, silica ($SiO_{2)}$, titanium dioxide (TiO_2), and zirconium dioxide (ZrO_2) have been added to polymer electrolytes to increase ionic conductivity and mechanical characteristics, limiting the formation of lithium dendrites. Using lithium salts that dissociate more readily can also boost the concentration of the charge carrier (Zhou et al., 2020). Despite the limitations provided by inorganic filler aggregation and poor dispersion, standard physical blending procedures have proven challenging and have not resulted in major improvements in ionic conductivity. Acknowledging this constraint, researchers have moved their emphasis to chemical crosslinking or grafting as alternatives to physical mixing, to address these long-standing difficulties (Nair et al., 2008).

Lithium bis(trifluoromethanesulfonyl)imide (LiN $(SO_2CF_3)_2$), commonly called LiTFSI, is establishing itself as the benchmark lithium salt in a new class of large lithium salts. These salts show immense charge delocalization, improving effective ionic dissociation qualitatively when combined with solvating polymers such as poly (ethylene oxide) (PEO). In addition, it demonstrates excellent chemical, electrochemical, and thermal stability, LiTFSI has plasticizing effect on the polymer matrix, lowering the crystallinity of the host polymer and thus allowing lithium ions to more easily mobilize in the electrolyte system.

For example, Chopade et al., 2017, created a new class of cross-linked polymer electrolytes by adding succinonitrile into a poly (ethylene oxide)/lithium salt matrix. This novel method produced outstanding ionic conductivity and mechanical characteristics at room temperature. Cross-linking has been shown to increase the dynamic elastic modulus of polymer electrolytes, improve thermal stability, prevent polymer crystallisation, and limit the formation of lithium dendrites (Zhou et al., 2020).

2.6.2 Polyvinyl Fluoride (PVDF)

Another SPE that was commonly used is polyvinylidene fluoride (PVDF). PVDF is a polymer electrolyte with excellent mechanical strength, thermal stability, and chemical stability that is widely utilised as a binder, separator, and polymer electrolyte in various battery systems. Despite these advantages, PVDF's homogeneous structure and low ionic conductivity prevent it from being used directly as an electrolyte (Ye et al., 2022). At this time, PEO has garnered considerable research attention due to its base on a major chain ether linkage bond that attaches itself to Li+ ions. Due to its high degree of crystallinity at room temperature, its chain segment motion and accompanying ionic diffusion ability, without other modification processes, are not good (Li et al, 2019). Several other polymers have since been developed as electrolytes, such as polyacrylonitrile (PAN) (L. Gao et al., 2020), polycarbonate (PC) (Saito et al., 2020), polymethyl methacrylate (PMMA) (Xiaolong et al., 2019), polyvinylidene fluoride (PVDF) (Lun et al., 2018), and polyvinylidene fluoride hexafluoropropylene copolymer (PVDF-HFP) (Y.F. et al., 2018).

PVDF is also compatible with conducting polymers such as PEDOT: PSS. PEDOT: PSS, being made up of thiophene and sulfonate units, does not crosslink directly with PVDF, allowing both polymers to coexist in a hybrid network without undesirable crosslinking or phase segregation. The non-ionic character of PVDF prevents disruption of the PEDOT: PSS electroactive network and ensures broad chemical stability in the composite, as confirmed in composite electrode and membrane research (Chen et al., 2025).

PVDF is an extremely resistant polymer with a number of beneficial characteristics, including being hardly flammable, gradually melting with minimal smoke emission, and being readily processed for a broad variety of product forms. It possesses reliability, optimum wear resistance, and required mechanical strength, and

is resistant to mechanical deterioration, surface wear, ozone, water, and corrosion. PVDF items can work over 50 years without diminishing physical and mechanical characteristics, showing slight deterioration when used outdoors. Additionally, it has low surface roughness, high flow rate, and better chemical resistance to most organic and inorganic aggressive fluids, even at elevated temperatures (Dallaev et al., 2022).

The applications of PVDF are diverse, with some applications in the chemical/petrochemical industry for non-flammable use, filtration, and storage of aggressive media; in the aviation industry for seals, linings, and gaskets; and in the aerospace industry for wiring coatings and 3D printing. It is also utilized in electronics/radio engineering as insulation, dielectric, and piezoelectric uses, such as those in lithium-ion batteries and sensors. In construction, PVDF is used as protective coatings, weather-resistant coatings, erosion-resistant coatings, and anti-corrosion coatings. It is also used in nuclear power engineering for treating nuclear waste since it is heat-resistant and radiation-resistant (Dallaev et al., 2022).

2.7 Lithium Bis (Trifluoromethanesulfonyl) Imide (LiTFSI) Salt

Lithium bis(trifluoromethanesulfonyl)imide (LiTFSI) has been recognized as the model' salt in the bulky lithium salt family owing to its high charge delocalization allowing ionic dissociation in solvating polymers such as poly (ethylene oxide) (PEO). LiTFSI can also be highly pliable and chemically, electrolytic and thermal stability as well as a plasticizing effect to the host polymer in turn making it less crystalline and ultimately facilitating ionic mobility. Solid polymer electrolytes (SPEs) are typically made up of lithium salts with a polymer matrix to enable ionic conduction. Various lithium salts have been a good example such as, LiTFSI, $LiClO_4$, $LiBF_4$, $LiPF_6$, $LiAsF_6$, $LiCF_3SO_3$, and $LiN(CF_3SO_2)_2$. Among of these salts, lithium bis(trifluoromethanesulfonyl)imide (LiTFSI) is especially known for its excellent thermal and chemical stability, excellent electrochemical performance, and high solubility, allowing for ease of ion dissociation (Mendes-Felipe et al., 2021).

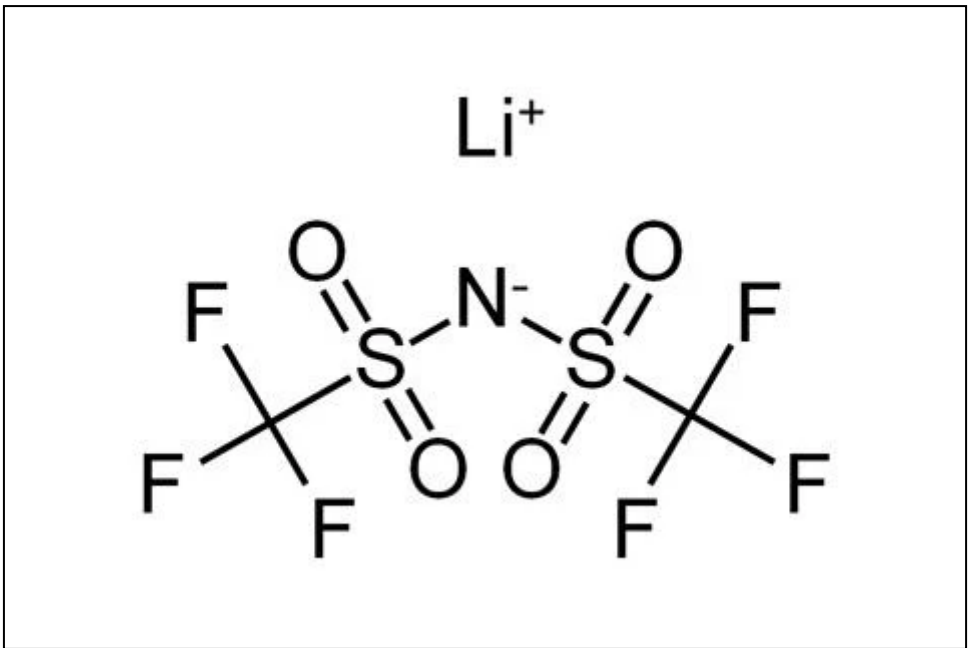

Figure 2. 8 Chemical Structure of LiTFSI Salt

LiTFSI in molecular structure figure 2.8, is a hydrophilic lithium salt with the formula C2F6LiNO4S2 and weight 287.09 g/mol and appears as white hygroscopic powder with remarkable solubility in water (approximately 21 molal). The compound has a melting point of 234 to 238 °C, is moisture sensitive, and is electrochemically stable. Its broad application ranges from lithium-ion batteries to organic semiconductors, and is an essential contributor to the development of energy storage and electronic technologies. LiTFSI produces less hazardous by-products compared to conventional salts used in electrolytes. All these characteristics contribute to battery performance improvement, increasing lifespan, and safety for the environment.

Many studies show that LiTFSI is typically completely dissociated in PEO hosts (H. S. Liu et al., 2021). PEO is a flexible macromolecular configuration that can move with a fair amount of Li+ ions being transported alongside (J. Wang et al., 2022). Simulation-based studies have identified several Li+ transport mechanisms including the diffusion along PEO chains, zig-zag complexations and decomplexations with anions, or even sporadically hopping between differing PEO chains. A researcher found that Li+ ions along PEO chains are more mobile than those that are hopping between PEO chains, which means that improved transport along the PEO chain can lead to improved Li+ diffusion (Borodin et al., 2006). PEO/LiTFSI solid polymer electrolyte (SPEs) offer attractive thermal stability, remarkable mechanical properties, and the ability to suppress lithium dendritic formation, addressing serious challenges for the

safety and durability of solid-state devices. The modular nature of PEO and the chemical stability of LiTFSI lend to this system as a viable future candidate for all-solid lithium batteries.

2.8 Interpenetrating Network (IPN)

Interpenetrating polymer networks (IPNs) are a type of polymer structure that is generated by the non-bonded combination of two different components, each in network form, intricately intertwined, and tightly entangled. IPNs are formed when one component is polymerized or cross-linked in the presence of another. As a result, the network structure is flexible and interconnected, combining the properties of both separate components (J. Liu et al., 2022). The IPN solid polymer electrolytes, besides showing high ionic conductivity, high flexibility, which permitted homogeneous current distribution, effectively suppressing Li dendrite growth, also had excellent compatibility with cathodes and were easily processed (Tong et al., 2018). IPN is needed in the solid polymer electrolyte as it can reduce the crystallinity of the material, which will result in high ionic conductivity (Jiang et al., 2023). Various ways have been used to reduce crystallinity and increase the ionic conductivity of polymer solid electrolytes. Polymer blending, the use of conductive polymers as polymer electrolyte membranes, and the integration of organic or inorganic components or ionic liquids (IL) as fillers are examples of these techniques (Li et al., 2019).

A study from (Fong et al., 2017) shows an incorporation of a mixture of PEDOT and PEO-based network to display the concepts of an interpenetrating network. Figure 2.9 shows the illustration of IPN. This polymer combination has been extensively researched in the field of semi-interpenetrating networks (s-IPNs) for use in actuators, electrochromic devices, and tactile sensors. However, its potential for supercapacitor applications has yet to be discovered. As the electrically conducting pseudocapacitive component of the semi-interpenetrating network (s-IPN), PEDOT offers various advantages. Chemical and thermal stability, biocompatibility, and a competitive theoretical specific capacitance of 210 F/g are among the benefits. Furthermore, PEDOT has a high conductivity, reaching up to 4500 S/cm, and can operate over a wider voltage range than many other conducting polymers. The ethylene oxide groups in the cross-linked PEO-based network within the s-IPN, on the other hand, achieve strong ionic conductivity. These groups can coordinate electrolyte metal cations, increasing

the material's polarity and enabling swelling in aqueous electrolytes. The presence of dangling chains in the matrix creates extra free space, which improves ion mobility (Fong et al., 2017).

PVDF (polyvinylidene fluoride) has a comparative ability to be applied in solid polymer electrolytes because it is known to be mechanically robust, chemically stable, and electrochemically compatible. Evidence shows that blending PVDF with PEO and LiTFSI salt can create free-standing membranes and electrolytes without compromising the properties of the respective pure polymer (Ushakova et al., 2020). In general, PVDF can provide mechanical strength and promote disorder of the polymer and LiTFSI salt dissociation to create a beneficial polymer matrix. Based on density functional theory studies and experimental evidence, PVDF can be involved with Li^+ coordination, whose multiple fluorine atoms could have a possible interaction with lithium ions, without affecting overall degrees of salt solubility, diffusion, or conductivity. In terms of PVDF, unlike being a plasticizer or disrupting PEO crystallinity, it helps maintain a homogeneous entangled network structure of polymers, which collectively provide beneficial mixtures for mechanical and electrochemical properties.

From studies, there is an optimal PVDF content (usually up to ~30 wt%) that may be incorporated without compromising ionic conductivity; instead, it is favourable for achieving good mechanical properties and tolerable ionic conductivity for solid-state lithium battery applications. Therefore, too much PVDF could dilute the conducting phase, disturbing percolation pathways (Ushakova et al., 2020). PVDF is a very compatible filler in the PEO/PEDOT: PSS matrix, promoting the formation of an interpenetrating, functional network with enhanced mechanical stability and maintained or enhanced ionic transport properties. This combination is appropriate for high-performance, flexible solid-state electrolyte membranes.

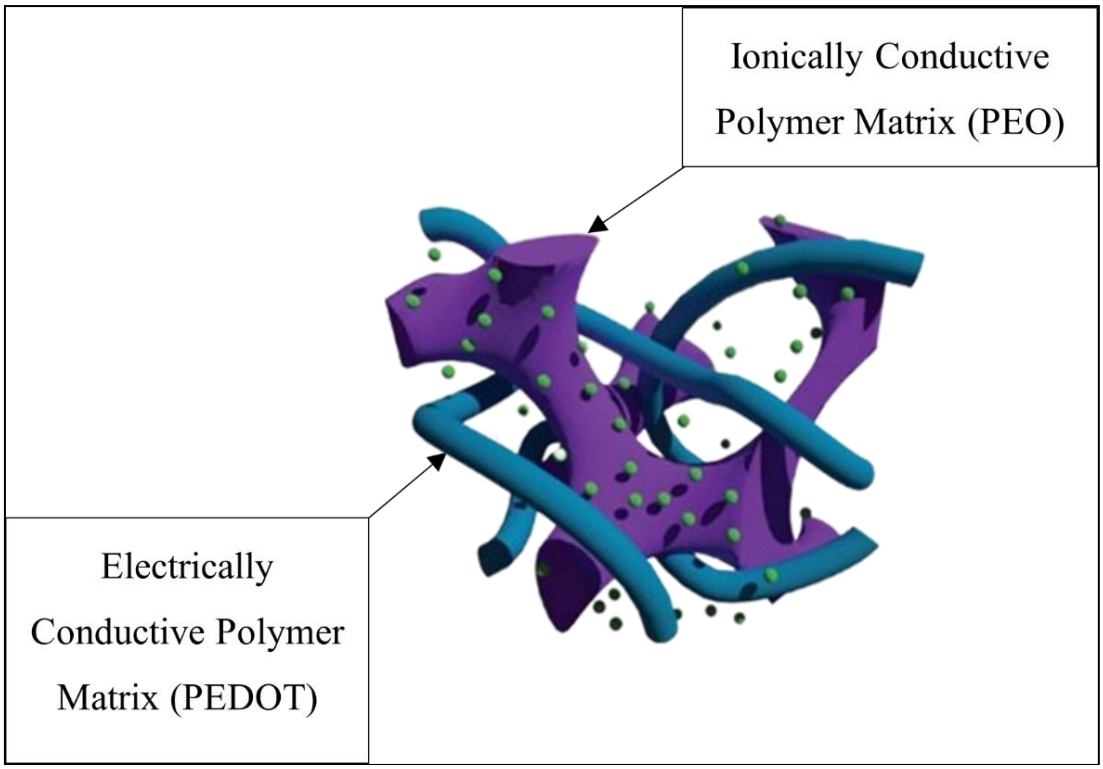

Figure 2. 9 Schematic Diagram of IPN For PEDOT/ PEO (Fong et al., 2017).

2.9 Conducting Polymer (CP)

Conducting polymers are materials that can conduct electricity. They can do this in two ways: by conducting ions or by conducting electrons. Some conducting polymers can conduct both ions and electrons. The way that a conducting polymer conducts electricity depends on its chemical structure and the presence of charged particles in its matrix. The matrix is the material that the charged particles are embedded in. For example, a conducting polymer with a conjugated backbone can conduct electrons. A conjugated backbone means that the polymer has alternating single and double bonds between its carbon atoms. This allows electrons to move freely along the polymer chain. A conducting polymer with ionizable groups in its structure can conduct ions. Ionizable groups are groups of atoms that can lose or gain protons (charged hydrogen atoms). When an ionizable group loses a proton, it becomes a negatively charged ion. When an ionizable group gains a proton, it becomes a positively charged ion. The presence of charged particles in the matrix of a conducting polymer is also important for conductivity. If there are no charged particles in the matrix, the polymer

will not be able to conduct electricity. Conducting polymers have a wide range of potential applications, including batteries, solar cells, and sensors (Li et al., 2015).

The addition of conducting polymers like PEDOT: PSS or polypyrrole into (SPEs) provides important ionic enhancement assisted by several synergistic mechanisms. First, the introduction of conducting polymers creates disorder in crystalline domains of host polymers (like polyethylene oxide (PEO)), which increases the amorphous regions of the polymer, where ionic conduction (Leš et al., 2020). This decrease in the size of crystalline domains promotes segmental motion of the polymer chains, so that lithium-ion, Li^+ transport can occur effectively.

One of the most significant uses of conducting polymers is their ability to enable salt dissociation through the use of electron-dense functional groups. Heteroatoms present in conducting polymers like PEDOT have a strong interaction with lithium salts such as LiTFSI, increasing the availability of free Li^+ ions to be transported (Leš et al., 2020). In addition, conducting polymers form interfacial regions that are preferential pathways for Li^+ migration, as indicated by solid-state nuclear magnetic resonance (NMR) and impedance spectroscopy measurements (Li et al., 2022). These interfaces decrease the activation energy required for ion transfer, enabling higher conductivity even at lower temperatures.

In addition to solely ionic effects, conducting polymers create beneficial electronic conductivity, to stabilize electrode-electrolyte interfaces. The mixed electronic and ionic conductivity results in lower interfacial resistance and reduced formation of lithium dendrites. This is among the most common failure mode of solid-state batteries (Hao et al., 2021). Conducting polymers provide a dual advance in that it not only promotes Li^+ mobility but also adds mechanical and electrochemical stability, both ultimately necessary for a high-performance SPE.

Given its great potential as an alternative to metallic conductors and semiconductors, it is significant that the progress of conductive polymers (CPs) increases. Several research groups have worked hard on modifying polymers to fulfill particular electrical, mechanical, optical, and thermal characteristics needs (Kumar et al., 1998). This accomplishment, like many others in scientific history, was preceded by necessary prerequisites such as theoretical discoveries from physicists and quantum chemists, as well as past work on conductive polymers. There are simple, adaptable, and cost-effective approaches for CP synthesis. CPs may be easily fashioned into

supramolecular structures with multifunctional properties using conventional electro-polymerization processes (Nezakati et al., 2018).

Whereas the conductivity of these polymers is a fascinating and useful trait in and of itself, the variability of their conductivity, for example, the ease with which the materials may be reversibly switched between their insulating and conducting states, is their most essential attribute (Kaneto, 2014).

There are several CPs, and they are classified depending on their electric charge types, such as delocalized electrons, conductive nanomaterials, and ions. In their work, many forms of conjugated CPs, their distinctive features, and synthesis processes will be thoroughly examined (Nezakati et al., 2018). Polypyrrole, polyaniline, and polythiophenes are the primary forms of CPs that are commonly discussed. These CPs, based on figure 2.10, find applications in organic electronics, sensors, actuators, energy storage devices, and other areas where electrical conductivity is desirable. The ability to control the conductivity and other properties of conducting polymers through chemical synthesis and processing has led to significant advancements in the field of organic electronics and flexible electronics.

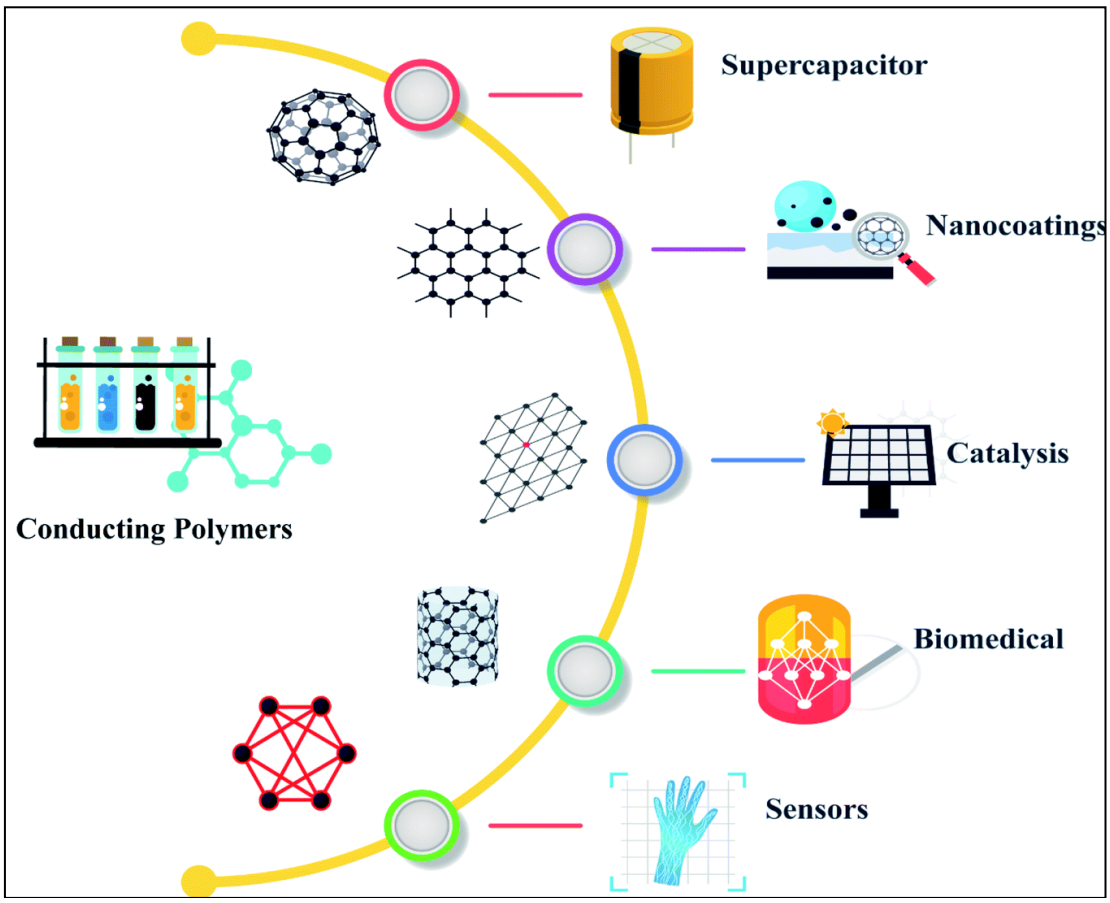

Figure 2. 10 Applications of Conducting Polymers And Their Composites Are Shown Schematically (Namsheer et al., 2021).

2.9.1 Polypyrrole

Polypyrrole (PPy) is another conducting polymer belonging to the class of intrinsically conducting polymers (CPs). It is formed by the oxidative polymerization of polypyrrole monomers, which can occur via chemical, electrochemical, or enzymatic methods. PPy, based on the chemical structure of Figure 2.11, has unique electrical, optical, and mechanical properties that make it a promising material for a variety of applications, including in sensors, actuators, energy storage devices, and electronic devices. It can be doped with different dopants to tune its electrical conductivity and optical properties.

PPy is an excellent conducting polymer that improves the performance of SPEs. PPy presents high electrical conductivity in the doped state (~10–100 S/cm), great compatibility with polymer matrices, and good environmental stability. The conjugated backbone of PPy is created from the nucleophilic polymerization of pyrrole monomers (C_4H_4NH), which have α–α′ linkages, and enable extensive π-electron delocalization that facilitates ionic and electronic charge transport. PPy is also redox-active in nature and can undergo oxidative doping, leading to charge carriers (polarons and bipolarons) that create pathways for a significant increase in the conductivity of a conducting polymer (Heeger, 1989).

As a conductive polymer, PPy offers various benefits, including simplicity of synthesis, low cost, and high processability. It is also ecologically stable, withstanding UV light and other environmental variables. Although it has many advantages, PPy also has some limitations, which are its relatively low electrical conductivity compared to metals and some other conductive materials. It can also be susceptible to oxidation and degradation in certain environments. Nevertheless, researchers are actively investigating ways to optimize the properties of PPy and other conductive polymers for specific applications, and they continue to show promise for a wide range of uses.

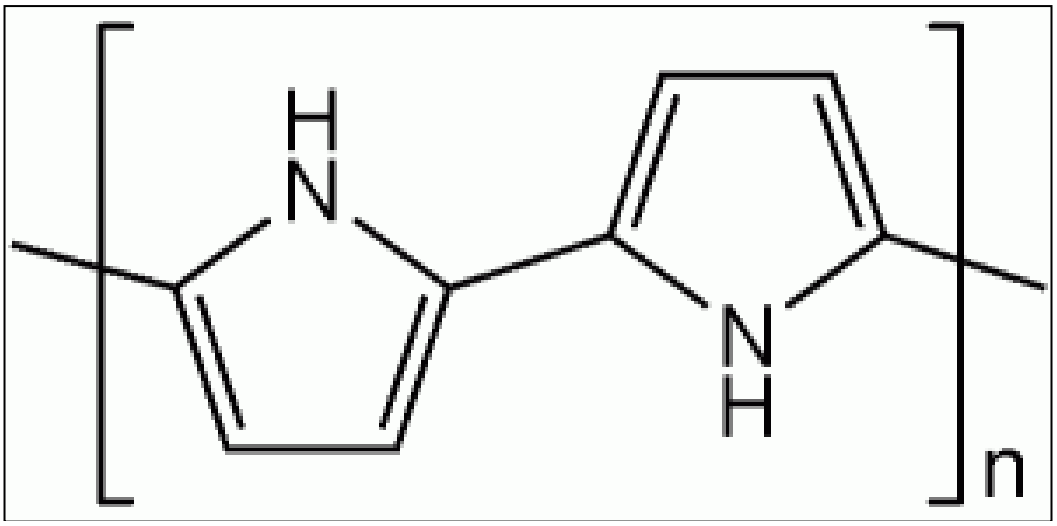

Figure 2. 11 Chemical Structure of Polypyrrole.

2.9.2 Polyaniline (PANI)

Another CPs that are widely used is polyaniline (PANI). PANI, as shown in Figure 2.12, stands out as the most extensively researched and promising member within the family of conducting polymers. PANI boasts remarkable attributes, including exceptional stability, excellent processability, and the capacity to fine-tune its electrical and optical properties. The conductivity of PANI is intricately linked to the concentration of dopants, and it attains conductivity akin to metals only under conditions where the pH is below 3 (Namsheer et al., 2021). PANI exists in 3 different types which are classified as leucoemeraldine, emeraldine, and pernigraniline. These types were classified based on their oxidation state. For instance, leucoemeraldine is in a reduced state, emeraldine in a partially oxidized and reduced state, and pernigraniline exists in a fully reduced state. PANI becomes conductive only when it is in a moderately oxidized state and acts as an insulator in a fully oxidized state.

The most commonly studied oxidation state is the emeraldine base (EB) form, which is an intermediate state between the fully reduced leucoemeraldine form and the fully oxidized pernigraniline form. The EB form of PANI is a blue- green colour and has good electrical conductivity. PANI has a wide range of potential applications, including in sensors, actuators, energy storage devices and electronic devices. It is attractive for these applications due to its low cost, ease of synthesis, and good processability. However, some challenges remain in optimizing the properties of PANI for specific applications, such as improving its stability and conductivity.

Generally, PANI in doped form is insoluble in organic solvents. Meanwhile, the undoped form of PANI is soluble in polar solvents such as N- methyl- 2- 2pyrrolidone (NMP), tetrahydrofuran (THF), dimethyl sulfoxide (DMSO), dimethylformamide (DMF), and many. Rather than being solubilized in the solvents, PANI will form a fine colloidal suspension. However, it is very critical in selecting a suitable dopant and tuning the synthesis conditions to improve the solubility of PANI in water and various organic solvents (Bhandari, 2017). Due to its powdery nature, PANI retains the ability to create a film on the electrode surface even after the electrodeposition process. Alternatively, free-standing PANI films can be produced by casting PANI solutions in NMP medium. Nevertheless, contemporary research primarily focuses on fabricating free-standing films by synthesizing composites with materials such as carbon nanotubes, carbon nanofibers, graphene oxide, and similar substances.

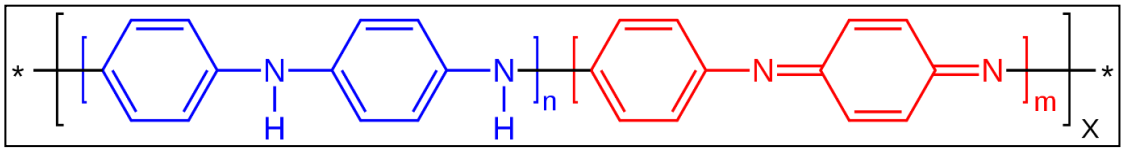

Figure 2. 12 Chemical Structure of PANI

2.9.3 Poly (3,4- ethylenedioxythiophene) (PEDOT)

PEDOT, a polythiophene derivative, is being widely explored for its exceptional electrical and electro-optical properties. The larger family of polythiophenes is being studied for the development of nonlinear optical devices, photochromic modules, polymer LEDs, and anti-corrosion coatings. Polythiophenes are also used in energy storage devices. Doping engineering or chemical alterations can be used to change the electrical and optical properties of polythiophenes. Polythiophenes have a band gap that ranges from 3 to 1 eV depending on the dopant and side chain used (Namsheer et al., 2021). PEDOT has a comparatively good stability when compared to other conducting polymers. Its conjugated polymer backbone, which contains alternating C-C double bonds, allows for significant orbital overlap throughout the molecule. PEDOT can also be doped with a variety of anions, including macromolecular polyanions such as poly (styrene sulfonate) (PSS). According to previous research, PEDOT is substantially

insoluble in the majority of solvents, electroactive in aqueous solutions, and has a reasonably high degree of conductivity (Ujvári et al., 2015).

The main challenge with the PEDOT derivative is its inability to dissolve in water. This problem was effectively solved by introducing a polyelectrolyte into the PEDOT matrix, such as poly sulfonates (PSS). PSS has a dual purpose of being a dopant and a stabiliser via a charge-balancing process. As a result, the PEDOT: PSS derivative has significant properties such as high conductivity, excellent mechanical flexibility, and long-term thermal stability (Namsheer et al., 2021).

Discovered in 1988, chemically polymerized PEDOT quickly found its first commercial application due to its capability to construct transparent and conductive films. Initially employed as an antistatic layer in photographic films, PEDOT has since diversified its presence across various markets. It has become integral in solid electrolyte capacitors, printed wiring boards, and packaging films, and is utilized in technologies such as touch screens. Additionally, PEDOT plays a crucial role as a hole transport layer in both organic light-emitting diodes (OLEDs) and organic photovoltaics (OPV) (Precious et al., 2014).

The conductivity of PEDOT films can be greatly improved if the dispersions comprise high-boiling polar solvents such as ethylene glycol (EG) or dimethyl sulfoxide (DMSO) in addition to water (Ouyang et al., 2004). 3-10% of such high boiling solvents are often included to the formulation. These solvents remain in the film longer than water during drying, improving the film formation process and influencing the resultant film morphology (Takano et al., 2012). This leads to the formation of a thermodynamically more favourable film morphology, characterized by the presence of enlarged PEDOT-rich domains. These domains are instrumental in facilitating the macroscopic transport of current (Timpanaro et al., 2004). With advancements in PEDOT synthesis and a deeper understanding of the film-forming process, there are now Clevios dispersions accessible, resulting in conductivities reaching 1000 S/cm.

2.9.4 Poly (3,4- Ethylenedioxythiophene): Poly (Styrene Sulfonate) (PEDOT: PSS)

Based on Figure 2.13, poly(3,4-ethylenedioxythiophene): poly (styrene sulfonate) (PEDOT: PSS), is one of the most commonly used CPs. The CPs consist of a conductive polymer (PEDOT) and a polyelectrolyte (PSS).

As one of the commonly used CPs, it has attracted much attention due to its high electrical conductivity. To achieve aqueous PEDOT: PSS dispersion, positively charged conjugated PEDOT might be chemically doped with negatively charged saturated PSS. PSS acts as a polymer surfactant, which helps PEDOT to disperse and stabilize in water and other solvents. It has several distinct features, making it an intriguing option for a low-cost, low-temperature, solution-processed electrode material for high-performance flexible and thin-film devices (Huseynova et al., 2019). It has many advantages compared to other conducting polymers. Bayer AG initially marketed it as an aqueous dispersion under the brand name Baytron, then H.C. Starck, and now Heraeus under the brand name CleviosTM. Agfa also introduced OrgaconTM, a PEDOT: PSS for large-scale printing applications (Fan et al., 2019). Various solution-processing processes, including spin casting, doctor blade, slot die coating, spray deposition, inkjet printing, screen printing, and so on, easily generate a continuous thin layer on either rigid or flexible substrate (Sun et al., 2015).

Post-treatments such as annealing, acid treatments, or dopant addition may greatly improve the conductivity of PEDOT: PSS. These treatments can improve the crystallinity of PEDOT, leading to enhanced charge transfer. However, these treatments may have an effect on the stability and other properties of the PEDOT: PSS composite. To produce polythiophene derivatives such as PEDOT, PEDOT: PSS, and poly (3-hexylthiophene) (P3TH), a composite was generated through diverse methods, encompassing green synthesis, synthesis in microfluidic systems, electro-polymerization, and other innovative techniques (Namsheer et al., 2021)

Synthesis of poly(3,4-ethylenedioxythiophene) doped with polystyrene sulfonate (PEDOT: PSS) by oxidative polymerization is shown in Figure 2.14, which has a multi-step mechanism pathway. The reaction begins with the dissociation of the oxidant sodium persulfate ($Na_2S_2O_8$) that undergoes cleavage to yield sodium ions (Na^+) and persulfate anions ($S_2O_8^{2-}$). These persulfate anions undergo homolytic cleavage to produce two sulfate radical anions ($SO_4^{\cdot -}$). The extremely reactive radical species serve as the oxidizing agents needed for initiation of the polymerization.

In the next step, the sulfate radicals oxidize the monomer 3,4-ethylenedioxythiophene (EDOT) to create EDOT radical cations. Oxidation is extremely critical as it activates the monomer by the creation of reactive sites and thereby facilitates further polymerization reactions by electron transfer from EDOT to the sulfate radicals.

On activation of the monomer, growth of the polymer chain is obtained via a sequence of radical coupling reactions. Two EDOT radical cations couple to form an EDOT dimer and then a dimer radical cation. This propagation is followed by successive coupling and deprotonation steps ($-2H^+$), producing trimers and higher PEDOT oligomers. Alternating oxidation and deprotonation reactions can produce extended chains of PEDOT.

The role of sodium polystyrene sulfonate (PSS) is of paramount importance in polymerization. As a polyelectrolyte with sulfonic acid and sulfonate functional groups, PSS serves two essential roles. Its sulfonate groups electrostatically interact with the positively charged PEDOT chains, doping and stabilizing the polymer charge in a polyelectrolyte complex. Second, PSS inhibits PEDOT chain aggregation, providing an aqueous dispersion enhancing processability and utility.

The final PEDOT: PSS complex comprises PEDOT chains tightly bonded with PSS due to coordination between sulfonate/sulfate groups and oxidized polymer segments. This structure enhances both electrical conductivity and mechanical stability, thereby positioning PEDOT: PSS as a promising material for diverse applications in electronics and energy storage (Sakunpongpitiporn et al., 2019).

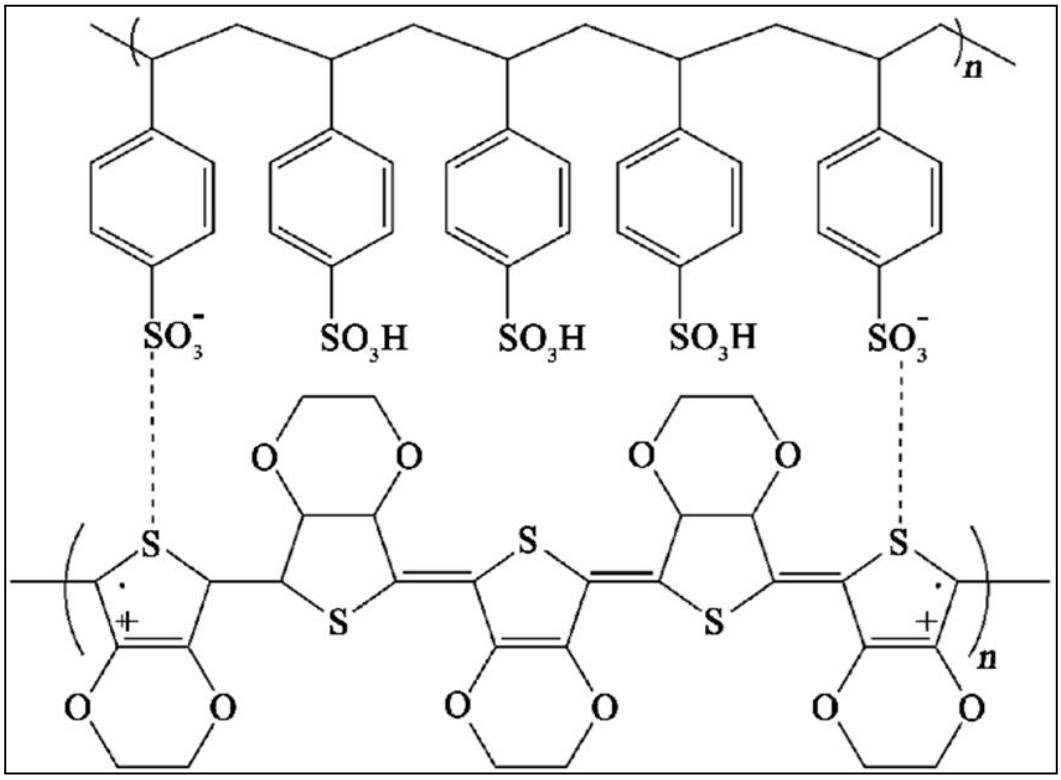

Figure 2. 13 Chemical Structure of Polymerized PEDOT: PSS

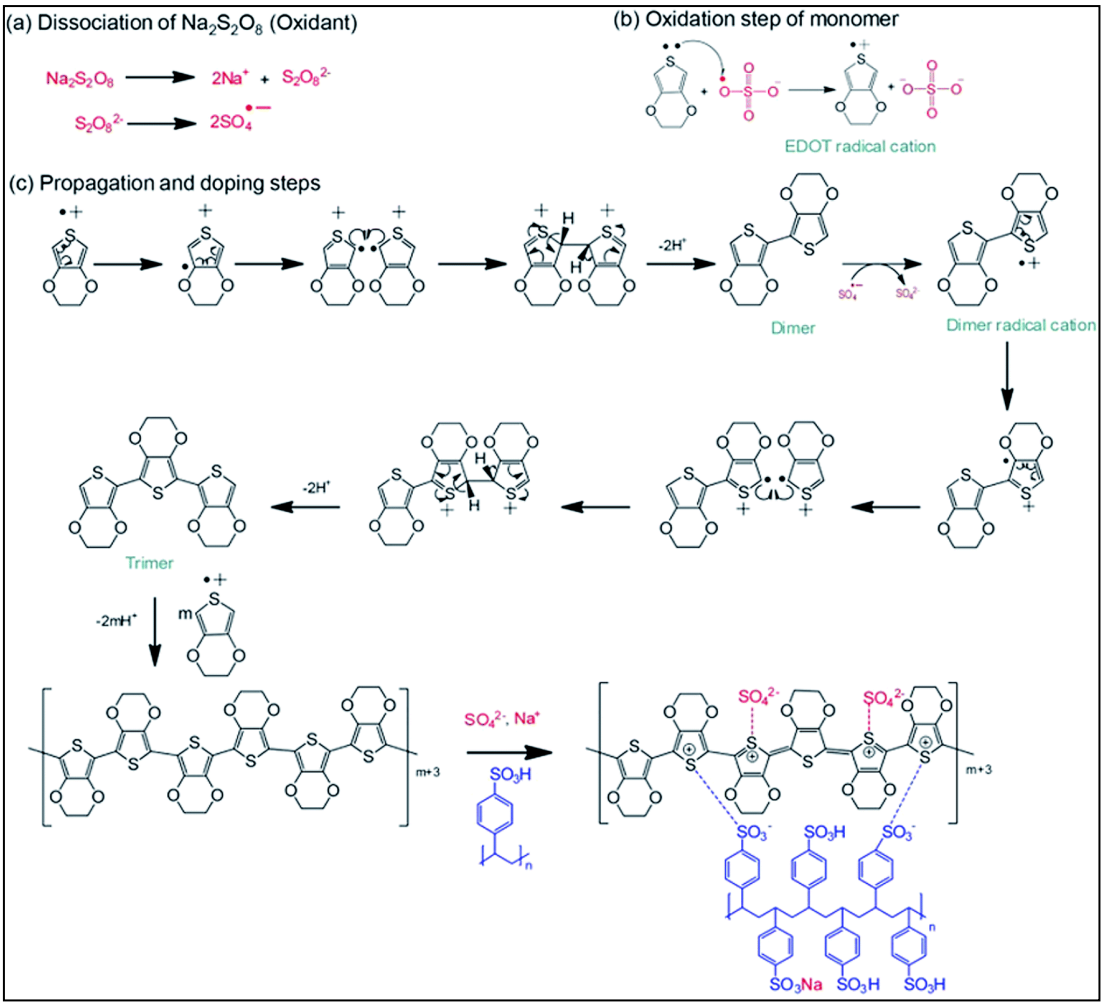

Figure 2. 14 Illustrated Mechanism Of PEDOT: PSS Formation Via Oxidative Polymerization (Sakunpongpitiporn et al., 2019).

2.10 Compatibility of Two Different Mix of Polymer

PEO and PEDOT: PSS constitute an attractive polymer blend system for solid polymer electrolytes (SPEs), emanating from their synergistic properties. PEO being semi-crystalline offers a significant amount of ionic conductivity by interacting through ether oxygen (–CH_2–O–CH_2–) units that solvate lithium salts, that is LiTFSI and thus facilitate the movement of Li^+ ions. However, its elevated crystallinity at room temperature tends to restrain the segmental movement of polymer chains; hence, it limits ionic conduction as well as mechanical flexibility (Huang et al., 2024). Contrastingly, PEDOT: PSS is a mixture of conductive polymers that includes the hydrophobic, π-conjugated PEDOT backbone associated with the hydrophilic PSS^- counterions. This set of properties gives PEDOT: PSS considerable electronic conductivity (~1–1000 S/cm) and superb solution processability, even though ionic

conductivity is low owing to limited ion mobility within PEDOT-dominated regions (Seiti et al., 2023).

Both the composite PEDOT: PSS/PEO electrode and the pure PEDOT: PSS electrode were analysed in their current configurations. From granular to filamentous, the morphology of the PEDOT: PSS film changed upon addition of the PEO network, based on Figure 2.15 (a)(b). This kind of morphological change is known to improve the electrical conductivity of PEDOT: PSS electrodes. Phase separation between the hydrophobic PEDOT domains and the hydrophilic PSS chains is caused by PEO, which helps to create a more continuous and well-connected network of PEDOT fibres. This intertwined fibrous form considerably improves the electrode's electrical charge transfer. Furthermore, predicted to rise dramatically from the combined action of PEO is the ionic conductivity inside the PEDOT: PSS layer. The observed improvements in the electrochemical characteristics of the composite electrodes (Rohtlaid et al., 2019) are possibly due to the resulting microstructure increasing the accessibility of ionic species to PEDOT domains. This data emphasizes how well-suited PEDOT: PSS and PEO polymers are together in producing composite electrodes with excellent performance.

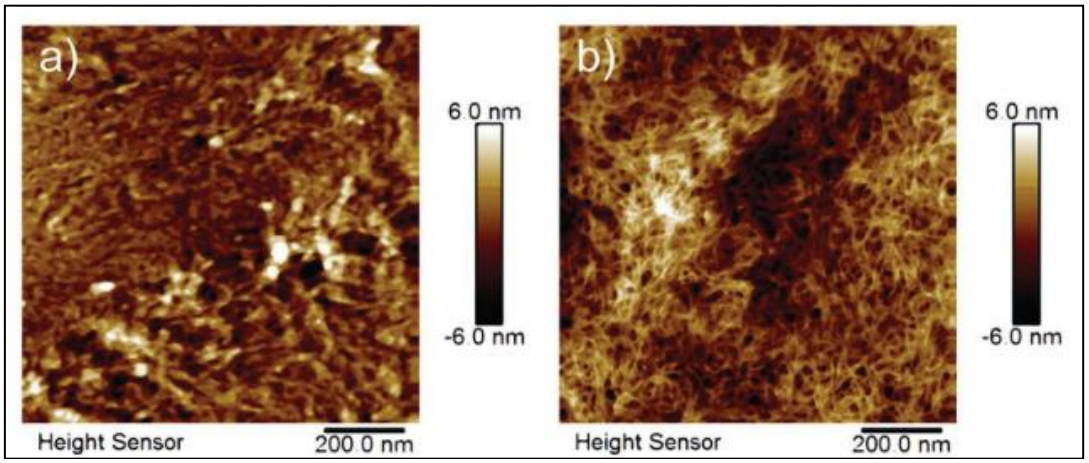

Figure 2. 15 AFM Images Of PEDOT: PSS Films: a) Pristine PEDOT: PSS; b) PEDOT: PSS/PEO.

2.11 Overoxidation of Conducting Polymer (CP)

Overoxidation commonly refers to exposing a substrate to a higher level of oxidation than was first expected or intended as well as it is the removal of electrons from a substrate (Holze, 2022). Cyclic voltammetry (CV) was widely used to study the

electrochemical overoxidation of the conducting polymer (Yongfang, 2000). 3 electrode system of cyclic voltammetry is used to conduct the electrochemical overoxidation treatment of the membrane separator. This 3-electrode system consists of a counter, working, and reference electrode. Increasing the electrode potential beyond a specific limit causes overoxidation. This value corresponds to the polymer's onset or oxidation peak potential. At this point, electrons are easily pulled from the conjugated backbone, exceeding the required doping level and causing unwanted reactions.

Irreversible molecular breakdown results from overoxidation of conductive polymers such as polypyrrole (PPy), polyaniline (PANI), and poly(3,4-ethylenedioxythiophene) (PEDOT), subjected to electrode potentials above a critical limit or strong chemical oxidants in solid polymer electrolytes (Holze, 2022). According to Holze, (2022) and Beck et al., (1993). This process breaks the conjugated backbone and produces carbonyl or carboxyl groups, hence lowering charge carrier mobility and electronic conductivity. Overoxidation is strongly influenced by the chemical composition of the electrolyte anions; some anions, such as perchlorate, offer better defense against nucleophilic attack than sulfate (Holze, (2022); Lippe et al., 1992). Besides this chemical degradation, morphological modifications such as polymer chain scission, cracking, and delamination compromise the material's mechanical stability and ionic transport capabilities (Holze, 2022) and Schultze et al., 2005).

Controlled overoxidation can be utilized to produce permselective membranes and sensor materials with improved selectivity by adding some functional groups and changing the porosity of the polymer, even though doing so affects conductivity (Witkowski et al., 1992). Limiting the potential window during electrochemical operation, employing radical scavengers, optimising dopant chemistry, and utilizing substituted monomers are all examples of techniques to reduce overoxidation (Debiemme-Chouvy et al., 2008). To improve the stability and performance of electrolytes based on conducting polymers in contemporary electrochemical devices, one must have thorough knowledge of overoxidation pathways and their effects (Holze, 2022).

Overoxidation, which exceeds the optimum doping level, might have detrimental consequences. The polymer's conductivity may decrease due to chain scission, the formation of insulating carbonyl groups, or the disruption of the π-conjugated system. Furthermore, the mechanical properties may be degraded, and undesirable byproducts may be produced (Holze, 2022). The structural differences

between conducting polymers contribute to varying susceptibilities to overoxidation. Polymers with longer conjugation durations often have lower onset potentials, making them more prone to overoxidation. For example, polythiophene (PTh) films can undergo overoxidation at potentials as low as +0.8 V versus Ag/AgCl, whereas polypyrrole (PPy) exhibits greater resistance, enduring higher potentials (>1.0 V).

Overoxidation can increase the ionic conductivity of the CP, whereas it can help the movement of the Li-ion. (Leš et al., 2020) had reported that the ion-selective properties of overoxidized CP produce unique 3D materials with greater ionic conductivity than solid polymer electrolytes (SPEs). Furthermore, these materials exhibit separator or selective ion-exchange membrane capabilities with high stability, supported by simple production techniques.

2.12 Properties or Characteristics of Conducting Polymer (CP)

2.12.1 X-Ray Diffraction (XRD)

X-ray diffraction (XRD) is a remarkable method that provides useful insights into both elemental and phase analysis. XRD is useful for stress measurements and texture analysis in addition to identifying chemical composition. It's important to remember that XRD analysis requires materials to have a crystalline structure; nonetheless, the method can reveal the degree of crystallinity in polymers.

While XRD was previously employed to analyse bulk materials, the development of new optical techniques has broadened its usefulness to thin film research. As previously stated, the essential concept driving XRD is Bragg's law of diffraction. An XRD experiment often produces a valuable dataset that provides a full insight of the crystalline nature of the substance under investigation (Nasrazadani, 2016).

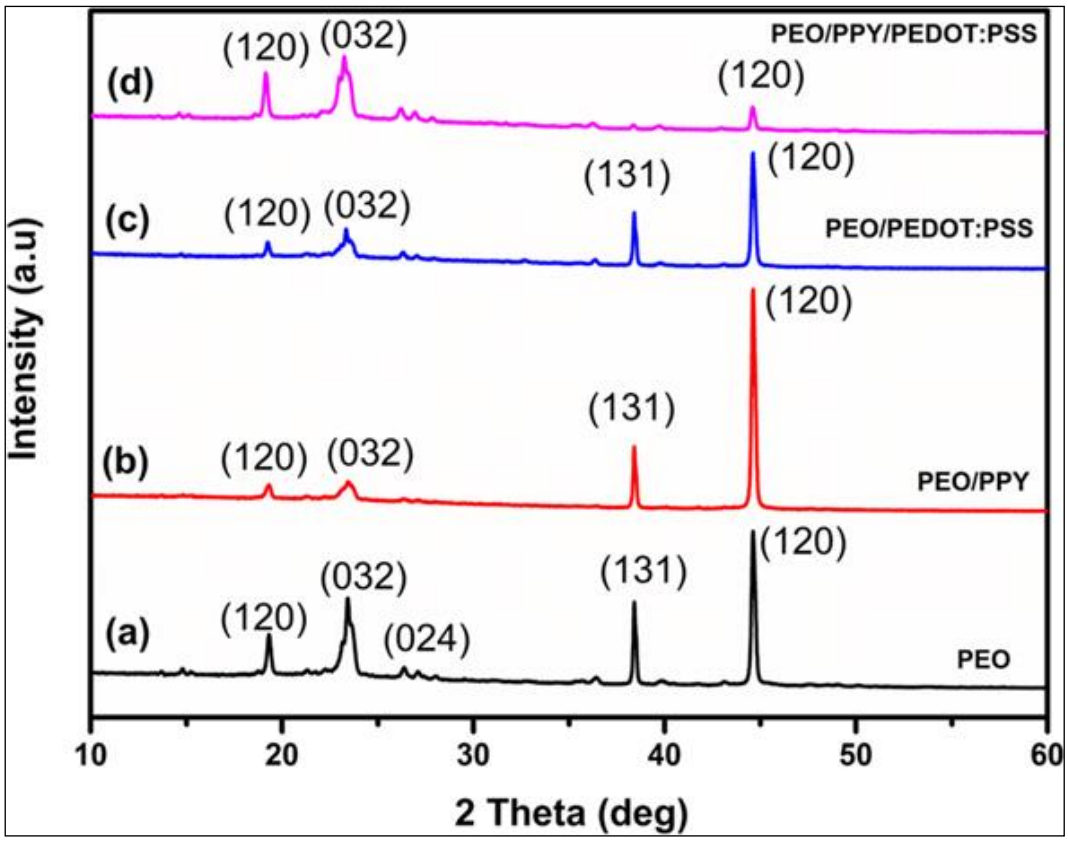

Figure 2. 16 Example Of XRD Spectra a) PEO, b) PEO/ PPy, c) PEO/ PEDOT: PSS, And d) PEO/ PPy/ PEDOT: PSS (Balaji et al., 2022).

The crystalline properties of the PEO, PEO/ PPy, PEO/ PEDOT: PSS and PEO/ PPy/ PEDOT: PSS are demonstrated using X-ray diffraction (XRD) analysis at room temperature, as shown in Figure 2.16. Figure 2.16 (a) shows the XRD pattern of PEO, and the peaks at 2θ= 19.1 ° and 23.2 ° correspond to (120) and (032) planes of PEO polymer, respectively. These two individual peaks represent the PEO polymer's crystalline nature. The (024) and (131) planes of PEO are responsible for the presence of two low-intensity peaks at 2θ = 26.3° and 27°, respectively. The crystalline structure of the polymer is shown by the existence of two peaks in the 33–45° range, which match to the (120) plane. Notably, the PEO material's semi-crystalline structure is implied by the presence of both crystalline and amorphous diffraction peaks. The PEO XRD results are consistent with other studies (Balaji et al., 2022).

As seen in Figure 12.4 (b), the XRD spectrum of the PEO/PPy composite lacks evident peaks characteristic of PPy, yet peaks associated with PEO are still abundant. Particularly, the composite's diffraction peaks for the (024) and (131) crystalline planes of PEO vanish completely, while the intensities of the (120) and (032) planes are dramatically lowered. This decline suggests that the addition of PPy destroys the ordered crystalline structure of PEO, therefore increasing the amorphous phase

concentration as a result of the disorganization of the polymeric chains of PEO. Furthermore, the PEO peaks' intensity falls even farther when PEDOT: PSS is introduced to the PEO/PPy system. The visible amorphous character of both conducting polymers, as indicated by the high disturbance of the crystalline structure of PEO, is supported by the commonly weak diffraction signals in the PEDOT: PSS composite of PEO/PPy (Maiz et al., 2012).

2.12.2 Fourier Transform Infrared Spectroscopy (FTIR)

Fourier transform (FT) may be used to separate the different absorption frequencies from an interferogram, generating a spectrum that is substantially identical to what a dispersive spectrometer would provide. The instrument is commonly known as a Fourier transform infrared spectrometer, or FTIR. The capacity of an FTIR instrument to capture the interferogram in less than a second is its primary benefit. This allows for the compilation of many interferograms for the same sample and storage in a computer's memory. A spectrum with an improved signal-to-noise ratio may be constructed by executing a Fourier transform on the total of these collected interferograms. As a result, an FTIR instrument outperforms a dispersion instrument in terms of speed and sensitivity (Pavia et al., 2013).

FTIR devices with computer interfaces operate in a single-beam mode. To construct a spectrum for a specific molecule, the chemist begins by capturing an interferogram of the "background." This background comprises infrared-active atmospheric gases, specifically carbon dioxide and water vapor (with oxygen and nitrogen being inactive in the infrared range). The obtained interferogram then undergoes a fourier transform, producing the spectrum corresponding to the background (Pavia et al., 2013).

Afterwards, the chemist puts the substance (sample) into the beam, resulting in the acquisition of a spectrum coming from the interferogram's Fourier transform. This spectrum includes absorption bands from the chemical as well as the background. The computer programme performs the smooth removal of the background spectrum from the sample spectrum, providing the spectrum particular to the molecule under investigation. Notably, the subtracted spectrum closely resembles the result of a normal double-beam dispersive instrument (Pavia et al., 2013).

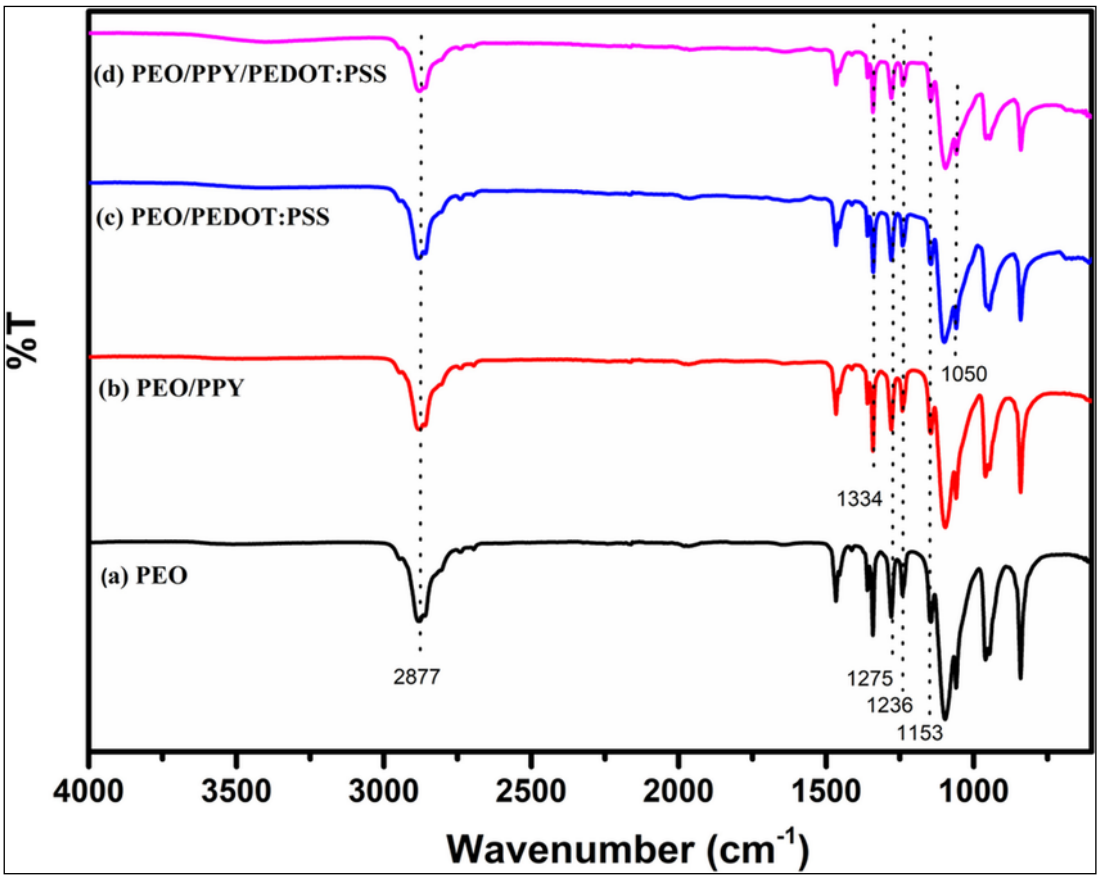

Figure 2. 17 Example of The FTIR Spectrum of a) PEO, b) PEO/PPY, c) PEO/ PEDOT: PSS And d) PEO/PPY/ PEDOT: PSS (Balaji et al., 2022).

For example, the FTIR spectra depicted in Figure 2.17 exhibit the compositions of PEO, PEO/PPy, PEO/PEDOT: PSS, and PEO/PPy/PEDOT: PSS. In Figure 2.17 (a), the FTIR spectra of PEO display peaks at 2877 cm−1, 1275 cm−1, 1236 cm−1, and 1156 cm−1, corresponding to symmetric CH2-stretching, asymmetric CH2-twisting, symmetric CH2-twisting, and C–O–C asymmetric stretching, respectively. Moving to Figure 2.17 (b), the FTIR analysis of PEO/PPy reveals the presence of characteristic PEO peaks along with a new band appearing at 1200–1050 cm−1, indicative of –C–O and –C–N stretching vibrations, confirming the formation of PPy conducting polymer. Figure 2.17 (c) demonstrates the FTIR spectra of PEO/PEDOT: PSS, where the characteristic PEO peaks are observable alongside new bands at 1050 cm−1, attributed to –SO3H bonding with PEDOT: PSS. Finally, in Figure 2.17 (d), the FTIR spectra of PEO/PPy/PEDOT: PSS display all characteristic bands of PEO, PEO/PPy, and PEO/PEDOT: PSS polymers, affirming the formation of these polymers and the strong interpolymer bonding crucial for their application in supercapacitors (Balaji et al., 2022).

2.12.3 Field Emission Scanning Electron Microscopy (FESEM)

Field Emission Scanning Electron Microscopy (FESEM) is an advanced microscopy technique that provides detailed topographical and elemental information at various magnifications, ranging from 10x until 300,000x. It is nearly unlimited depth of field ensures that features at different heights within a specimen are simultaneously in focus, offering a comprehensive view of the sample. FESEM also significantly improves spatial resolution, allowing researchers to discern finer details within a sample. This heightened resolution, often three to six times better than traditional SEM, is crucial for studying nanoscale structures.

In contrast to conventional scanning electron microscopy (SEM), FESEM generates sharper images with minimized electrostatic distortions. This improvement is attributed to the employment of a field emission electron gun, emitting electrons from a sharply pointed emitter. This high-brightness electron source elevates the spatial resolution of FESEM images significantly, reaching levels as fine as 1 1/2 nanometres

In summary, FESEM is a powerful tool in the field of microscopy, offering improved magnification, depth of field, and spatial resolution. Its ability to provide detailed topographical and elemental information makes it invaluable for a wide range of scientific and industrial applications, from materials science to biological research.

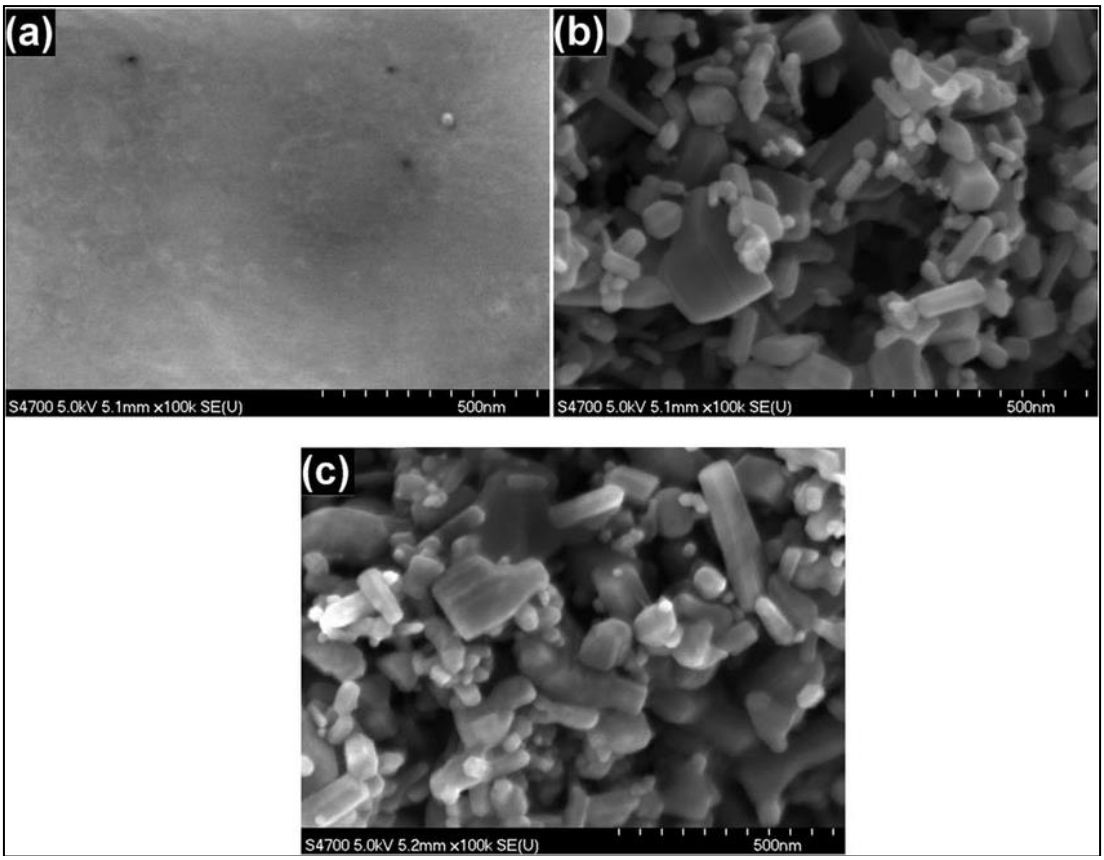

Figure 2. 18 Example Illustration Of a) PEDOT: PSS, b) ZnO and c) PEDOT: PSS/ ZnO (H. Wang et al., 2015).

Figure 2.18 illustrates the surface morphologies of PEDOT: PSS, ZnO, and their composite. In Figure 2.18 (a), a flat and smooth surface morphology is evident for PEDOT: PSS, while ZnO nanoparticles exhibit a combination of sphere-like and rod-like morphologies with diameters ranging from 50 to 100–200 nm. In the ZnO/PEDOT: PSS composite, as anticipated, ZnO nanoparticles are dispersed onto the surface of PEDOT: PSS, facilitating contact between them, a crucial aspect for electron transfer between ZnO and conductive PEDOT: PSS in DSSCs. Additionally, ZnO nanoparticles are expected to serve as active sites for the catalytic reduction of I_{3-} in the electrolyte (H. Wang et al., 2015).

2.12.4 Electrochemical Impedance Spectroscopy (EIS)

Electrochemical impedance spectroscopy (EIS) is a main technique commonly used to examine the mobility of ions, charge transfer at interfaces, and the overall electrochemical properties of solid polymer electrolytes (SPEs) found in energy storage

devices. By using a little alternating current (AC) disruption across several frequencies, EIS measures the system's impedance. In solid polymer electrolyte (SPE) systems, such as those using poly (ethylene oxide) (PEO), the electrochemical impedance spectroscopy (EIS) spectra normally show a mix of bulk resistance, interfacial charge transfer resistance, and ion diffusion resistance. This process allows resistive and capacitive components related to different physical events occurring within the solid polymer electrolyte (SPE) and at the electrode's surface to be identified and measured. Often shown in Nyquist plots as semicircles and straight Warburg tails. This makes it possible to fully understand how ions move throughout the polymer structure as well as how quickly charges are transferred between the electrode and electrolyte interfaces (Isaac et al., 2022). EIS is primarily used to respond to and measure the response of an electrochemical system to an applied voltage. The sample was clipped with two stainless steel disc electrodes having a diameter of 1 cm, (figure 2.19). EIS operates by applying little cyclical or time-varying voltage across the sample and measuring the resultant current through the sample. For each operating frequency, the impedance was measured. The conductivity value was measured after plotting the Nyquist plot (Che Roslan, 2020).

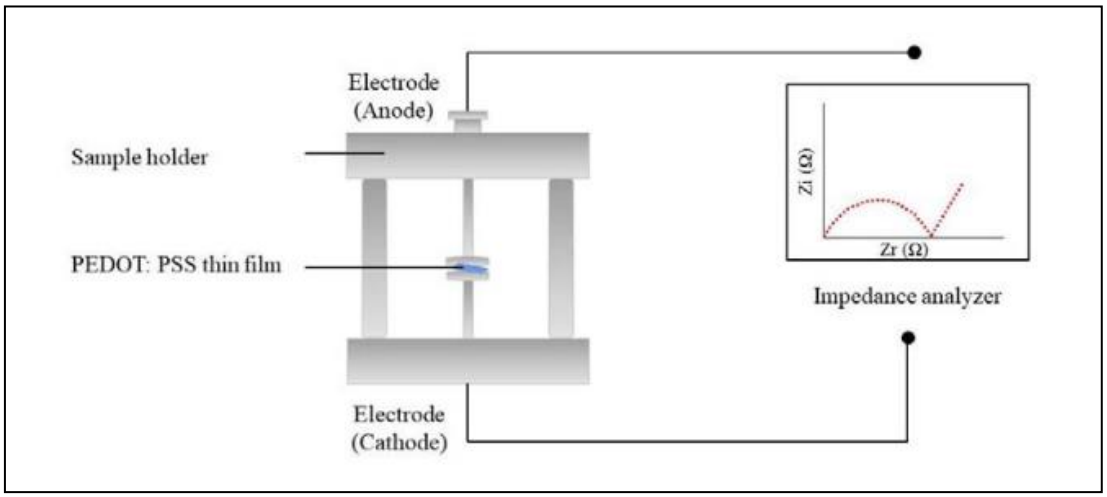

Figure 2. 19 Schematic Representation of The EIS Measurement System Used To Analyze The Impedance Response of The Thin-Film Solid Polymer Electrolyte (Asri et al., 2022).

Previous study indicated PEDOT: PSS had an influence on the ionic conductivity of chitosan-based SPEs (Eren, 2018). The SPE had an ionic conductivity of 4.2×10^{-4} S/cm with PEDOT: PSS, but only 3.40×10^{-4} S/cm without it. The useful electrostatic interactions between chitosan and PEDOT: PSS helped with ion transport, which led to a decrease in bulk resistance (Rb) which is shown in figure 2.120. For

optimum efficiency, electrochromic devices (ECDs) typically need conductivities exceeding 10^{-4} S/cm; hence, the observed conductivity values satisfy their requirements. The made ECD had a faster switching speed because it conducted electricity better. It took 0.29 seconds to change colour and 3 seconds to go back to normal. With conductivities ranging from 10^{-5} to 10^{-4} S/cm, these findings were consistent with those of other polysaccharide-based electrolytes described in the literature including pectin and erbium triflate-doped chitosan systems. The research makes clear that chitosan SPEs modified with PEDOT: PSS could be good choices for use in electrochromic and other optoelectronic gear.

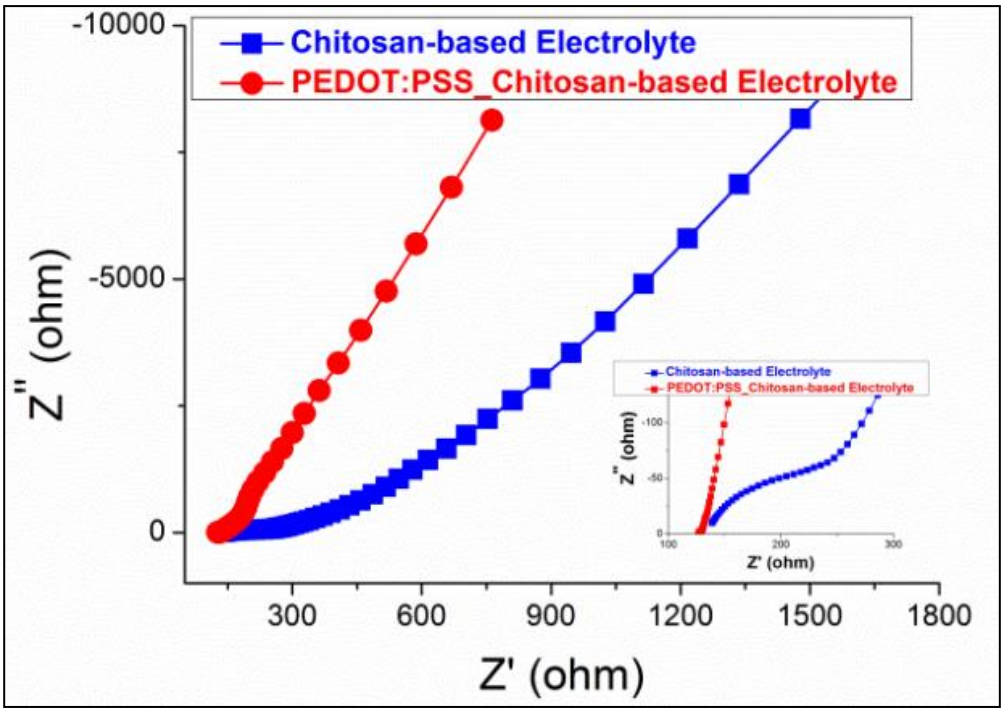

Figure 2. 20 Electrochemical Impedance Spectroscopy (EIS) Nyquist Plots Comparing Ionic Conductivity of Chitosan-LiTRIF-PC Electrolytes With And Without PEDOT:PSS (Eren, 2018).

2.12.5 Transference Number (TN)

One of the primary limitations on the rapid charging and discharging of lithium and lithium-ion batteries is the formation of a salt concentration gradient within the cell when in operation (Mindemark et al., 2018) (Choo et al., 2020). This is because the reason that the anion flux through migration must be offset by diffusion flux at steady state. Consequently, it is highly desirable for the electrolyte material to possess a high

cation transference number, meaning a higher proportion of migrating cations, in order to restrict concentration gradients. The cation transference number is thus a critical parameter in designing superior electrolyte materials. But conventional liquid electrolytes typically possess relatively low cation transference numbers, and the issue is worsened in solid-state polymer electrolytes, particularly those containing polyether systems (Shao et al., 2022).

The transference number is defined as the ratio of the electric current derived from the cation to the total electric current. It is thought that the permissible values of transport numbers solely fall within the range of 0 to 1, although there is debate about the potential for negative values to be possible and have physical significance. A value close to 1 indicates that the ion-conducting performance in the polymer electrolyte is primarily governed by the cation. A higher transference number can mitigate concentration polarization during charge–discharge cycles, leading to increased power density. Achieving a transference number close to 1 for lithium ions is highly desirable in an electrolyte system. However, many current electrolyte systems, whether liquid or polymeric, have transference numbers below 0.5 (Ye et al., 2010).

The Hittorf method is definitively the most direct and accurate way of determining the ion transference number; it consists of a direct chemical analysis of differing sections of the electrolyte after passing through a defined amount of charge. The Hittorf method is a straightforward way to determine the fraction of current carried by specific ionic species by measuring the differences of ion transports in multiple samples. Both the Hittorf method and the electrolyte may be very exact but the method demands a lot of labour and technical expertise, especially for those electrolytes that can be readily distracted by outside influences such as water vapor (humidity) or oxidation (oxygen). Lithium ion conducting electrolytes typically fall into this category of electrolytes as their properties may be easily altered by outside influences. Therefore, the Hittorf method is not easily applicable for routine examination of a varying number of lithium ion conducting systems (Xu, 2022).

Apart from the pulsed-field gradient nuclear magnetic resonance (pfg-NMR), the Bruce-Vincent method is one of the most popular methods for the measurement of the lithium-ion transference number. The Bruce-Vincent method is an electrochemical technique method that taps into alternating current (AC) impedance spectroscopy and direct current (DC) polarization. It is also the most used technique for measuring electrolyte transport properties and accounts for almost 50% of the recorded Li^+

transference values. The method comprised the construction of an electrochemical cell that had symmetric electrodes, usually lithium metal (Li^0), ensuring at least one ionic species, such as Li^+, faced no barrier to the electrode. With a constant voltage DC polarization was applied across the cell and monitored current against time until a steady state value was established. Initially, the total current (i_0) is the result of the migration of cations and anions. Under steady-state conditions, the current where i_{ss} is set, and the electrodes block anions, then the current will be dominated by cation migration. Thus, the cation transference number can be determined using the current readings and resistances (Xu, 2022).

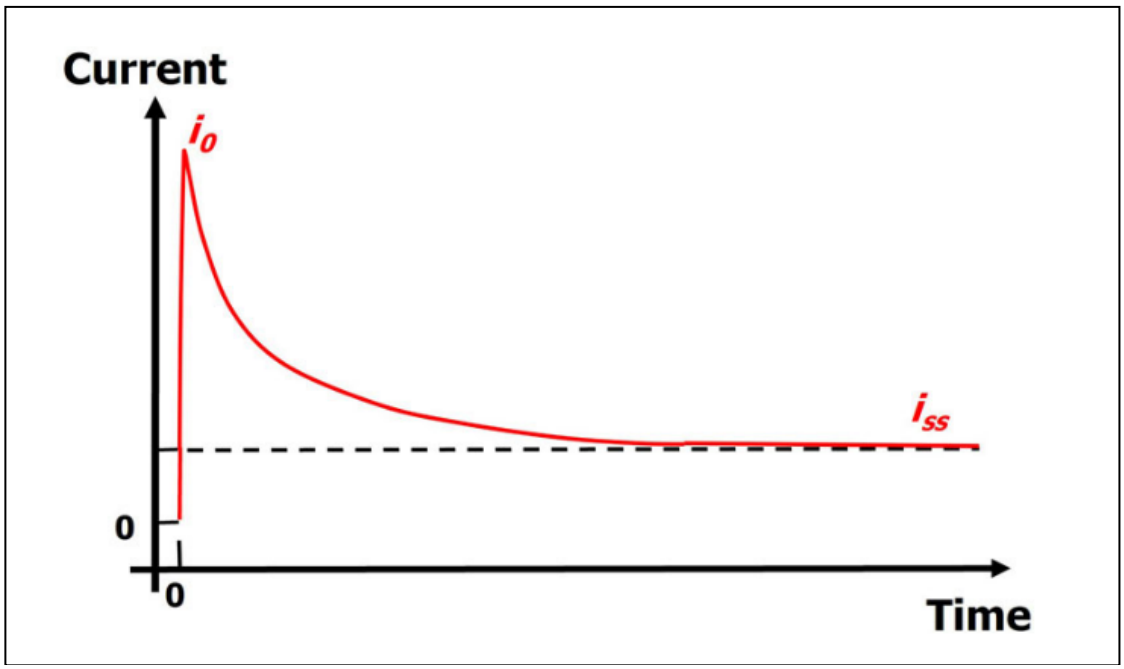

Figure 2. 21 Li^+ Transference Number (t_+) Determination by Bruce-Vincent Method (Xu, 2022).

CHAPTER 3
RESEARCH METHODOLOGY

3.1 Materials

Polyethylene oxide (PEO) with average viscosity molecular weight Mv~ 400,000 (Sigma Aldrich, product 372773) and EDOT monomer with molecular weight Mw~ 142.18 (Sigma Aldrich, product 483028) and PSS solution with an average Mw ~70,000 were bought from Sigma-Aldrich, product 243051. Deionized (DI) water will be used as solvent to dissolve the mixture. EDOT: PSS is polymerized by adding the ammonium persulfate (APS) (ACS reagent, ≥98.0%, Mw~ 228.20) into the solution was also bought from Sigma- Aldrich. Then, PEO solution will be used at different concentration which are (0,3,5,7,9) wt% from adding dimethylformamide (DMF) solvent (anhydrous, 99.8%) which was also supplied from Sigma- Aldrich. After the mixing, PVDF powder with Mw~ 534,000 from Sigma- Aldrich, 182702, was added directly added into the PEO solution. Bis (trifluoromethane) sulfonimide lithium (LiTFSi) with Mw~ 287.09 from Sigma- Aldrich was also used to help improving the movement of lithium ion.

3.2 Sample Preparation

3.2.1 Flow of Synthesis Works

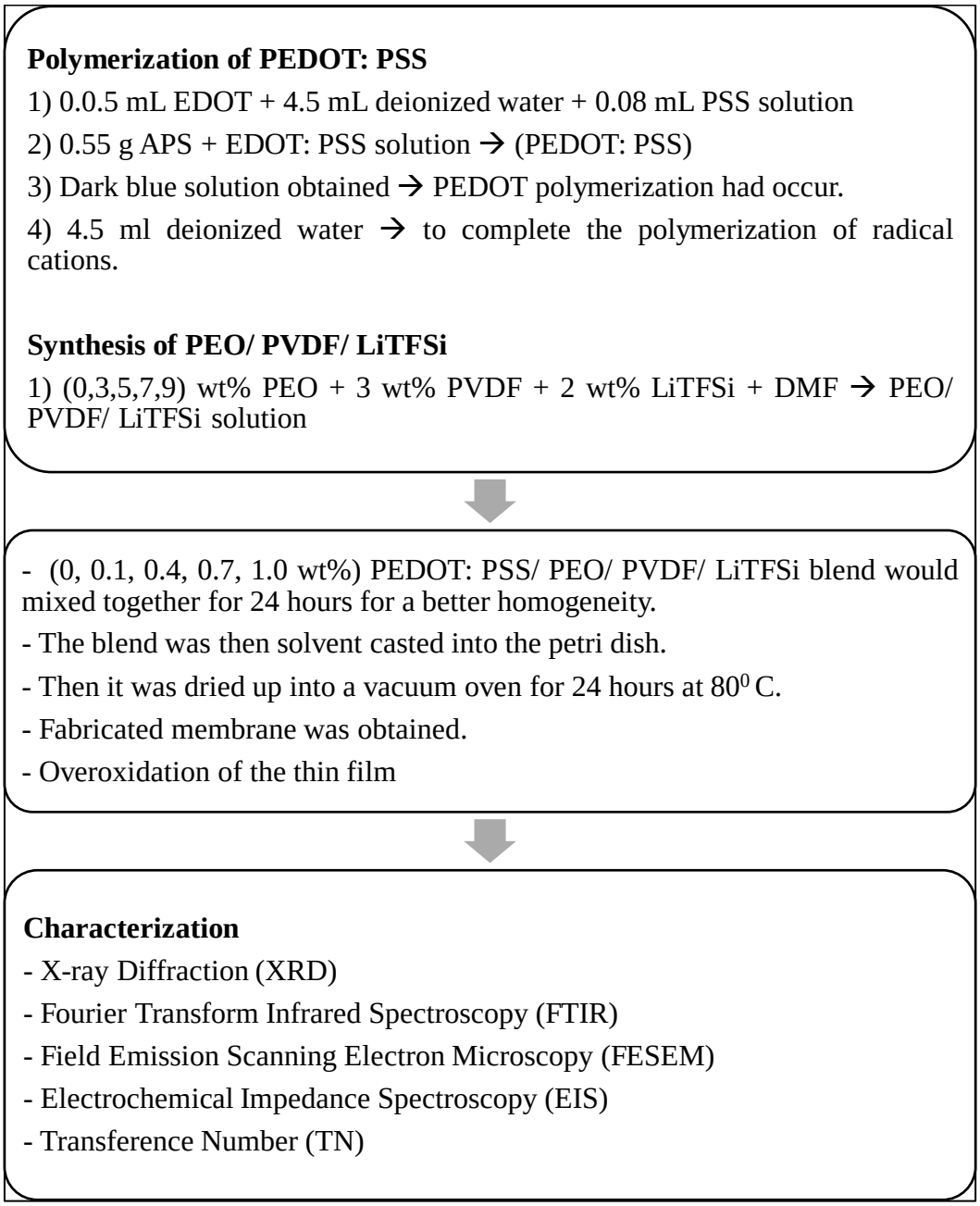

Figure 3. 1 The Overall Synthesis Workflow Was Illustrated

3.2.2 EDOT: PSS Polymerization

0. 05 mL of hydrophobic EDOT was added into 4.5 mL of deionized water. Then, 0.08 mL of hydrophilic PSS was added into the solution. The solution was left

stirring for an hour at room temperature to obtain EDOT: PSS. After an hour, 0.55g of ammonium persulfate (APS) acting as an oxidizing agent was added into the solution. APS was added to initiate the polymerization of EDOT. After 24 hours of stirring, a dark blue solution was obtained, which indicated that the polymerization of PEDOT had occurred. Then, 4.5 mL of deionized water was gradually added to the PEDOT: PSS solution over 30 minutes and left under continuous stirring. The process facilitates the completion of oxidative polymerization because it allows sufficient time for any residual radical cations of the EDOT monomers to fully react, hence providing the possibility for the development of an electrically conductive and homogenous PEDOT: PSS complex. As a result, the final dispersion has improved conjugation polymer chain interactions, which are directly related to improvements in membrane formation.

The production of PEDOT: PSS typically entailed chemically polymerizing 3,4-ethylenedioxythiophene (EDOT) utilizing an oxidizing agent and a polymeric acid like poly (styrene sulfonic acid) (PSS). The synthesis mechanism involved oxidizing EDOT monomers to generate a radical cation, followed by the polymerization process to form PEDOT chains. PSS functioned as both a dopant and stabilizer for the PEDOT chains, resulting in a blend that exhibited conductivity. The synthesized PEDOT: PSS found diverse applications, including use in organic photovoltaics, electrochromic displays, and sensors.

3.2.3 Synthesis of PEO/ PVDF/ LiTFSI Solution

(0, 3, 5, 7, and 9) wt% PEO, 3 wt% PVDF, and 2 wt% LiTFSI were weighed and dissolved in DMF solvent, as shown in Table 3.1. The mixture was stirred for at least 5 hours to ensure everything dissolved completely and mixed well. The amounts of PVDF and LiTFSI salt came from the method by Gonçalves et al., 2019. The amounts of PEO and DMF were then adjusted to finalize the formulation.

Table 3. 1
Concentration Table Of PEO/ PVDF/ LiTFSI

Solution	PEO (wt%)	PVDF (wt%)	LiTFSi (wt%)	DMF (wt%)
C0	0	3	2	95
C1	3	3	2	92
C2	5	3	2	90
C3	7	3	2	88
C4	9	3	2	86

3.2.4 PEDOT: PSS/ PEO/ PVDF/ LiTFSI Blend

Table 3.2 indicated the formulation of PEDOT: PSS/ PEO/ PVDF/ LiTFSi solution which was to be blended according to the weight ratio that was determined. The blend was then stirred for 24 hours to make it homogenous so that agglomeration would not form.

Table 3. 2
Formulation Of Solution Mixing.

Samples	PEO/ PVDF/ LiTFSi (wt%)	PEDOT: PSS (wt%)
PP0	100	0
PP1	99.9	0.1
PP2	99.6	0.4
PP3	99.3	0.7
PP4	99.0	1.0

3.2.5 Fabricated PEDOT: PSS/PEO/PVDF/LiTFSI Membrane

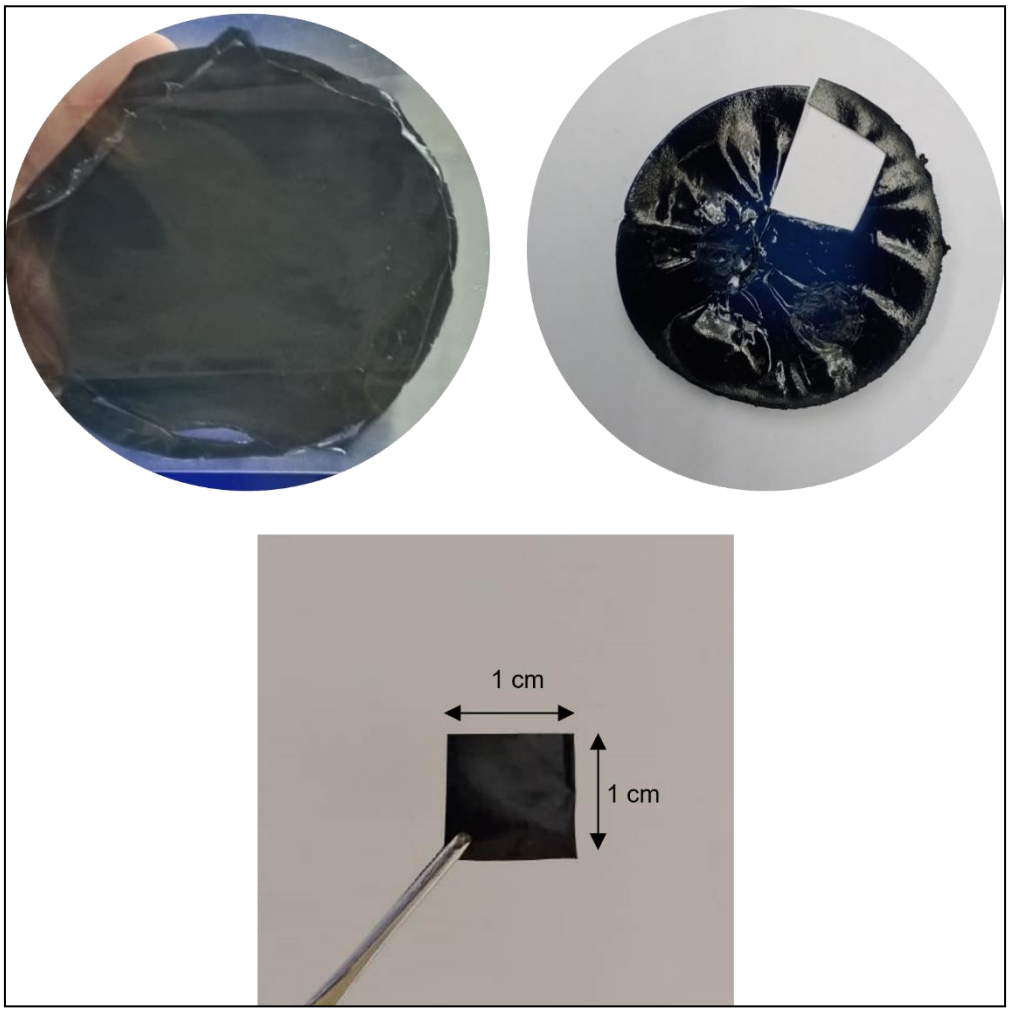

Figure 3. 2 PEDOT: PSS/ PEO Film Membrane.

All mixtures were mixed for 24 hours to allow for proper blending to ensure an even distribution of materials. After the mixing, the resulting solution was solvent-cast into petri dishes for thin films. The thin films were dried in a vacuum oven at 80 °C for 24 hours to rid the membranes of any remaining solvent and allow the films to form in figure 3.2. In addition, the thin films were overoxidized before and after drying to make changes to the polymer and possibly optimize the electrochemical properties of the membrane.

3.2.6 Overoxidation Treatment on PEDOT: PSS/ PEO/ PVDF/ LiTFSI Membrane

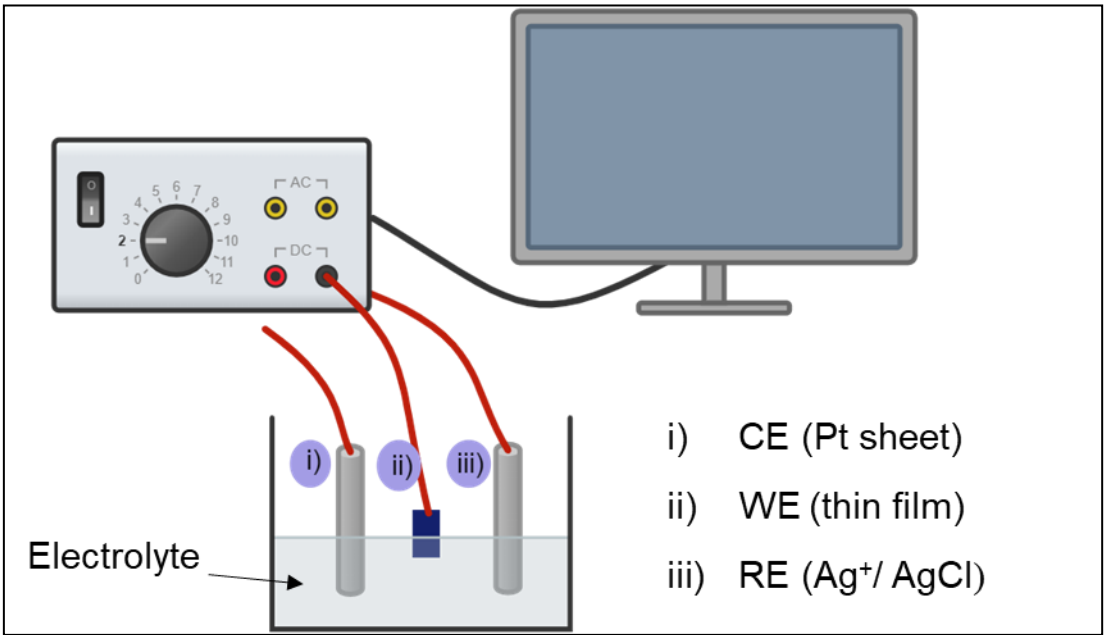

Figure 3. 3 Illustration of Overoxidation Treatment On Membrane

Overoxidation of the thin film was conducted using a Metrohm Autolab potentiostat. The overoxidation treatment was carried out using a cyclic voltammetry procedure. This method used a 3- electrode system based on the illustration on figure 3.3, which consisted of PEDOT: PSS/ PEO/ PVDF/ LiTFSi membrane as the working electrode (WE), a platinum sheet as the counter electrode (CE), and Ag/ AgCl as the reference electrode (RE). The voltage supplied ranged from -0.3V to 1.5V. 1M of sodium sulfate (Na_2SO_4) was used as an electrolyte for this system. The voltage range of -0.3V to 1.5V was chosen because of the known properties of PEDOT: PSS. In the cathodic area below 0V at -0.3V, PEDOT: PSS is in a reduced state and has lower conductivity. This starting point is chosen to make PEDOT: PSS is de-doped before it starts to oxidize. This gives a baseline for later electrochemical treatment. When the voltage goes from 0V to about 1.2V PEDOT: PSS enters a doping phase. In this phase, PEDOT can experience oxidation. If the voltage goes above 1.2V and reaches 1.5V, PEDOT: PSS gets overoxidized (Ma et al., 2012). This results in permanent damage to its backbone. Within this timeframe, the structure of PEDOT: PSS gradually breaks down. This breakdown happens via chain scission and reduction of conjugation length. Ultimately, it leads to a decrease in electronic conductivity. This controlled degradation

is important for changing the membrane. The choice of using 1M Na_2SO_4 as the electrolyte is studied. Na_2SO_4 is neutral and is known to be inert hence, it will not chemically react with the polymer structure. Studies have shown that overoxidation is greatly dependent on the electrolyte composition and pH, whereby higher pH results in lower overoxidation potential. (Tehrani et al., 2007)

3.3 Characterization Methods for The Samples

3.3.1 X- Ray Diffraction (XRD)

Figure 3. 4 PANanalytical X-Pert Pro XRD Instrument

The X-ray diffraction (XRD) profile for the PEDOT: PSS/PEO membrane was acquired using a PANalytical X-Pert Pro XRD instrument based on Figure 3.4, employing Cu-Kα (λ=0.154nm) radiation. The XRD measurements were conducted over a 2θ range spanning from 5° to 90°, which allowed for sufficient angular coverage to capture the low- and high-angle diffraction peaks corresponding to the crystalline phases of the sample. The X-ray emission initiated once the instrument's conditions reached 45 kV and 40 mA. Analysis of the XRD pattern involved the utilization of 'X'pert High Score Plus' software and Origin PRO to delve deeper into the membrane's properties.

3.3.2 Fourier Transform Infrared Spectroscopy (FTIR)

Figure 3. 5 Perkin Elmer 100 Infrared Spectrum Analyzer

FTIR analysis was done to identify the functional groups present, and different FTIR spectra were obtained from PEDOT: PSS, PEO, PVDF and LiTFSi. This was done using a Perkin Elmer 100 infrared spectrum analyser as indicated in Figure 3.5. The spectra were collected from the wave number range of 500 to 4,500 cm−1 with 16 scans at a resolution of 4 cm−1 using a PerkinElmer infrared spectrum analyser.

3.3.3 Field Emission Scanning Electron Microscopy (FESEM)

Figure 3. 6 FESEM Apreo 2 Instrument

Images of the morphology at the surface of the specimens will be captured by using field emission scanning electron microscopy, as pictured in Figure 3.6 which is FESEM Apreo 2. Apreo 2 is distinguished as the sole SEM capable of achieving a 1-nanometer resolution when operating at an analytical working distance of 10 millimetres. The PEDOT: PSS/ PEO thin film will be cut to the necessary dimensions in order to equip them in the material holder of the microscope. The sample is coated with gold (Au) to enhance the conductivity before placing it inside the instrument.

3.3.4 Electrochemical Impedance Spectroscopy (EIS)

Figure 3. 7 HIOKI 3520 LCR Hi- Ester Electrochemical Impedance Spectroscopy (EIS)

The conductivity of the membrane with the different ratio of PEDOT: PSS/ PEO was determined using HIOKI 3520 LCR Hi- ester electrochemical impedance spectroscopy (EIS) shown in Figure 3.7 in a frequency range of 100 Hz to 10,000 Hz at room temperature.

3.3.5 Transference Number (TN)

Transference number (TN) is Wagner's polarisation method with blocking electrodes will be used to determine the ionic transference number. The PEDOT: PSS/ PEO/ PVDF/ LiTFSI thin film will be deposited between two stainless steel disc electrodes, each measuring 1 cm in diameter. A potentiostat will be used in this

approach to deliver a direct current (DC) voltage across the blocking electrodes, thereby among the material. To achieve both a practical amount and a stable sufficient initial polarize effect, the peak polarizing (DC) voltage current generated from the DC supply was required prior to the application of voltage to be high enough to produce a polarized steady-state current within a sufficiently reasonable time (Zurita, 2024). The potentiostat, in turn, will apply a DC voltage of 4 V across the electrodes. 4V was chosen as the highest possible potential that could be used with the PEDOT: PSS/PEO/PVDF/LiTFSI membrane to make sure that the experiments are performed within a practically and electrochemically viable voltage window for applications involving lithium ions. Furthermore, PEDOT: PSS is an electrically conductive material and limiting the applied voltage to 4V will help to eliminate the possibility of creating non-ideal leakage currents and polarisation errors that could otherwise hinder accurate measurements of the transport of ions through the composite membrane (Diederichsen et al., 2017).

In more technical terms based on equation (3.1), the transference number (tion)is defined as the ratio of the electric current carried by lithium ions (i_{Li^+}) to the total electric current (itotal).

$$t_{ion} = \frac{i_{Li^+}}{i_{total}} \tag{3.1}$$

If the transference number is close to 1, it implies that the majority of the electric current is carried by lithium ions. This is desirable for lithium-ion batteries because a higher transference number indicates efficient ion transport, which can lead to benefits such as reduced concentration polarization during charge and discharge cycles and improved power density. Initiatives are undertaken to create and optimise electrolyte materials and compositions in order to get the lowest possible transference number. Low transference numbers, generally less than 0.5, might indicate considerable electronic conduction or contributions from other ions, resulting in poor battery performance. Wagner's polarisation technique, for example, may be used to practically measure the transference number in various electrolyte systems.

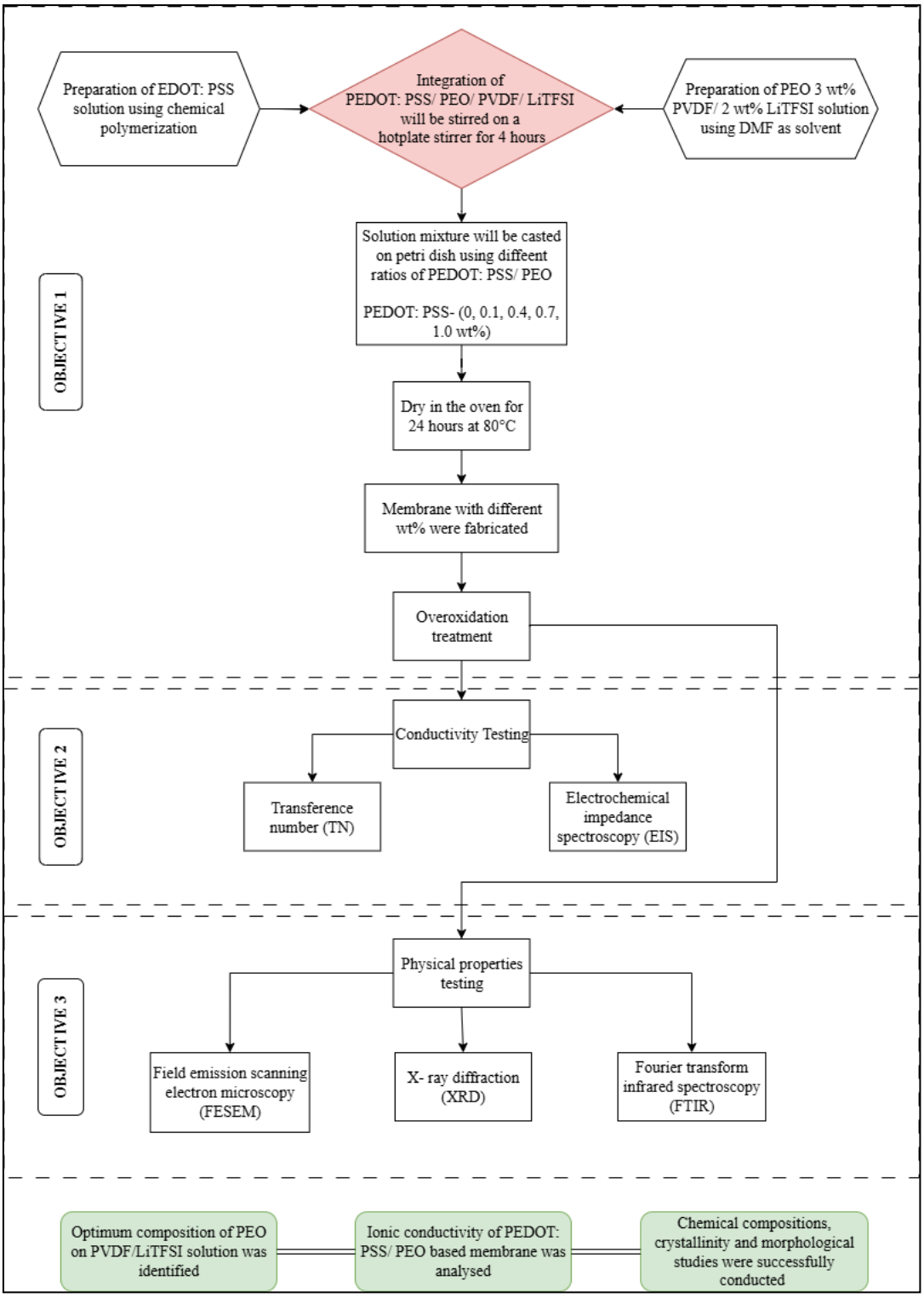

Figure 3. 8 Flowchart Of The Methodology

Various analytical techniques were used in this study to address the three research objectives proposed for the project. The FTIR technique was used for the first research objective, which was to determine the composition of PEO by observing the presence of the C-O-C ether peak that proves Li^+ coordination in the PVDF/LiTFSI

solution. The XRD technique confirmed the crystalline nature of the polymer matrix to prove the presence of adequate amorphous areas for ion migration. For the second research objective of determining the effect of PEDOT: PSS composition on ionic conductivity, EIS was used to observe ionic conductivity at different concentrations of PEDOT: PSS, and TN calculation was used to quantify Li^+ transference number. FESEM, FTIR, and XRD techniques were used in the third research objective that involved the determination of chemical, crystallinity, and morphology characteristics of the system.

CHAPTER 4
RESULTS AND DISCUSSION

4.1 Morphological Characterization of Membrane

Figure 4.1 (a) shows the pure membrane, which contains PEO/PVDF/LiTFSI salt without the addition of PEDOT: PSS. In (a), the polymer film consists of a composite polymer electrolyte made of PEO and PVDF, where the natural immiscibility between the hydrophilic PEO and hydrophobic PVDF results in distinct phase-separated regions. The microstructural segregation is particularly evident under field emission scanning electron microscopy (FESEM) at 5,000× magnification. Typically, PEO-rich domains exhibit smooth, semi-crystalline lamellae, whereas PVDF-rich domains exhibit more porous or fibrillar morphologies. Where LiTFSI salt is not homogeneously dissolved within the matrix, lustrous micron-scale salt aggregates are also observed.

In Figure 4.1 (b), the integration of 0.1 wt% PEDOT: PSS into PEO/PVDF membranes manages the role of a multifunctional nanostructured conductive filler, greatly enhancing the electrochemical and mechanical properties of the systems. The sulfonate ($-SO_3^-$) groups in PSS enhance ionic transport by promoting the dissociation of LiTFSI,salt, whereas the conjugated PEDOT backbone offers electronic conductivity. Moreover, PEDOT: PSS contributes to mechanically linking the otherwise immiscible PEO and PVDF phases. FESEM images reveal a significantly smoother surface than in membranes without PEDOT: PSS, which is indicative of reduced phase separation. The presence of bright micron-sized LiTFSI salt aggregate suggests it does not correctly distribute into the acrylate matrix (Leš et al., 2020). Because of its interactions with the PEO/PVDF matrix, incomplete lithium salt dissolution roughens the film surface, resulting in deficiencies (Li et al., 2020).

Figure 4.1 (c), at higher loading levels, particularly 0.4 wt%, the incorporation of PEDOT: PSS into composite membranes showed a significant morphological alteration. At these elevated amounts, phase integration was promoted, which improved interfacing between the naturally immiscible PEO and PVDF phases, hence diminishing respective phase separation. This compatibilization favoured the dispersion of PEDOT: PSS fibrils in the polymer matrix to create the continuous conductive network; thus, even the distribution of LiTFSI salt improved, whereas with FESEM, the lesser extent

of bright salt aggregate formations indicated the lesser ionic aggregation. The surface of the membranes looked very smooth with PEDOT: PSS filling in the small voids generated after solvent evaporation. The self-assembled nanofibrillar structures enabled the establishment of continuous high-conductivity pathways, while the absence of visible cracks demonstrated an improvement in the mechanical performance of the material.

Figure 4.1 (d), the resultant micrograph demonstrates an extremely smooth surface, because, in addition to filling remaining voids, PEDOT: PSS will also adhesively link the hydrophilic PEO with the hydrophobic PVDF phases. PEO/PVDF with the addition of 0.7 wt% PEDOT: PSS should present nanofibrillar networks supporting the PEDOT: PSS in links of conductive channels, which improves mechanical and electrical conductivity. It is noteworthy that the membrane surface exhibits no cracking, indicating a significant enhancement in mechanical strength with increasing PEDOT: PSS loading. The uniform grayscale contrast observed in the FESEM images reflects a well-mixed composite with homogeneous phase distribution, while the absence of bright, micron-sized spots confirms complete dissolution of LiTFSI salt, resulting in a uniform ionic environment and elimination of salt clustering in localized regions

As illustrated in Figure 4.1(e), the micrograph reveals a densely packed interpenetrating network within the PEO/PVDF matrix. The surface is notably free of visible cracks or voids, indicating the structural integrity. The formation of the IPN under this high load is shown through several unique features of the FESEM image, which include the fibrous, porous, and highly interconnected network structure indicating the formation of a conductive path through PEDOT: PSS in the polymer matrix, absence of a phase boundary confirming the entanglement of PEO and PVDF instead of their separation in terms of phases, evenness of the grayscale showing equal dispersion of all components, and absence of cracks or cavities revealing good mechanical compatibility between the polymer phases (Fong et al., 2017, Rohtlaid et al., 2019). These interconnected networks not only facilitate cohesion between the immiscible polymer phases but also establish efficient pathways for lithium-ion transport, enhanced by the dissociation of LiTFSI salt through interactions with the sulfonate groups in PSS. The relatively uniform grayscale contrast and the absence of large, bright salt clusters indicate a homogenous distribution and low salt crystallinity, both of which are crucial for achieving high ionic conductivity, potentially on the order

of ~10^{-3} S/cm. The most extensive of IPN morphology at 1.0 wt% is associated with FTIR, indicating the highest intensity of PEDOT: PSS and $TFSI^-$ bands, the lowest degree of crystallinity is shown by XRD analysis, and the highest value of conductivity of 6.16×10^{-4} S/cm is obtained by EIS analysis. However, at this optimal loading, TN shows a slight decrease in maximum ionic selectivity with t_+ decreasing from 0.99 at 0.7 wt% to 0.95 at 1.0 wt%, implying that the closely interconnected network of PEDOT rich in structure that ensures conductivity also generates minor electronic channels (Holze, 2022). However, the advantages associated with these structural features reduce at the smallest loading (0 wt%), owing to poor percolation, while the maximum loading (1.0 wt%) offers the optimal SPE efficiency for the investigated material composition.

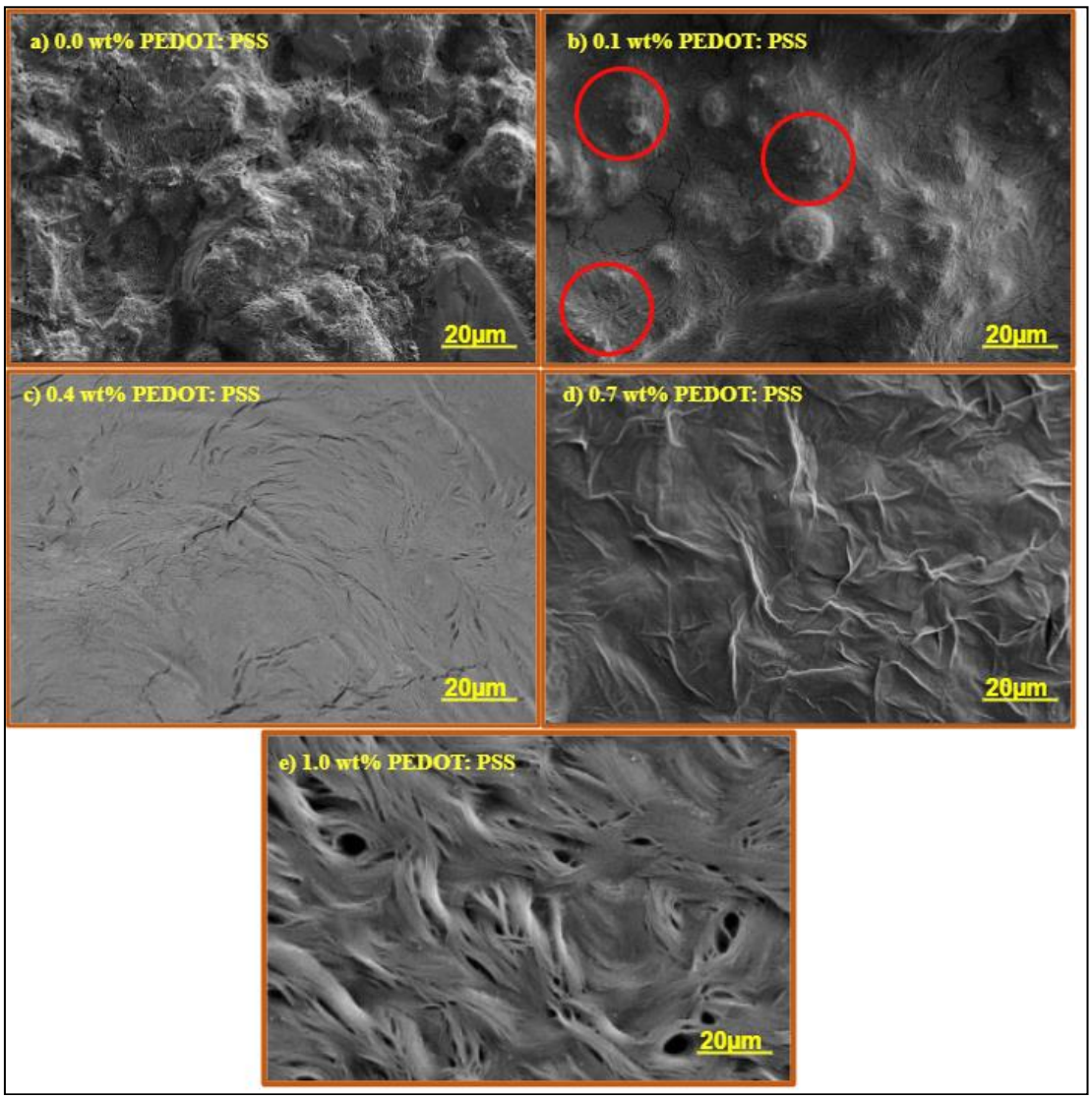

Figure 4. 1 FESEM Micrographs Of Membranes With 0–1.0 Wt% PEDOT:PSS. The Morphology Evolves From Rough, Phase-Segregated Surfaces At 0 Wt% To A Fibrous, Porous, And Interconnected Microstructure At 1.0 Wt%, Indicative Of An Interpenetrating Network (IPN). Comparable IPN

Morphologies Have Been Shown To Improve Charge Transport Efficiency In Conductive Polymer Composites (Fong et al., 2017).

4.2 Structural Confirmation and Elemental Identification of Membrane

FTIR spectroscopy is an instrumental and valuable method to investigate molecular interactions and verify the molecular structure of chemical species in polymer electrolyte systems. In the current study, FTIR spectroscopy was used to analyse the molecular vibrations and associated interaction of the composite electrolyte formulated with polyethylene oxide PEO/PVDF/PEDOT: PSS/LiTFSI. Since the vibrational signatures of each component and their interactions are informative of the collective analytical features of the composite, FTIR analysis was useful in establishing structural information and fundamental functions of the composite electrolyte.

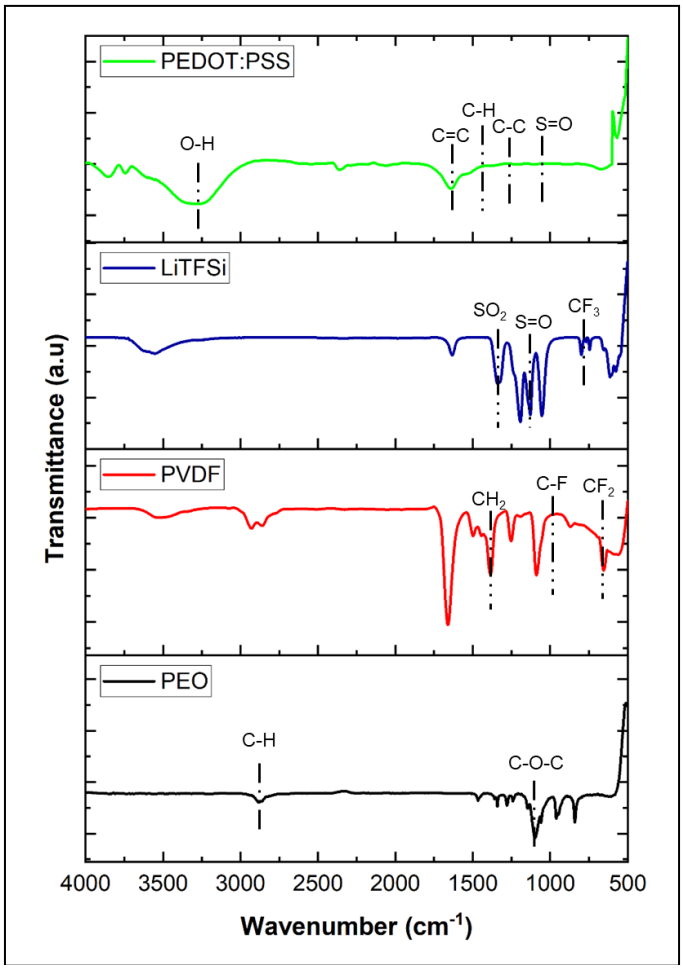

Figure 4. 2 Fourier Transform Infrared (FTIR) Spectra Of Pure PEO, PVDF, LiTFSi, And PEDOT: PSS

The PEDOT: PSS complex is conductive and shows characteristic FTIR transmittance peaks of both PEDOT and PSS. A broad peak near 3290 cm^{-1} is ascribed to O–H stretching vibrations from the sulfonic acid groups in PSS, which present hydrogen bonding sites (Kirchmeyer et al., 2005). The C=C stretching mode due to the thiophene backbone of PEDOT arises near 1641 cm^{-1}, confirming the conjugated nature of the polymer (Crispin et al., 2003). PSS sulfonate groups (SO_3^-) show a strong S=O stretching band at about 1050 cm^{-1} (Ouyang et al., 2004). C–C and C–H vibrations in the PEDOT ring system appear in the range 1200–1400 cm^{-1} (Xia et al., 2012). The detection of LiTFSI is established from the vibrational modes of the anion, which include the asymmetric stretching vibration of the sulfonyl (SO_2) groups observed close to 1335 cm^{-1}, and the symmetric S=O stretching vibration found near 1126 cm^{-1} (Rey et al., 1998). Note that the CF_3 bending vibration recorded near 740 cm^{-1} corresponds to the trifluoromethyl groups in the $TFSI^-$ anion (Edman, 2000). Poly (vinylidene fluoride) (PVDF) shows distinct crystalline peaks such as the CF_2 bending vibration around 840 cm^{-1}, which signifies the β-phase characterized by increased polarity and piezoelectricity, along with the C–F bond stretching near 1070 cm^{-1}, and the CH_2 wagging mode around 1400 cm^{-1} supports its semi-crystallinity. Poly (ethylene oxide) (PEO), a linear polyether, showed the ether backbone with the C–O–C strong stretching band observed at around 1100 cm^{-1} and the C–H stretching vibrations at 2880 cm^{-1}; all of these features provide evidence of the presence of PEO and its structural integrity in the composite.

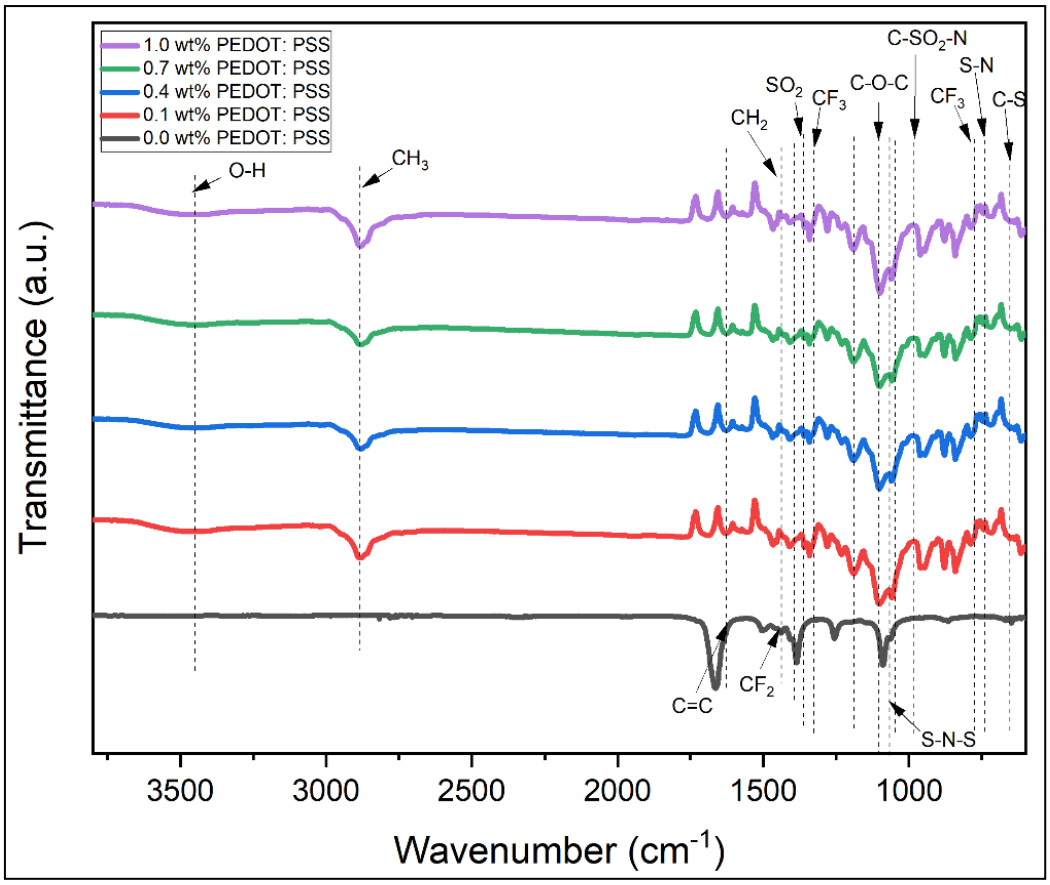

Figure 4. 3 Fourier Transform Infrared (FTIR) Transmittance Spectra Of Pure Poly(3,4-Ethylenedioxythiophene):Poly(Styrenesulfonate) (PEDOT:PSS) And PEO/PVDF/LiTFSI Salt Composite Polymer Electrolytes With Different PEDOT:PSS Loadings (0.1 Wt% To 1.0 Wt%).

Table 4. 1
Characteristic FTIR Absorption Bands of Pure PEO, PVDF, LiTFSI, PEDOT, And PSS, Used To Identify Molecular Interactions Within The Composite Membranes.

Sample	Functional group	Wavenumber (cm^{-1})
PEO	C-O-C	~1100
PVDF	CF_2 and S-N-S	~1180 and ~ 800- 900
$TFSI^-$	SO_2 and CF_3	~ 1350 and ~ 740
PEDOT	C=C thiophene ring	~ 1510
PSS	S=O	~ 1180

In Figure 4.3, the FTIR spectra of the PEO/PVDF/LiTFSI composite membranes with increasing concentration of the conductive polymer PEDOT: PSS (0 - 1.0 wt%) enable one to study structural changes and molecular interactions occurring during formation of the composite membranes. The spectra presented above exhibit distinct absorption bands attributable to the functional groups of each component, providing valuable insights into their contributions to ionic conduction and the structural morphology of the polymer matrix.

In the FTIR spectra of the composite membrane without any PEDOT: PSS (0.0 wt%), typical peaks observed were C=C stretching (~1650 cm--^{1}), CF_2 bending (~1180 cm-^{1}), and S–N–S stretching (~800–900 cm-^{1}), and are indicative of the crystalline regions of the PVDF. Concerning the PEO component, the C–O–C ether stretching vibration is seen around ~1100 cm-^{1}, indicating its semi-crystalline state. LiTFSI functional groups were observed to have associated features such as SO_2 stretching (~1350 cm^{1}) and CF_3 bending (~740 cm^{1}), but they are relatively weak, indicating limited salt dissociation and also low ionic conductivity (~10^{-6} S/cm) in the absence of any significant lithium- ion speculation due to the lack of conductive polymer.

The increase in PEDOT: PSS content in the middle range, 0.1 to 0.7 wt%, leads to significant changes in the FTIR spectra, which include broadening and lowering of the wavenumber of the C-O-C ether bond stretching mode. This implies stronger interaction between Li^+ ions and the ether oxygen in PEO, attributable to an increased amorphous phase content of the polymer, improving the mobility of ions (Ouyang et al., 2004, Xia & Ouyang, 2012). Furthermore, the characteristic peaks of PEDOT (C=C stretch at about 1510 cm^{-1}) and PSS (S=O stretch between 1050 and 1180 cm^{-1}) become more apparent due to their higher content, denoting the formation of ion-conductive networks (Kirchmeyer & Reuter, 2005), Crispin et al., 2003).

At 0.7 wt% PEDOT: PSS, which is the highest possible intermediate weight percent, the membrane displays a strong PSS-Li^+ binding ability, and enhanced $TFSI^-$ signal strength, implying proximity to the ionic conductivity threshold with a conductivity value of 5.91 × 10^{-4} S/cm, without compromising peak ionic selectivity (t_+ = 0.99) (Leš et al., 2020, Yao et al., 2019). Notably, at the highest weight percent of 1.0 wt% PEDOT: PSS, the spectra show the greatest peak broadening effects, while PEDOT: PSS and $TFSI^-$ signals reach their peaks, indicating ideal conductive path formation for Li^+ ions transport, maximum salt dissociation, and uniform elemental distribution (Kim et al., 2020). The formation of the interpenetrating network (IPN) can be attributed to different FTIR properties: the gradual broadening and shift of the C–O–C peak in the range of 1100 cm^{-1} show that the chains of PEO are tightly mixed with PEDOT: PSS and PVDF, leading to the destruction of their initial crystallinity; the appearance of enhanced peaks of the S=O group of PSS in the region of 1050-1180 cm^{-1} implies that the sulfonate groups bind with Li^+ ions and the two polymer phases and act as a compatibilizer; the presence of peaks of $TFSI^-$ with higher intensity demonstrates that an IPN has a polar microenvironment for dissociation of the salt; and the absence

of additional peaks proves that there is no covalent linking, which is critical for the creation of a real IPN with retention of the initial chemical nature of each polymer (Fong et al., 2017). However, at the peak concentration of 1.0 wt% where IPN structure formation is maximal and conductivity is highest (6.16×10^{-4} S/cm), the small decline in ionic selectivity ($t_+ = 0.95$ versus 0.99 at 0.7 wt%) suggests that the strong, interconnected PEDOT network that is associated with high conductive properties also produces small electronic conduction paths (Holze, 2022). This statement is further supported by complementary morphological (FESEM) and electrochemical impedance spectroscopy (EIS) measurements, which show that at a 1.0 wt% concentration, the IPN exhibits the largest network formation and conductivity, but lower ionic selectivity compared to the intermediate concentration of 0.7 wt%, which provides an optimal combination of conductivity and ionic selectivity.

Critically, the enhancement of these favourable effects does not appear to occur to the detriment of the polymer matrix when the maximum level of utilization of 1.0 wt% PEDOT: PSS is reached. The spectral profiles at this concentration are indicative of a compromise whereby maximum conductive pathways exist for Li^+ ion transport, and the amount is also optimal for the beneficial amount of salt dissociation and even dispersal. It is often thought that the disadvantages of needing to be concerned with the excess of PEDOT: PSS aggregation with higher PEDOT: PSS loadings are offset by the 1.0 wt% concentration. In this case, the impacts of PEDOT: PSS concentration offset with membrane homogeneity and mechanical stability, combined with the fact that it appears enhanced ionic conductivity can be achieved without compromising mechanical stability. This finding is under complementary morphological (FESEM) and electrochemical impedance spectroscopy data, which lends evidence for 1.0 wt% PEDOT: PSS to be the maximum loading to maximise Li^+ mobility and electronic percolation in the composite membrane.

4.3 Phase Study of the Membrane

The use of XRD can reveal the crystallographic characteristics of any given substance, making it a powerful technique. Crystalline materials exhibit well-defined diffraction peaks at certain 2θ angles, which are caused by constructive interference from atomic planes (Bragg's Law: $n\lambda=2d \sin \theta$). Due to the absence of long-range order, amorphous materials, however, generate wide humps or halos.

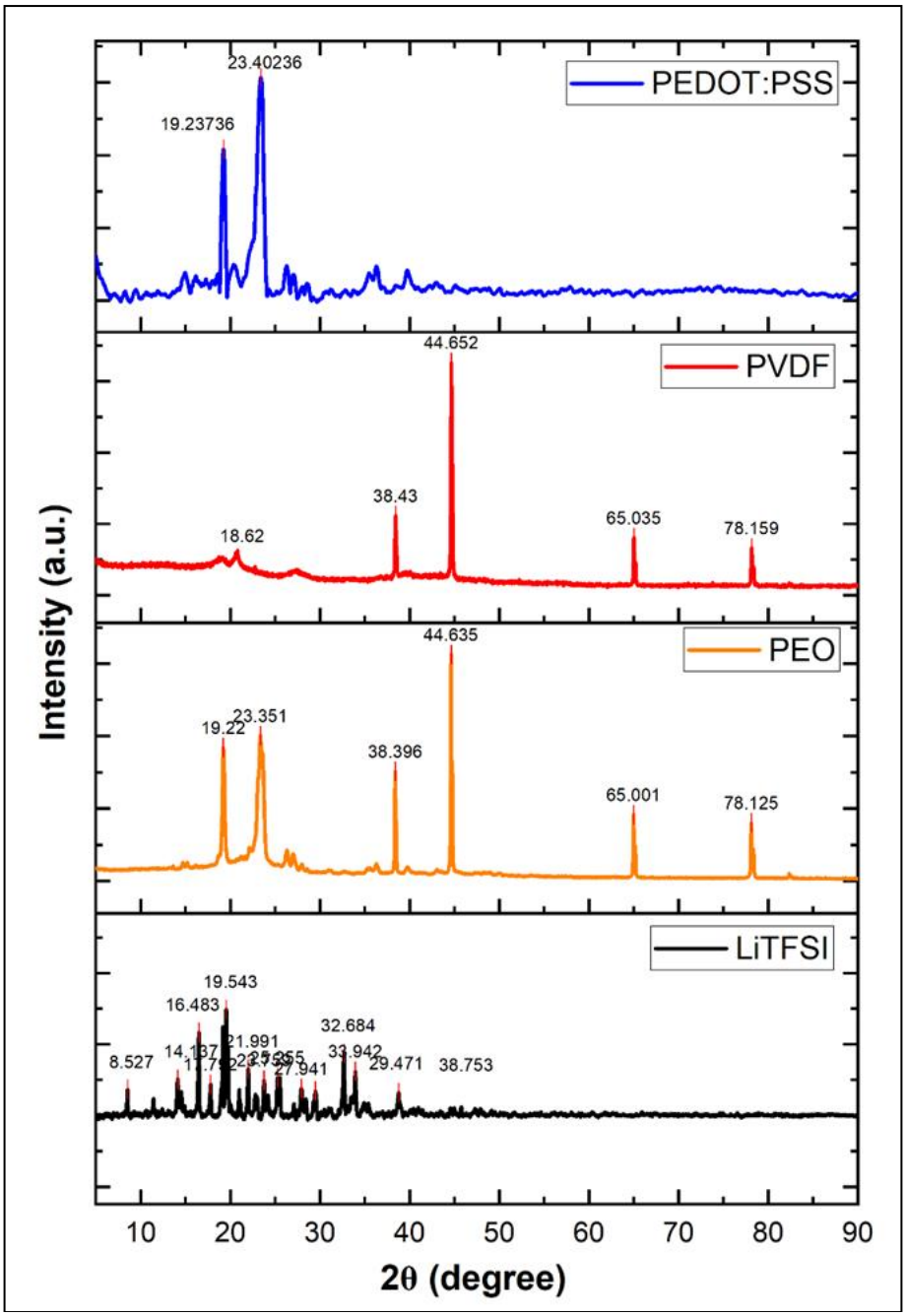

Figure 4. 4 XRD Patterns Of The Pure Components: Lithium Bis(Trifluoromethanesulfonyl)Imide (LiTFSi), Poly(Ethylene Oxide) (PEO), Poly(Vinylidene Fluoride) (PVDF), And Poly(3,4-Ethylenedioxythiophene):Poly(Styrenesulfonate) (PEDOT:PSS).

LiTFSI salt exhibits sharp and intense diffraction peaks in the XRD pattern at 8.57°, 14.13°, 16.48°, 19.54°, 21.99°, 23.75°, 25.59°, 27.94°, 29.47°, 32.68°, 33.94°and 38.75°, affirming that it is a highly crystalline material. These distinct peaks result from the orderly arrangement of LiTFSI ions in the solid state. A crystalline state is usually expected when present in its pure form, although, on the other hand, it is generally considered detrimental in polymer electrolytes since these crystalline domains restrict

salt dissociation and thereby hinder the lithium-ion mobility. Therefore, an effective strategy for developing high-performance electrolyte systems involves reducing the crystallinity of LiTFSI through polymer blending, thereby enhancing ionic conductivity. The XRD pattern of PEO exhibits distinct diffraction peaks at 19.24°, 23.35°, 38.39°, 44.63°, 65.00°, and 78.12°, indicative of its semi-crystalline nature. These reflections correspond to the crystalline lamellae formed by the helical conformation of the PEO polymer chains. Even though there are crystalline areas, the ionic conduction in PEO mainly happens in its amorphous phase, where the movement of polymer chain segments helps ions travel. The XRD pattern of PVDF reveals peaks at 18.62°, 38.43°, and 44.66°. The peak at 18.43° is linked to the α-phase (020), while the prominent peak at 38.43° is attributed to the β-phase (110/200) which the electroactive and polar crystalline form of PVDF. Additionally, the reflection at 44.66° corresponds to the α-phase (021). This pattern suggests that PVDF has a mixed-phase structure, with the β-phase being the most prominent, as shown by the intensity of the 38.43° peak. The β-phase is particularly advantageous in electrochemical systems because of its high polarity and improved dielectric constant, which can boost ion transport and interfacial stability in the composite electrolyte. The diffraction pattern of PEDOT: PSS reveals a at 23.4°, accompanied by a less intense hump around 19.2°.

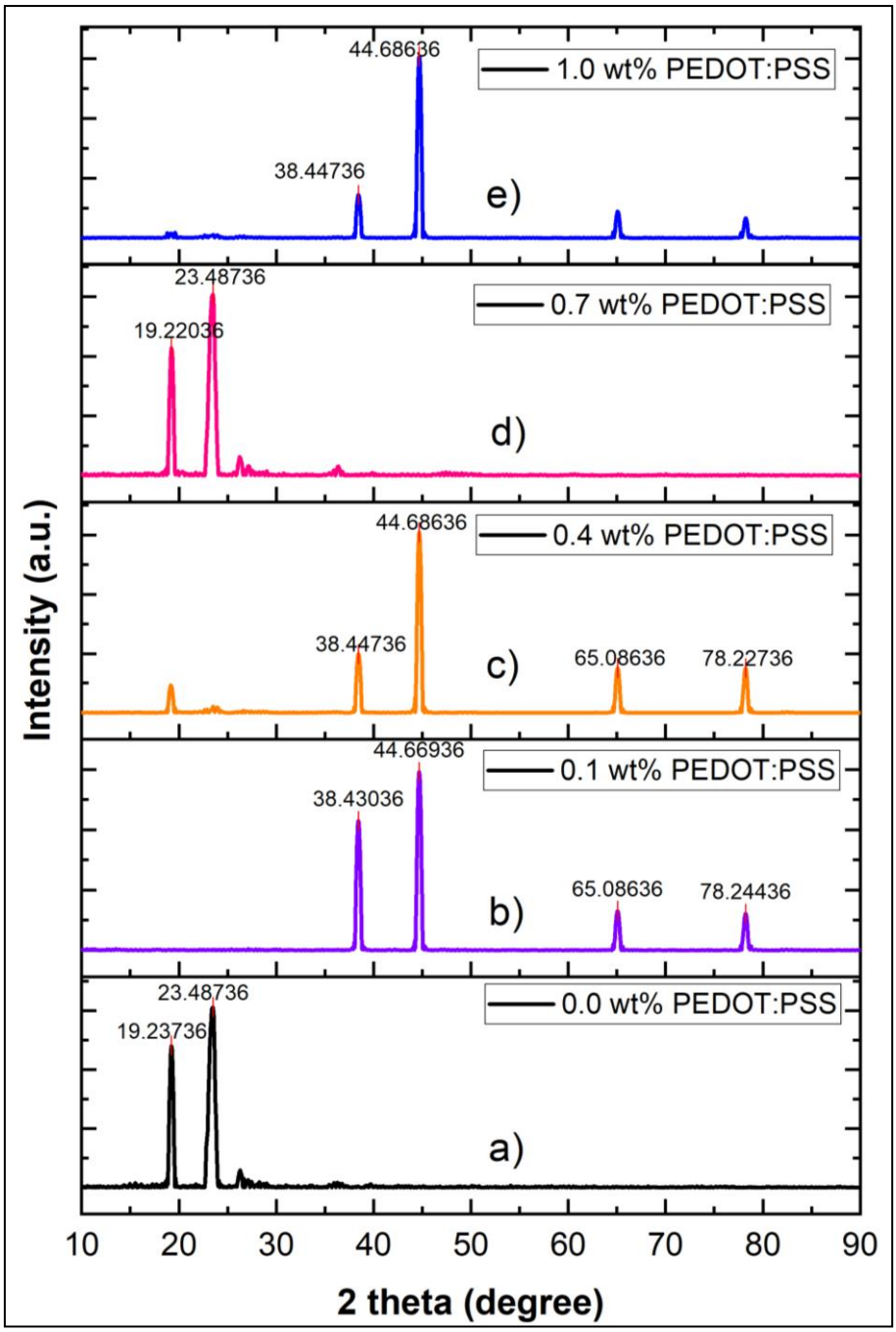

Figure 4. 5 XRD Patterns Of PEO/PVDF/LiTFSi Composite Polymer Electrolytes With Varying Poly(3,4-Ethylenedioxythiophene):Poly(Styrenesulfonate) (Pedot:Pss) Loadings: (A) 0.0 Wt%, (B) 0.1 Wt%, (C) 0.4 Wt%, (D) 0.7 Wt%, And (E) 1.0 Wt%.

The lack of significant broadening or distinct hump features in the XRD patterns following the addition of PEDOT: PSS suggests that the crystalline structure of the PEO/PVDF polymer matrix is largely preserved. This indicates that the inclusion of PEDOT: PSS, at the concentrations investigated, does not lead to considerable disruption or modification of the crystalline domains, thereby maintaining the composite's inherent semi-crystalline nature. Such retention of crystallinity aligns with

existing literature, which states that PEDOT: PSS primarily functions as a well-dispersed filler or conductive matrix without causing detectable lattice distortion or rearrangement of polymer chains as observed through XRD (Morsi et al., 2024) and (Prabakaran et al., 2015). Additionally, the presence of both crystalline and amorphous phases within PEO/PVDF blends is well established, and the stability of the crystalline phase is frequently supported by PVDF and salt components, which can reduce structural disruptions caused by additives (Ruan et al., 2018) (Morsi et al., 2024).

The fact that the XRD patterns of various samples display peaks at identical 2θ positions, even if their intensity or sharpness differs, can be attributed to the consistency in the fundamental crystalline phases and lattice structures of the PEO/PVDF polymer matrix, regardless of the changes in PEDOT: PSS loading. These constant peak positions reflect the inherent crystal planes of PEO and PVDF that do not change regardless of the content of the additive. Changes in peak intensity or width usually represent variations in the degree of crystallinity, crystallite size, or order of polymer chains rather than the crystal structure. Small intensity variations are attributable to changes in the packing density of the polymer chains, small variations in crystallite size, or differences in sample thickness and preferred orientation when measuring. The existence of the PEDOT: PSS additive may affect these properties by altering the surrounding local environment, resulting in small changes in the size or direction of the crystalline domains without forming new crystalline phases or the relocation of existing lattice planes. Thus, the XRD data show that while the addition of PEDOT: PSS affects the degree of crystallinity as reflected in intensity variation, it does not alter the crystal structure or add new phases, as can be seen from the invariance of characteristic peak positions for all samples. This implies that the composite samples contain identical semi-crystalline polymer phases but with quantitative variations in crystallinity.

However, the XRD spectra revealed a unique non-linear correlation exists in where samples (a) 0 wt% and (d) 0.7 wt% form one group that consists of a full range of crystalline peaks including PEO (120) at 19.24°, and PVDF (032)/(112) at 23.49°, whereas samples (b) 0.1 wt%, (c) 0.4 wt%, and (e) 1.0 wt% belong to another group that possesses a reduced number of peaks, particularly at 38.44°, and 44.68° but lacks the PEO peak at 19.24° and high-angle peaks (Khan et al., 2025, (Prabakaran et al., 2015). In the case of sample (a) having the lowest composition of 0 wt%, the whole peak profile should be expected because there is nothing that can hinder the crystalline structure due to the absence of PEDOT: PSS. For sample b at 0.1 wt% and sample c at

0.4 wt%, the presence of a low-intensity peak set indicates that only small amounts of PEDOT: PSS molecules are effective in blocking some crystal planes, including that of PEO (120) plane at 19.24°, while still leaving others discernible (Morsi et al., 2024). For sample d at 0.7 wt%, which represents a middle concentration level that approaches maximum concentration, all peak intensities disappear nearing the PVDF peak, implying that PEDOT: PSS molecules are effectively dispersed within the composite, thus providing enough room for the PEO chains to retain crystallinity along with high ionic conductivity (5.91 x 10^{-4} S/cm) and maximum ionic selectivity ($t_+ = 0.99$) (Holze, 2022). For sample e, at the maximum concentration of 1.0 wt%, again, the appearance of low intensity peaks means that the high concentration of PEDOT:PSS molecules forms a continuous chain leading to a major disruption of crystallinity and loss of 19.24° and other high-angle peaks. However, the latter condition results in the highest conductivity (6.16 x 10^{-4} S/cm) but slightly lower ionic selectivity ($t_+ = 0.95$) (Holze, 2022, Ruzaidi et al., 2021).

XRD spectra for PEO/PVDF/LiTFSI composite with 1.0 wt% PEDOT: PSS shows that the crystalline nature of the polymer matrix remains unaffected. The diffraction peak positions remain stable and there are no broad amorphous humps which suggests that even at this concentration, PEDOT: PSS does not interfere with the organized crystalline domains, and it coexists within the semi-crystalline polymer framework. This behaviour is similar to previous observations in the literature, which demonstrates that PEDOT:PSS acts mainly as a conductive filler which improves charge transport pathways without any substantial changes in the structural attributes (Morsi et al., 2024) and (Prabakaran et al., 2015). Although XRD shows structure stability, PEDOT: PSS may still positively affect the electrochemical performance due to increased ionic conductivity and mechanical flexibility. The mixed ionic/electronic conductivity of PEDOT: PSS and its ability to induce lithium salt dissociation through interactions with ionic groups would help to improve lithium-ion mobility in the amorphous regions and would do so without requiring a large increase in the amorphous phase (Kee et al., 2020) and (Song et al., 2020). These conductive networks are critical for ensuring efficient ion transport within solid polymer electrolytes and mechanical stability.

In addition, at the highest amount of PEDOT:PSS used in this experiment of 1.0 wt%, an appropriate balance was achieved between improved electrical conductivity without compromising the crystal formation, which is crucial. However, if the

concentration of PEDOT: PSS exceeds this point, for example, up to 1.5 wt% or even 2.0 wt%, then increased disruption of crystallinity will affect the integrity of the composite in terms of mechanical properties, as has been found out in previous research (Ahmad Ruzaidi et al., 2021). Alternatively, when the amount of PEDOT: PSS becomes too low, approaching 0 wt%, charge transfer pathways become unable to connect with each other fully, hence forming poor conductive channels leading to the least conductivity. It has been observed in various studies that the addition of a conductive polymer to composites improves electrochemical behaviour by reducing resistance and improving charge transfer without compromising the phase (Prabakaran et al., 2015, Kee et al., 2020). Although the XRD results show a small impact on crystallinity, with the lowest amount of crystallinity achieved at the highest loading (1.0 wt%), further testing needs to be conducted in terms of electrochemistry, especially above 1.0 wt%. Therefore, in the tested concentration range (0-1.0 wt%), 1.0 wt% of PEDOT:PSS has the greatest conductive properties, although further studies are needed to determine whether it represents the highest possible value across all concentrations.

4.4 Electrochemical Impedance Spectroscopy (EIS) Analysis

At 0 wt% of PEDOT: PSS, the unmodified PEO/PVDF/LiTFSI membrane shows the least ionic conductivity value, 4.76×10^{-4} S/cm, as seen in Figures 4.6 and Table 4.1, and this can be attributed to four interlinked reasons. Firstly, in the absence of PEDOT: PSS, no conductive fillers will be present for the formation of new paths through which charges can be conducted whereas PEDOT: PSS, according to Mengistie et al., 2013, forms fibers with three-dimensional structures enhancing conductivity, whereas Namsheer and Rout, (2021) explained that conductive fillers form a percolation network reducing resistance levels significantly hence, its absence forces the membrane to use the low ionic conductivity of the polymer-salt combination only. Secondly, the hydrophilic PEO and hydrophobic PVDF inherently do not mix, and thus there will be phase separation, leading to discontinuous ion channels. According to Zhu et al., (2025), mixing PEO and PVDF directly causes macroscopic phase separation, and no coupling is achieved, whereas Cui et al., (2008) found that the PVDF/PEO blends, without compatibilizers, have significant phase separation, which is directly related to low ionic conductivity. The phase separation effect in this sample is evident from FESEM results shown in Figure 4.1a. This shows a rough surface consisting of phase-separated

domains with clear domain boundaries, which block ion transport (Banitaba and Semnani, 2019). Thirdly, PEO polymer possesses high crystallinity at ambient conditions, since Li^+ ion transport occurs in amorphous zones in which polymer segmental motions occur, therefore higher crystallinity reduces ionic mobility, Krause et al., (2024), mentioned that conduction of ions in solid polymer electrolyte occurs due to the movement of polymer chain segments, which is significantly low in crystalline PEO at temperatures less than 60°C, further reported the conductivity of unmodified PEO-based solid polymer electrolyte to be extremely low with value of only 2.16×10^{-6} S cm^{-1} at 30°C, caused by high crystallinity whereas Xue et al., (2015) reported that conductivity in amorphous zone is described by the Vogel-Tammann-Fulcher (VTF) equation, however it deviates in crystalline zone. Significant crystallinity at 0wt% is further confirmed by XRD results in Figure 4.4a, showing sharp peaks indicating the highest crystallinity. Fourth, PEDOT: PSS not being present in the system, LiTFSI salt does not dissociate fully, thus leading to fewer free Li^+ ions available for conduction which is according to Kim et al., (2020), it is possible to determine the extent of salt dissociation using FTIR by analysing the peaks of $TFSI^-$ anions as well as shifts in the PEO C-O-C peak, hence, since LiTFSI remains undissociated in the presence of low polymer-salt interaction, Zhou et al., (2019) stated that the concentration of free charge carriers depends on the ratio of salt lattice energy to polymer solvation energy, and, according to Leš & Jordan, (2020), free Li^+ ions increase by up to 40% due to PEDOT: PSS presence compared to other systems. All four phenomena mentioned above are interconnected, which is separation into distinct phases with high crystallinity, resulting in the reduction of available volume for ions, and insufficient salt dissociation further lowers the number of available charge carriers within this volume. Finally, the lack of PEDOT: PSS indicates that there is no method available to address any of these constraints (Zhu et al., 2025, Leš & Jordan, (2020). Consequently, the lowest conductivity at 0 wt% indicates the actual baseline efficiency of the unaltered polymer-salt system, used as a reference for assessing enhancements at greater PEDOT: PSS concentrations.

At intermediate amounts of 0.1 wt%, 0.4 wt%, and 0.7 wt% of PEDOT: PSS, the ionic conductivities of the PEO/PVDF/LiTFSI composite membrane are progressively enhanced by 5.13×10^{-4} S/cm, 5.67×10^{-4} S/cm, and 5.91×10^{-4} S/cm shown in Figure 4.6 and Table 4.1, revealing an evident direct correlation between the PEDOT: PSS concentration and conductivity, which changes from a minimum at 0 wt%

to a maximum at 1.0 wt%. Under 0.1 wt%, which is the lowest concentration of PEDOT: PSS at intermediate levels, there is still an increase in the ionic conductivity of the polymer matrix; this is attributed to the creation of PEDOT: PSS fibers, as reported by Mengistie et al., (2013). However, at this concentration level, PEDOT: PSS remains below the percolation point. FESEM in Figure 4.1b, at 0.1 wt%, presents a smoother surface compared to 0 wt%, while at the same time, phase separation remains partially evident, and salt clusters are visible. From the XRD results in Figure 4.4, one can observe the slight reduction in the intensities of crystalline peaks, indicating partial crystal modification and a certain level of PEO disruption, but only to a limited extent. With a higher PEDOT: PSS content, at 0.4 wt%, there appear more and more conductive domains interconnected close to the percolation threshold; according to Namsheer and Rout, (2021), percolation typically occurs between 0.5 wt% and 2.0 wt%. FESEM in Figure 4.1c shows improved morphology, decreased phase separation, and reduced salt cluster formation.

At 1.0 wt% PEDOT: PSS, the highest composition examined in this study, the PEO/PVDF/LiTFSI composite membrane shows the peak ionic conductivity of 6.16×10^{-4} S/cm, as illustrated in Figure 4.6 and Table 4.1. This increased conductivity results from the effective creation of an interpenetrating polymer network (IPN) that mitigates the issues identified at 0 wt%. Initially, incorporating PEDOT: PSS adds a conductive filler that establishes extra charge transport routes (Mengistie et al., 2013). Generally, increased compositions of PEDOT: PSS imply a higher number of conductive paths, hence improving the conductivity of the membrane (Namsheer and Rout, 2021). This is because PEDOT behaves as a conductive polymer (Kim et al., 2014). The increased conductivity within a certain range of compositions is associated with high compositions of PEDOT: PSS which however, according to literature findings, the conductivity may slightly decrease with continued increase beyond a certain range, such as 1.5 wt% and 2.0 wt% (Dania Adila et al., 2021). Thus, although 1.0 wt% PEDOT: PSS is the highest composition in this study and gives the highest conductivity achieved, further research is required to determine whether this particular composition is the percolation point or not. The FESEM results in Figure 4.1e validate the formation of fibrous pores with an interconnected structure that allows ions to flow along continuous channels efficiently. PEDOT: PSS serves as a compatibilizer and helps prevent the phase separation of two immiscible PEO and PVDF polymers. Zhu et al., (2025) observed that adding compatible substances can eliminate the natural immiscibility of

two phases of PEO and PVDF, whereas Leš and Jordan (2020) discovered that PEDOT: PSS causes molecular blending because of the interaction of sulfonate groups with both phases. The FESEM image in Figure 4.1e shows a uniform surface without any phase boundaries.

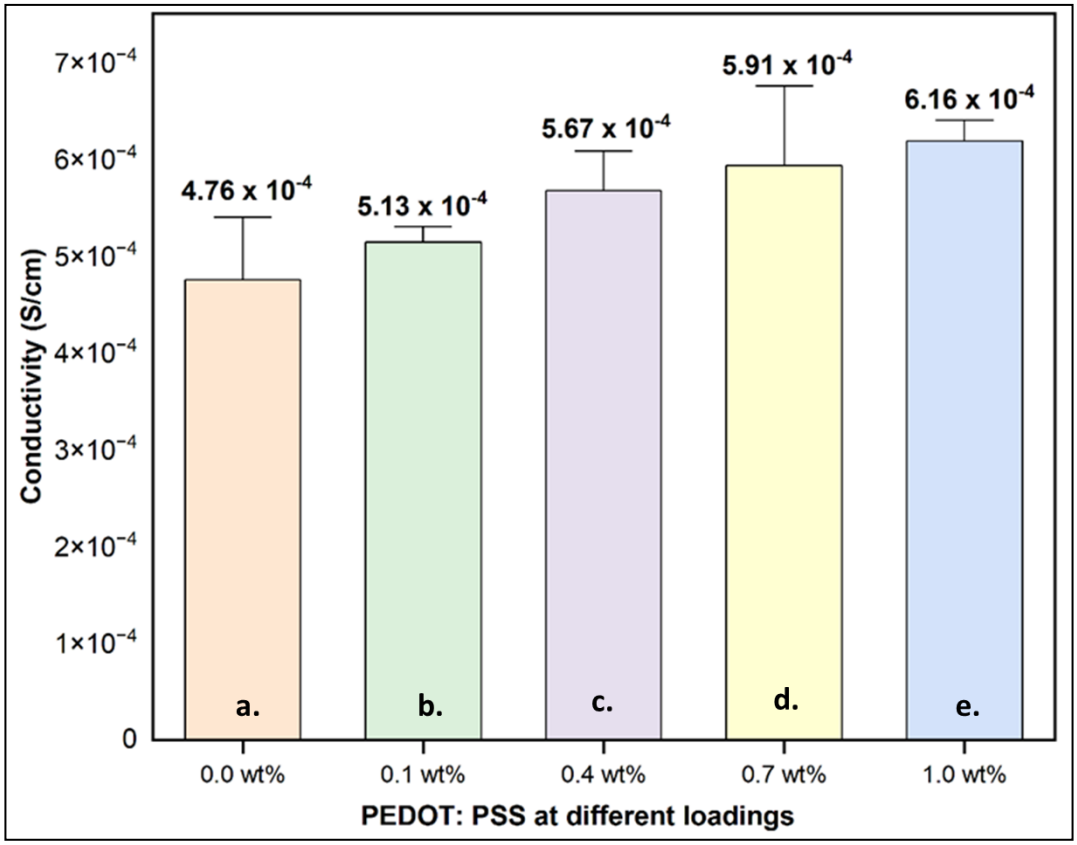

Figure 4. 6 PEO/PVDF/LiTFSI Composite Membranes Ionic Conductivity with Various Weight Percentages of PEDOT: PSS (0%, 0.1%, 0.4%, 0.7%, and 1.0%). The Maximum Ionic Conductivity Value Of 6.16 × 10^{-4} S/Cm Was Recorded For The Sample With The Maximum Weight Percentage Of PEDOT: PSS of 1.0%. This Indicates A Positive Relationship Between The Concentration Of PEDOT: PSS And The Ionic Conductivity Studied Range.

FESEM micrographs also further illustrate this morphological evolution. The pure membrane (0 wt%) was rough, with phase-separated domains with low connectivity, as it should be for crystalline barriers in XRD. With progressive addition of PEDOT: PSS (0.1–0.7 wt%), the morphology becomes denser and more uniform, and at 1.0 wt%, a highly well-connected fibrous and porous network is developed. This type of morphology is characteristic of an interpenetrating network (IPN), since PEDOT-rich areas are distributed evenly throughout the PEO/ PVDF matrix. This type

of IPN provides a twofold improvement, enhancing free volume and mobility of polymer chains to allow Li^+ conduction by amorphous PEO, and dynamic PEDOT backbones would provide conductive bridges, decreasing the small degree of tortuous nature in the porous membrane and bulk resistance. This leads to an additive enhancement of ionic and electronic conducting pathways.

Therefore, the enhancements in conductivity characterized by EIS directly correspond to these changes in structure, that is, the IPN-like morphology development (FESEM), allowing for greater Li^+ dissociation, higher segmental mobility, and shorter lengths of conduction paths. Optimal performance at 1.0 wt% PEDOT: PSS results from the optimum balance among salt dissociation, amorphization, and network formation. In addition to this loading, literature indicates that crowding and aggregation can disrupt the IPN, restoring transport barriers partially (Dania Adila et al., 2021).

Table 4. 2
Ionic Conductivity Of PEO/PVDF/LiTFSI Composite Membranes At Varying PEDOT: PSS loadings (0 wt%, 0.1 wt%, 0.4 wt%, 0.7 wt%, and 1.0 wt%). Five Independent Measurements (A–E) Are Shown, Demonstrating A Progressive Increase In Conductivity With Higher PEDOT: PSS Content. The Minimum Conductivity Of 4.76×10^{-4} S/Cm Is Recorded At 0 Wt%, While The Maximum Conductivity Of 6.16×10^{-4} S/Cm Is Achieved At 1.0 Wt% PEDOT: PSS.

PEDOT: PSS	Conductivity (S/m)
0.0 wt%	4.76E-04
0.1 wt%	5.13E-04
0.4 wt%	5.67E-04
0.7 wt%	5.91E-04
1.0 wt%	6.16E-04

4.5 Transference Number (TN) Analysis

In solid polymer electrolytes, ions and electrons are active. Therefore, to understand the increase in ionic conductivity, it is essential to separate the contribution from the ions and the contribution from the electrons (Arya et al., 2019). The main aim of this study is to measure the ionic transference number of the electrolyte, which in this case is a PEO/PVDF/PEDOT: PSS/LiTFSi composite. The transference number (t_+) is important in determining the ion-selective ability of polymer electrolyte membranes and it represents the fraction of the current carrying lithium ions (Li^+) in comparison with the electrons.

Deviations from this expected curve start to occur at a 1.0 wt% PEDOT: PSS concentration where current fluctuations can be seen, which show that some electronic conduction is noticeable in figure 4.7. This approach could be attributed to the formation of multiple, defined, and persistent PEDOT-enriched regions within the polymer matrix, which enhances ionic conductivity, but may be creating leakage pathways and losing the purely ionic nature of the transport described in reference to their different approaches with various copolymer concentrations (Yao et al., 2019) and (Lu et al., 2023). There seems to be a trade-off between these two factors in terms of the concentration range investigated which is the 1.0 wt% formulation, which represents the highest PEDOT: PSS content examined, exhibits the highest ionic conductivity (6.16×10^{-4} S/cm), whereas 0.4–0.7 wt% formulations exhibit higher ionic selectivity (t_{ion}=1), keeping t_+ at its maximum value of around 1.00.

This trade-off between conductivity and transference number has been similarly reported in other polymer electrolyte systems modified with conducting fillers, where excessive filler loading promoted aggregation and partial electronic conduction (Xiaowei Li et al., 2019) and (Xue et al., 2015). It can be seen that 1.0 wt% PEDOT: PSS, which is the highest percentage studied here, leads to the largest enhancement in conductivity, while 0.4-0.7 wt% PEDOT: PSS provides the maximum stability in ionic transference. This study shows that the choice of percentage depends upon what is important for a particular use of the material, which is higher conductivity in the case of 1.0 wt%, and better selectivity in the case of 0.4-0.7 wt%.

With a composition of 0 wt% PEDOT: PSS, no value for the transference number is presented because of the impossibility of conducting reliable measurements via the Bruce-Vincent method because of a low ionic conductivity of 4.76×10^{-4} S/cm, phase separation, high crystallinity, and the partial dissociation of LiTFSI ((Bruce et al., 1987, Zhou et al., 2019, Kim et al., 2020). With the composition of 0.1 wt% PEDOT: PSS, the transference number is estimated at around 0.98, meaning that 98% of the charge transfer occurs through Li^+ ions, and 2% of the charge transfer occurs through other ions, indicating that PEDOT: PSS aggregates have not formed electronic conductors but still act as clusters that promote ion dissolution (Yao et al., 2019, (Leš and Jordan, 2020). The value of 0.98 is substantially higher than the values of the transference number in liquid electrolytes ($t_+ \approx$ 0.2-0.5) and many solid polymers ($t_+ \approx$ 0.3-0.6) (Shao et al., 2022). When the PEDOT: PSS content reaches 0.4 wt%, the transference number slightly increases to 0.99. It shows the best ion selectivity observed

in this study. In addition, it can be inferred that the current carried by the Li^+ ions is approximately 99%. The reason for the increase from 0.98 is due to additional sulfonate groups brought in by PSS to enhance the salt dissociation and Li^+ coordination (Namsheer and Rout, 2021, Kim et al., 2020). At 0.7 wt% PEDOT: PSS, the transference number remains at approximately 0.99, indicating that the membrane maintains purely ionic conduction with no detectable electronic contribution despite a higher PEDOT: PSS concentration. The sustained t_+ value of 0.99 is significant because it shows that the percolation threshold for electronic conduction has not yet been reached even as the membrane approaches maximum conductivity (Yao et al., 2019). The FESEM image in Figure 4.1d shows uniformity on the surface, and the XRD pattern in Figure 4.5d results in the synergistic effect of high conductivity (5.91×10^{-4} S/cm) and ionic selectivity peaks ($t_+ = 0.99$). Thus, 0.7 wt% is an optimal loading for such practical applications, where efficient transport and high-purity Li^+ conductance are desired (Zhou et al., 2019, Tarascon and Armand, 2001).

With a maximum composition of 1.0 wt% PEDOT:PSS, the value of transference number decreases to approximately 0.95, which means that the 95% of current is carried by Li^+ ions while 5% is carried by electrons from PEDOT, indicating the start of electronic conductivity as highly dense and well-connected PEDOT-rich regions provide a continuous pathway for electrons throughout the thickness of the membranes (Holze, 2022, Leš and Jordan, 2020). FESEM at 1.0 wt% (Figure 4.1e) is consistent with this result showing the formation of fibrous-porous interconnected network providing a continuous path for both ion and electron transport, however, despite the decrease to 0.95, the transference number is still quite adequate for most battery systems as transference number values above 0.9 are generally considered good for solid polymer electrolyte (Diederichsen et al., 2017). The values of transference numbers over the entire range of compositions indicate a clear trade- off where intermediate compositions in the range 0.4 – 0.7 wt% show the highest ionic selectivity value of 0.99 along with high conductivity values reaching up to 5.91×10^{-4} S/cm, while the highest loading (1.0%) gives the highest conductivity value of 6.16×10^{-4} S/cm but with slightly lower t_+ of 0.95.

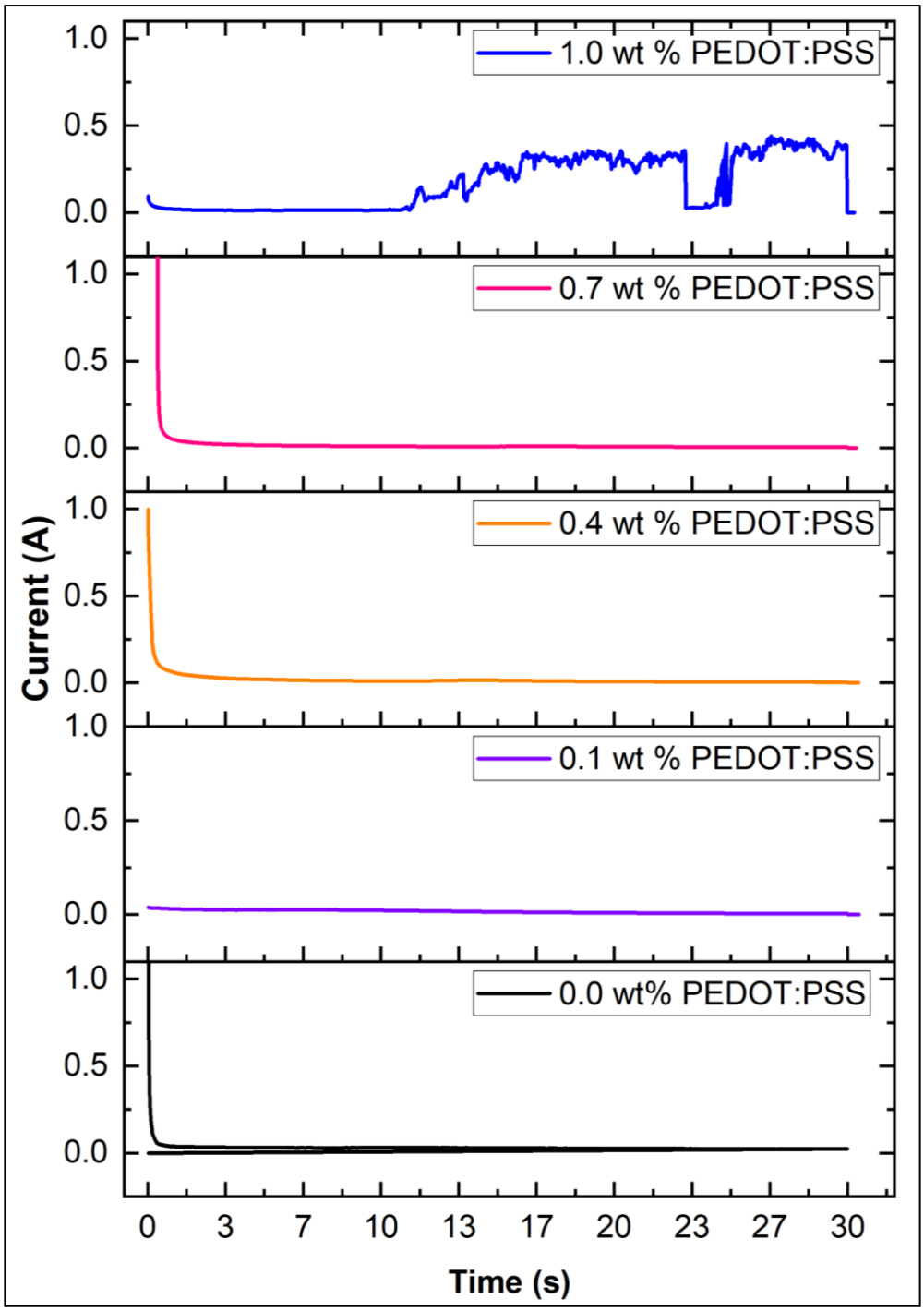

Figure 4. 7 Current–Time Polarization Curves For PEO/PVDF/LiTFSI Membranes With Different Levels Of PEDOT: PSS Doping (0.0–1.0 Wt%). All The Membranes Display A Decline In Current Before Stabilizing, Which Demonstrates That Ionic Transport Is The Primary Transport Mechanism In These Membranes. The Membranes Doped With 0.0–0.7 Wt% Demonstrate Consistent Current Decay To Zero, Which Corresponds To High Values Of Ionic Transference Number.

CHAPTER 5
CONCLUSION AND RECOMMENDATIONS

5.1 Conclusion

This study successfully characterized PEDOT: PSS as a conducting polymer in PEO/PVDF/LiTFSI composite membranes for lithium-ion separators, addressing the need for sustainable and efficient lithium-ion battery recycling. The primary objectives were to investigate the optimal PEO composition in PVDF/LiTFSI solutions, evaluate the effect of PEDOT: PSS on ionic conductivity, and examine the chemical, crystallinity, and morphological properties of the composite membranes. The methodology involved synthesizing PEDOT: PSS via oxidative polymerization, blending it with PEO/PVDF/LiTFSI solutions at varying concentrations (0–1.0 wt%), and characterizing the membranes using FESEM, FTIR, XRD, and EIS.

FESEM images displayed a significant transformation in the membrane's morphology, with higher PEDOT: PSS concentrations promoting a shift from rough, phase-segregated surfaces to a dense, fibrous, and highly interconnected interpenetrating network (IPN) at a maximum composition of PEDOT: PSS which is 1.0 wt%. This network morphology enhanced the mobility of polymer chains and facilitated efficient lithium-ion pathways, which are crucial for high-performance solid polymer electrolytes. FTIR confirmed molecular interactions through progressive broadening of the C-O-C peak (~1100 cm^{-1}) and enhanced $TFSI^-$ peaks (~1350 and ~740 cm^{-1}) with increasing PEDOT:PSS loading, indicating greater Li^+ coordination and salt dissociation. XRD confirmed that the semi-crystalline structure of PEO/PVDF was preserved, with stable peak positions indicating that PEDOT: PSS acts as a dispersed conductive additive without disturbing crystal packing.

Further confirmation came from EIS, which revealed a gradual increase in ionic conductivity with rising PEDOT: PSS content, peaking at 1.0 wt%. This ideal loading strikingly balanced maintaining membrane uniformity, optimizing salt dissociation, and enhancing conductive pathways which it is resulting in improved lithium-ion transport while preserving the mechanical strength of the composite. From TN analysis, there was a compromise in that at 0.4-0.7 wt%, the maximum transference number of Li^+ (t^+ = 0.99) was obtained but dropped to t^+ = 0.95 at 1.0 wt% due to electronic effects from

regions rich in PEDOT. Therefore, 1.0 wt% is optimal for high conductivity, ensuring efficient charge transfer while 0.4-0.7 wt% favors selectivity, which enables effective separation of lithium ions from other substances. The research establishes various range of loading parameters according to target properties between conductivity and transference stability which enables better customization of solid polymer electrolytes for modern lithium-ion battery applications.

In summary, this thesis demonstrates that the incorporation of PEDOT: PSS into the PEO/PVDF/LiTFSI system considerably improves the functional characteristics of of SPE membranes, the maximum loading of which is 1.0 wt%, which gives the greatest electrical conductivity, while intermediate values (0.4–0.7 wt%) give better ionic selectivity.

5.2 Recommendations

Based on the findings of this study, several recommendations are proposed to guide future research on PEO/PVDF/PEDOT: PSS/LiTFSI composite electrolytes:

a) Future research should focus on extensive and prolonged studies to assess wearability and longevity of PEO/PVDF/PEDOT: PSS/LiTFSI composites under a wide range of conditions. The investigation should consider the environmental conditions, such as exposure to ultraviolet (UV) light, changes in humidity, and temperature fluctuations that wearables and flexible electronics may encounter when actually used. Understanding how these factors can affect mechanical integrity, ionic conductivity, and structural stability, over time, is critical in tailoring the composite for real-world field use in wearable and flexible devices.

b) Further research is recommended to investigate a wider assortment of PEDOT: PSS formulations and concentrations, which may enhance ionic conductivity and overall electrochemical performance. In addition, research should focus on improving miscibility and compatibility of the PEDOT: PSS in the PEO/PVDF matrix- This may be explored via alternative mixing tactics or in the use of compatibilizing agents that may lead to improved dispersion of the PEDOT: PSS as well as improved interfacial interactions, thus leading to improved uniformity and functional properties of the composite electrolyte.

c) Alternative fabrication techniques, such as spin coating, should be investigated in an effort to achieve better uniformity and consistency in these materials. Not only can spin coating yield uniform thickness films in some cases, it can also produce films with precisely designed thickness and structure, leading to a more even comprised distribution of PEDOT: PSS in the polymer matrix. The technique could also improve the electrode/electrolyte interface improving ion transport pathways and subsequently improve device performance.

d) Transitioning from solvent casting on the laboratory scale to methods that can be scaled up to industrial levels, including roll-to-roll coating, doctor blade casting, or slot-die coating should be paid attention. There is still a

need for future research on problems associated with thickness homogeneity, defect control, manufacturing rate, and material wastage. Furthermore, techno-economic analysis and LCA should be conducted in order to estimate the ecological and economic benefits of membrane recycling compared with conventional pyrometallurgy and hydrometallurgy approaches.

e) Future research should carry out charge-discharge cycling tests (>500 cycles) to determine the stability of the membrane's mechanical and electrochemical properties under practical operating conditions. Accelerated aging tests should be carried out at various temperature ranges (25-80^{o}C), humidity levels (20-80% RH), and ultraviolet radiation to understand how long the membrane can operate and to establish modes of failure, such as polymer chain scission, PEDOT overoxidation, or LiTFSI leaching.

REFERENCES

Aannir, M., & Hakkou, R. (2023). *Towards a closed loop recycling process of end-of-life lithium-ion batteries : Recovery of critical metals and electrochemical performance evaluation of a regenerated LiCoO 2*. *580*(April). https://doi.org/10.1016/j.jpowsour.2023.233341

Ahmad Ruzaidi, D. A., Mahat, M. M., Mohamed Sofian, Z., Nor Hashim, N. A., Osman, H., Nawawi, M. A., Ramli, R., Jantan, K. A., Aizamddin, M. F., Azman, H. H., Chang, Y. H. R., & Hamzah, H. H. (2021). Synthesis and characterization of porous, electro-conductive chitosan–gelatin–agar-based pedot: Pss scaffolds for potential use in tissue engineering. *Polymers*, *13*(17), 1–21. https://doi.org/10.3390/polym13172901

Arya, A., & Sharma, A. L. (2019). *Tailoring of the Structural , Morphological , Electrochemical , and Dielectric Properties of Solid Polymer Electrolyte*. *April*. https://doi.org/10.1007/s11581-019-02916-7

Asri, N. A. N., Amir, B., Ramli, A. S., Safian, M. F., Zakaria, A., Jani, N. A., & Mahat, M. M. (2022). The effect of ethylene glycol post-treatment on the electrical conductivity of PEDOT: PSS thin films. *Journal of Physics: Conference Series*, *2169*(1). https://doi.org/10.1088/1742-6596/2169/1/012036

Bae, H., Hwang, S. M., Seo, I., & Kim, Y. (2016). *Electrochemical Lithium Recycling System toward Renewable and Sustainable Energy Technologies*. *163*(7), 199–205. https://doi.org/10.1149/2.0691607jes

Bae, H., & Kim, Y. (2021). *Materials Advances Technologies of lithium recycling from waste lithium ion batteries : a review †*. https://doi.org/10.1039/d1ma00216c

Balaji, J., Aruchamy, K., & Oh, T. H. (2022). Binder-free PEO/PPy/PEDOT:PSS layer coated on nickel foam for high-performance asymmetric supercapacitor applications. *Ionics*, *28*(10), 4867–4880. https://doi.org/10.1007/s11581-022-04692-3

Banitaba, S. N., & Semnani, D. (2019). Advances in Textile Engineering Nanofibrous Membranes Applicable in. *Advances in Textile Engineering*, 1–14.

Bankole, O. E., Gong, C., & Lei, L. (2013). Battery Recycling Technologies: Recycling Waste Lithium Ion Batteries with the Impact on the Environment In-View. *Journal of Environment and Ecology*, *4*(1), 14.

https://doi.org/10.5296/jee.v4i1.3257

Baum, Z. J., Bird, R. E., Yu, X., & Ma, J. (2022). Lithium-Ion Battery Recycling─Overview of Techniques and Trends. *ACS Energy Letters*, *7*(2), 712–719. https://doi.org/10.1021/acsenergylett.1c02602

Beck, F., Barsch, U., & Michaelis, R. (1993). Corrosion of conducting polymers in aqueous media. *Journal of Electroanalytical Chemistry*, *351*(1–2), 169–184. https://doi.org/10.1016/0022-0728(93)80232-7

Bhandari, S. (2017). Polyaniline: Structure and Properties Relationship. In *Polyaniline Blends, Composites, and Nanocomposites*. Elsevier Inc. https://doi.org/10.1016/B978-0-12-809551-5.00002-3

Borodin, O., & Smith, G. D. (2006). Mechanism of ion transport in amorphous poly(ethylene oxide)/ LiTFSI from molecular dynamics simulations. *Macromolecules*, *39*(4), 1620–1629. https://doi.org/10.1021/ma052277v

Bruce, G., Vincent, A., & Andrews, S. (1987). *Steady State Current Flow in Solid Binary Electrolyte Cells*. *225*, 1–17.

Chattopadhyay, J., Pathak, T. S., & Santos, D. M. F. (2023). Applications of Polymer Electrolytes in Lithium-Ion Batteries: A Review. *Polymers*, *15*(19). https://doi.org/10.3390/polym15193907

Che Roslan, N. (2020). *MORPHOLOGICAL AND CONDUCTIVITY STUDIES OF POLYANILINE FABRIC DOPED PHOSPHORIC ACID*. *24*(5), 698–706.

Chen, S., Liang, L., Zhang, Y., Lin, K., Yang, M., Zhu, L., Yang, X., Zang, L., Lu, B., & Nws, A. (2025). *PEDOT : PSS-based electronic materials : Preparation , performance tuning , processing , applications , and future prospect*. *166*. https://doi.org/10.1016/j.progpolymsci.2025.101990

Choo, Y., Halat, D. M., Villaluenga, I., Timachova, K., & Balsara, N. P. (2020). Diffusion and migration in polymer electrolytes. *Progress in Polymer Science*, *103*, 101220. https://doi.org/10.1016/j.progpolymsci.2020.101220

Chopade, S. A., Au, J. G., Li, Z., Schmidt, P. W., Hillmyer, M. A., & Lodge, T. P. (2017). Robust Polymer Electrolyte Membranes with High Ambient-Temperature Lithium-Ion Conductivity via Polymerization-Induced Microphase Separation. *ACS Applied Materials and Interfaces*, *9*(17), 14561–14565. https://doi.org/10.1021/acsami.7b02514

Contestabile, M., Panero, S., & Scrosati, B. (2001). Laboratory-scale lithium-ion battery recycling process. *Journal of Power Sources*, *92*(1–2), 65–69.

https://doi.org/10.1016/S0378-7753(00)00523-1

Crispin, X., Marciniak, S., Osikowicz, W., Zotti, G., Gon, A. W. D. V. A. N. D. E. R., Louwet, F., Fahlman, M., Groenendaal, L., Schryver, F. D. E., & Salaneck, W. R. (2003). *Stability of Poly (3 , 4-ethylene dioxythiophene)– Poly (styrene sulfonate): A Photoelectron Spectroscopy Study*. 2561–2583.

Cui, Z., Xu, Y., Zhu, L., Wang, J., Xi, Z., & Zhu, B. (2008). *Preparation of PVDF / PEO-PPO-PEO blend microporous membranes for lithium ion batteries via thermally induced phase separation process*. *325*, 957–963. https://doi.org/10.1016/j.memsci.2008.09.022

Dallaev, R., Pisarenko, T., Sobola, D., Orudzhev, F., & Ramazanov, S. (2022). *Brief Review of PVDF Properties and Applications Potential*. 1–29.

Dania Adila, A. R., Mahat, M. M., Sofian, Z. M., Adli, N., Hashim, N., Osman, H., Nawawi, M. A., Ramli, R., Jantan, K. A., Aizamddin, M. F., Azman, H. H., Hui, Y., Chang, R., & Hamzah, H. H. (2021). Synthesis and Characterization of Porous , Electro-Conductive Potential Use in Tissue Engineering. *Polymers*, *13*(2901), 1–20.

Debiemme-Chouvy, C., & Tran, T. T. M. (2008). An insight into the overoxidation of polypyrrole materials. *Electrochemistry Communications*, *10*(6), 947–950. https://doi.org/10.1016/j.elecom.2008.04.024

Deng, D. (2015). Li-ion batteries: Basics, progress, and challenges. *Energy Science and Engineering*, *3*(5), 385–418. https://doi.org/10.1002/ese3.95

Diederichsen, K. M., McShane, E. J., & McCloskey, B. D. (2017). Promising Routes to a High Li+ Transference Number Electrolyte for Lithium Ion Batteries. *ACS Energy Letters*, *2*(11), 2563–2575. https://doi.org/10.1021/acsenergylett.7b00792

Edman, L. (2000). *Ion Association and Ion Solvation Effects at the Crystalline - Amorphous Phase Transition*. 7254–7258.

Eren, E. (2018). Li+ doped chitosan-based solid polymer electrolyte incorporated with PEDOT:PSS for electrochromic device. *Journal of the Turkish Chemical Society, Section A: Chemistry*, *5*(3), 1413–1422. https://doi.org/10.18596/jotcsa.433901

Fakui, L., Congcong, W., Chi, Z., Hui, G., Jiazheng, N., Wensheng, M., Zhangquan, P., Yanwen, B., & Zhonghua, Z. (2019). Operando X-ray diffraction analysis of the degradation mechanisms of a spinel LiMn 2 O 4 cathode in different voltage windows. *Journal of Energy Chemistry*, *xxxx*. https://doi.org/10.1016/j.jechem.2019.09.011

Fan, X., Nie, W., Tsai, H., Wang, N., Huang, H., Cheng, Y., Wen, R., Ma, L., Yan, F., & Xia, Y. (2019). PEDOT:PSS for Flexible and Stretchable Electronics: Modifications, Strategies, and Applications. *Advanced Science*, *6*(19). https://doi.org/10.1002/advs.201900813

Flexer, V., Baspineiro, C. F., & Galli, C. I. (2018). Lithium recovery from brines: A vital raw material for green energies with a potential environmental impact in its mining and processing. *Science of the Total Environment*, *639*, 1188–1204. https://doi.org/10.1016/j.scitotenv.2018.05.223

Fong, K. D., Wang, T., Kim, H. K., Kumar, R. V., & Smoukov, S. K. (2017). Semi-Interpenetrating Polymer Networks for Enhanced Supercapacitor Electrodes. *ACS Energy Letters*, *2*(9), 2014–2020. https://doi.org/10.1021/acsenergylett.7b00466

Gonçalves, R., Miranda, D., Almeida, A. M., Silva, M. M., Meseguer-Dueñas, J. M., Ribelles, J. L. G., Lanceros-Méndez, S., & Costa, C. M. (2019). Solid polymer electrolytes based on lithium bis(trifluoromethanesulfonyl)imide/poly(vinylidene fluoride -co-hexafluoropropylene) for safer rechargeable lithium-ion batteries. *Sustainable Materials and Technologies*, *21*, 1–31. https://doi.org/10.1016/j.susmat.2019.e00104

Goodenough, J. B., & Park, K. (2013). *The Li-Ion Rechargeable Battery : A Perspective*.

Hanna, F., Somers, C., & Anctil, A. (2025). *Life Cycle Assessment of Lithium-Ion Battery Recycling : Evaluating the Impact of Recycling Methods and Location*.

Hao, S., Liang, S., Sewell, C. D., Li, Z., Zhu, C., Xu, J., & Lin, Z. (2021). *Lithium-Conducting Branched Polymers : New Paradigm of Solid- State Electrolytes for Batteries*. *2021*(2).

Harper, G., Sommerville, R., Kendrick, E., Driscoll, L., Slater, P., Stolkin, R., Walton, A., Christensen, P., Heidrich, O., Lambert, S., Abbott, A., Ryder, K., Gaines, L., & Anderson, P. (2019). Recycling lithium-ion batteries from electric vehicles. *Nature*, *575*(7781), 75–86. https://doi.org/10.1038/s41586-019-1682-5

Heeger, A. J. (1989). Feature Article. *Remedial and Special Education*, *10*(3), 8. https://doi.org/10.1177/074193258901000304

Holze, R. (2022). Overoxidation of Intrinsically Conducting Polymers. *Polymers*, *14*(8). https://doi.org/10.3390/polym14081584

Huang, B., Pan, Z., Su, X., & An, L. (2018). Recycling of lithium-ion batteries:

Recent advances and perspectives. *Journal of Power Sources*, *399*(June), 274–286. https://doi.org/10.1016/j.jpowsour.2018.07.116

Huang, Y., Tang, L., & Jiang, Y. (2024). Chemical Strategies of Tailoring PEDOT:PSS for Bioelectronic Applications: Synthesis, Processing and Device Fabrication. *CCS Chemistry*, *6*(8), 1844–1867. https://doi.org/10.31635/ccschem.024.202403858

Huseynova, G., Kim, Y. H., Lee, J., & Lee, J. (2019). Rising advancements in the application of PEDOT : PSS as a prosperous transparent and flexible electrode material for solution-processed organic electronics. *Journal of Information Display*, *0*(0), 1–21. https://doi.org/10.1080/15980316.2019.1707311

Isaac, J. A., Mangani, L. R., Devaux, D., & Bouchet, R. (2022). Electrochemical Impedance Spectroscopy of PEO-LATP Model Multilayers: Ionic Charge Transport and Transfer. *ACS Applied Materials and Interfaces*, *14*(11), 13158–13168. https://doi.org/10.1021/acsami.1c19235

Jiang, Y., Guo, N., Dong, F., Xie, H., & Liu, J. (2023). Semi-interpenetrating-network PEO-based polymer electrolytes with fast Li-ion conduction for solid Li-metal batteries. *Journal of Energy Storage*, *73*(PA), 108809. https://doi.org/10.1016/j.est.2023.108809

Joulié, M., Laucournet, R., & Billy, E. (2014). Hydrometallurgical process for the recovery of high value metals from spent lithium nickel cobalt aluminum oxide based lithium-ion batteries. *Journal of Power Sources*, *247*, 551–555. https://doi.org/10.1016/j.jpowsour.2013.08.128

Kaneto, K. (2014). Conducting polymers. In *Soft Actuators: Materials, Modeling, Applications, and Future Perspectives* (Vol. 9784431547). https://doi.org/10.1007/978-4-431-54767-9_7

Kasri, M. A., Mohd Halizan, M. Z., Harun, I., Bahrudin, F. I., Daud, N., Aizamddin, M. F., Amira Shaffee, S. N., Rahman, N. A., Shafiee, S. A., & Mahat, M. M. (2024). Addressing preliminary challenges in upscaling the recovery of lithium from spent lithium ion batteries by the electrochemical method: a review. *RSC Advances*, *14*(22), 15515–15541. https://doi.org/10.1039/d4ra00972j

Kee, S., Kim, N., Park, H., Kim, B. S., Teo, M. Y., Lee, S., Kim, J., & Lee, K. (2020). Tuning the Mechanical and Electrical Properties of Stretchable PEDOT:PSS/Ionic Liquid Conductors. *Macromolecular Chemistry and Physics*, *221*(23), 1–8. https://doi.org/10.1002/macp.202000291

Khan, K. H., & Haleem, A. (2025). RSC Advances ion batteries : strategies in composites , blends ,. *RSC Advances*, *15*, 20629–20656. https://doi.org/10.1039/D5RA02951A

Kim, K., Kuhn, L., Alabugin, I. V, & Jr, D. T. H. (2020). *Lithium Salt Dissociation in Diblock Copolymer Electrolyte Using Fourier Transform Infrared Spectroscopy*. *8*(September), 1–17. https://doi.org/10.3389/fenrg.2020.569442

Kim, N., Kee, S., Lee, S. H., Lee, B. H., Kahng, Y. H., Jo, Y., Kim, B., & Lee, K. (2014). *Highly Conductive PEDOT : PSS Nanofi brils Induced by Solution-Processed Crystallization*. 2268–2272. https://doi.org/10.1002/adma.201304611

Kirchmeyer, S., & Reuter, K. (2005). *Scientific importance , properties and growing applications of*. 2077–2088. https://doi.org/10.1039/b417803n

Krause, D. T., Förster, B., Dulle, M., Krämer, S., Böckmann, S., Mönich, C., Hansen, M. R., Schönhoff, M., Siozios, V., Grünebaum, M., Winter, M., Förster, S., & Wiemhöfer, H. (2024). *A Super-Ionic Solid-State Block Copolymer Electrolyte*. *2404297*, 1–15. https://doi.org/10.1002/smll.202404297

Kumar, D., & Sharma, R. C. (1998). *REVIEW ARTICLE ADVANCES IN CONDUCTIVE POLYMERS*. *34*(8).

L. Gao, J. Li, B., Sarmad, B. Cheng, W. Kang and N. DengL. Gao, J. Li, B., & Sarmad, B. Cheng, W. K. and N. D. (2020). *Nanoscale*. https://doi.org/10.1039/D0NR04244G

Leš, K., & Jordan, C.-S. (2020). Ionic conductivity enhancement in solid polymer electrolytes by electrochemical: In situ formation of an interpenetrating network. *RSC Advances*, *10*(68), 41296–41304. https://doi.org/10.1039/d0ra07966a

Li, J., Zhu, K., Wang, J., Yan, K., Liu, J., & Yao, Z. (2020). Optimisation of conductivity of PEO / PVDF-based solid polymer electrolytes in all-solid-state Li-ion batteries. *Materials Technology*, *00*(00), 1–8. https://doi.org/10.1080/10667857.2020.1827873

Li, Xiaohui, Liu, S., Yang, J., He, Z., & Zheng, J. (2023). Electrochemical methods contribute to the recycling and regeneration path of lithium-ion batteries. *Energy Storage Materials*, *55*(December 2022), 606–630. https://doi.org/10.1016/j.ensm.2022.12.022

Li, Xiaolong, & Wang, X. (2019). *Preparation and performance of poly (ethylene oxide) -based composite solid electrolyte for all solid-state lithium batteries*. *47498*, 1–9. https://doi.org/10.1002/app.47498

Li, Xiaowei, Zheng, Y., Pan, Q., & Li, C. Y. (2019). *Polymerized Ionic Liquid-Containing Interpenetrating Network Solid Polymer Electrolytes for All-Solid-State Lithium Metal Batteries*. https://doi.org/10.1021/acsami.9b09985

Li, Y., Sun, Z., Shi, L., Lu, S., Sun, Z., Shi, Y., Wu, H., Zhang, Y., & Ding, S. (2019). *Poly (ionic liquid) -polyethylene oxide semi-interpenetrating polymer network solid electrolyte for safe lithium metal batteries*. *375*(June). https://doi.org/10.1016/j.cej.2019.121925

Li, Z., Yu, R., Weng, S., Zhang, Q., Wang, X., & Guo, X. (2022). *Tailoring polymer electrolyte for high-voltage solid- state Li metal batteries working at ultra-low temperatures*. 1–21.

Lippe, J., & Holze, R. (1992). The anion-specific effect in the overoxidation of polyaniline and polyindoline. *Journal of Electroanalytical Chemistry*, *339*(1–2), 411–422. https://doi.org/10.1016/0022-0728(92)80465-G

Liu, H. S., Chen, K. Y., Fang, C. E., & Chiu, C. cheng. (2021). Comparing the effects of polymer binders on Li+ transport near the liquid electrolyte/LiFePO4 interfaces: A molecular dynamics simulation study. *Electrochimica Acta*, *375*, 137915. https://doi.org/10.1016/j.electacta.2021.137915

Liu, J., Miao, P., Zhang, W., Song, G., Feng, J., Leng, X., & Li, Y. (2022). Synthesis and characterization of interpenetrating polymer networks (IPNs) based on UV curable resin and blocked isocyanate/polyols. *Polymer*, *256*(August). https://doi.org/10.1016/j.polymer.2022.125254

Lu, X., Wang, Y., Xu, X., Yan, B., Wu, T., & Lu, L. (2023). Polymer-Based Solid-State Electrolytes for High-Energy-Density Lithium-Ion Batteries – Review. *Advanced Energy Materials*, *13*(38). https://doi.org/10.1002/aenm.202301746

Lun, P., Chen, Z., Zhang, Z., Tan, S., & Chen, D. (2018). *RSC Advances*. 34232–34240. https://doi.org/10.1039/c8ra06856a

Lv, W., Wang, Z., Cao, H., Sun, Y., Zhang, Y., & Sun, Z. (2018). A Critical Review and Analysis on the Recycling of Spent Lithium-Ion Batteries. *ACS Sustainable Chemistry and Engineering*, *6*(2), 1504–1521. https://doi.org/10.1021/acssuschemeng.7b03811

Ma, J., Wang, X., & Jiao, X. (2012). Electrocatalytic Reduction of Oxygen on PEDOT-Modified Glassy Carbon Electrode. *International Journal of Electrochemical Science*, *7*(2), 1556–1563. https://doi.org/10.1016/S1452-3981(23)13435-3

Maiz, J., Martin, J., & Mijangos, C. (2012). *Con fi nement E ff ects on the Crystallization of Poly (ethylene oxide) Nanotubes*.

Makuza, B., Tian, Q., Guo, X., Chattopadhyay, K., & Yu, D. (2021). Pyrometallurgical options for recycling spent lithium-ion batteries : A comprehensive review. *Journal of Power Sources*, *491*(January), 229622. https://doi.org/10.1016/j.jpowsour.2021.229622

Manthiram, A. (2020). *A re fl ection on lithium-ion battery cathode chemistry*. 1–9. https://doi.org/10.1038/s41467-020-15355-0

Maroufi, S., Assefi, M., Khayyam Nekouei, R., & Sahajwalla, V. (2020). Recovery of lithium and cobalt from waste lithium-ion batteries through a selective isolation-suspension approach. *Sustainable Materials and Technologies*, *23*, 2–6. https://doi.org/10.1016/j.susmat.2019.e00139

Mcdonald, M., & Hammond, P. T. (2018). *Efficient Transport Networks in a Dual Electron / Lithium-Conducting Polymeric Composite for Electrochemical Applications*. https://doi.org/10.1021/acsami.8b01519

Mendes-Felipe, C., Barbosa, J. C., Gonçalves, R., Miranda, D., Costa, C. M., Vilas-Vilela, J. L., & Lanceros-Mendez, S. (2021). Lithium bis(trifluoromethanesulfonyl)imide blended in polyurethane acrylate photocurable solid polymer electrolytes for lithium-ion batteries. *Journal of Energy Chemistry*, *62*, 485–496. https://doi.org/10.1016/j.jechem.2021.01.030

Mengistie, A. D., Wang, P.-C., & Chu, C.-W. (2013). Highly Conductive PEDOT:PSS Electrode Treated with Polyethylene Glycol for ITO-free Polymer Solar Cells. *The Electrochemical Society*, *58*(11), 49–56.

Meshram, P., Pandey, B. D., & Mankhand, T. R. (2015). Recovery of valuable metals from cathodic active material of spent lithium ion batteries: Leaching and kinetic aspects. *Waste Management*, *45*, 306–313. https://doi.org/10.1016/j.wasman.2015.05.027

Mindemark, J., Lacey, M. J., Bowden, T., & Brandell, D. (2018). Beyond PEO—Alternative host materials for Li+-conducting solid polymer electrolytes. *Progress in Polymer Science*, *81*, 114–143. https://doi.org/10.1016/j.progpolymsci.2017.12.004

Morsi, M. A., Abdelrazek, E. M., Tarabiah, A. E., & Salim, E. (2024). Preparation and tuning the optical and electrical properties of polyethylene oxide/polyvinyl alcohol/poly(3,4-thylenedioxythiophene): polystyrene sulfonate/CuO-based

quaternary nanocomposites for futuristic energy storage devices. *Journal of Energy Storage*, *80*(November 2023), 110239. https://doi.org/10.1016/j.est.2023.110239

Nair, J. R., Gerbaldi, C., Meligrana, G., & Bongiovanni, R. (2008). *UV-cured methacrylic membranes as novel gel – polymer electrolyte for Li-ion batteries*. *178*, 751–757. https://doi.org/10.1016/j.jpowsour.2007.08.004

Namsheer, K., & Rout, C. S. (2021). Conducting polymers: a comprehensive review on recent advances in synthesis, properties and applications. *RSC Advances*, *11*(10), 5659–5697. https://doi.org/10.1039/d0ra07800j

Nasrazadani, S. (2016). Chapter 2 - Modern analytical techniques in failure analysis of aerospace, chemical, and oil and gas industries. In *Handbook of Materials Failure Analysis with Case Studies from the Oil and Gas Industry*. Elsevier Ltd. https://doi.org/10.1016/B978-0-08-100117-2.00010-8

Nezakati, T., Seifalian, A., Tan, A., & Seifalian, A. M. (2018). Conductive Polymers: Opportunities and Challenges in Biomedical Applications [Review-article]. *Chemical Reviews*, *118*(14), 6766–6843. https://doi.org/10.1021/acs.chemrev.6b00275

Ouyang, J., Xu, Q., Chu, C., Yang, Y., Li, G., & Shinar, J. (2004). *On the mechanism of conductivity enhancement in through solvent treatment*. *45*, 8443–8450. https://doi.org/10.1016/j.polymer.2004.10.001

Pavia, D. L., Lampman, G. M., Kriz, G. S., & Vyvyan, J. R. (2013). *INTRODUCTION TO SPECTROSCOPY*.

Pengcheng Li, K. S. J. O. (2015). *Stretchable and Conductive Polymer Films Prepared by Solution Blending*. https://doi.org/10.1021/acsami.5b04492

Poinsignon, C. (1989). Polymer electrolytes. *Materials Science and Engineering B*, *3*(1–2), 31–37. https://doi.org/10.1016/0921-5107(89)90175-X

Prabakaran, K., Mohanty, S., & Nayak, S. K. (2015). Improved electrochemical and photovoltaic performance of dye sensitized solar cells based on PEO/PVDF-HFP/silane modified TiO2 electrolytes and MWCNT/Nafion® counter electrode. *RSC Advances*, *5*(51), 40491–40504. https://doi.org/10.1039/c5ra01770j

Precious, H., Gmbh, M., & Leverkusen, C. (2014). *PEDOT — Properties and Applications 1*. *56*(1), 135–143. https://doi.org/10.1134/S1811238214010068

Rey, I., Lasse, J. C., Servant, L., Grondin, J., Cristalline, Â., & Ce, T. (1998). *Infrared and Raman study of the PEO-LiTFSI polymer electrolyte*. *43*, 1505–1510.

Rohtlaid, K., Nguyen, G. T. M., Soyer, C., Cattan, E., & Vidal, F. (2019). *Polyethylene Oxide Electrodes with Improved Electrical and Electrochemical Properties for Soft Microactuators and Microsensors*. *1800948*, 1–11. https://doi.org/10.1002/aelm.201800948

Ruan, L., Yao, X., Chang, Y., Zhou, L., Qin, G., & Zhang, X. (2018). Properties and applications of the β phase poly(vinylidene fluoride). *Polymers*, *10*(3), 1–27. https://doi.org/10.3390/polym10030228

Ruzaidi, D. A. A., Mahat, M. M., Shafiee, S. A., Sofian, Z. M., Sabere, A. S. M., Ramli, R., Osman, H., Hamzah, H. H., Ariffin, Z. Z., & Sadasivuni, K. K. (2021). Advocating electrically conductive scaffolds with low immunogenicity for biomedical applications: A review. *Polymers*, *13*(19), 1–26. https://doi.org/10.3390/polym13193395

Saito, K., Jehanno, C., Meabe, L., Olmedo, J., Mecerreyes, D., And, K. F., & Sardon, H. (2020). *Materials Chemistry A*. https://doi.org/10.1039/x0xx00000x

Sakunpongpitiporn, P., & Phasuksom, K. (2019). RSC Advances Facile synthesis of highly conductive PEDOT : PSS via surfactant templates. *RSC Advances*, *9*, 6363–6378. https://doi.org/10.1039/C8RA08801B

Schultze, J. W., & Karabulut, H. (2005). Application potential of conducting polymers. *Electrochimica Acta*, *50*(7–8), 1739–1745. https://doi.org/10.1016/j.electacta.2004.10.023

Seiti, M., Giuri, A., Corcione, C. E., & Ferraris, E. (2023). Advancements in tailoring PEDOT: PSS properties for bioelectronic applications: A comprehensive review. *Biomaterials Advances*, *154*(September). https://doi.org/10.1016/j.bioadv.2023.213655

Shao, Y., Gudla, H., Brandell, D., & Zhang, C. (2022). *Transference Number in Polymer Electrolytes: Mind the Reference- Frame Gap*. 7583–7587. https://doi.org/10.1021/jacs.2c02389

Sisodia, A., & Monteiro, J. (2018). Lithium-Ion Battery Management System: A Lifecycle Evaluation Model for the Use in the Development of Electric Vehicles. *MATEC Web of Conferences*, *144*, 1–9. https://doi.org/10.1051/matecconf/201714404020

Sojka, R., Pan, Q., & Billmann, L. (2020). *Comparative study of Li-ion battery recycling processes*.

Song, I., Yeon Park, N., Seung Jeong, G., Hwan Kang, J., Hwa Seo, J., & Choi, J. Y.

(2020). Conductive channel formation for enhanced electrical conductivity of PEDOT:PSS with high work-function. *Applied Surface Science*, *529*, 147176. https://doi.org/10.1016/j.apsusc.2020.147176

Sun, K., Zhang, S., Li, P., Xia, Y., Zhang, X., Du, D., Isikgor, F. H., & Ouyang, J. (2015). Review on application of PEDOTs and PEDOT:PSS in energy conversion and storage devices. *Journal of Materials Science: Materials in Electronics*, *26*(7), 4438–4462. https://doi.org/10.1007/s10854-015-2895-5

Takano, T., Masunaga, H., Fujiwara, A., Okuzaki, H., & Sasaki, T. (2012). PEDOT nanocrystal in highly conductive PEDOT:PSS polymer films. *Macromolecules*, *45*(9), 3859–3865. https://doi.org/10.1021/ma300120g

Tarascon, J.-M., & Armand, M. (2001). *Issues and challenges facing rechargeable lithium batteries*. *414*(November), 359–367.

Taylor, P., Zeng, X., Li, J., & Singh, N. (2013). *Critical Reviews in Environmental Science and Technology Recycling of Spent Lithium-Ion Battery : A Critical Review*. *October 2014*, 37–41. https://doi.org/10.1080/10643389.2013.763578

Tehrani, P., Kanciurzewska, A., Crispin, X., Robinson, N. D., Fahlman, M., & Berggren, M. (2007). The effect of pH on the electrochemical over-oxidation in PEDOT:PSS films. *Solid State Ionics*, *177*(39–40), 3521–3527. https://doi.org/10.1016/j.ssi.2006.10.008

Teo, L. P., & Buraidah, M. H. (2021). *Development on Solid Polymer Electrolytes for*.

Thackeray, M. M., Wolverton, C., & Isaacs, E. D. (2012). *Environmental Science going beyond , lithium-ion batteries*. 7854–7863. https://doi.org/10.1039/c2ee21892e

Timpanaro, S., Kemerink, M., Touwslager, F. J., De Kok, M. M., & Schrader, S. (2004). Morphology and conductivity of PEDOT/PSS films studied by scanning-tunneling microscopy. *Chemical Physics Letters*, *394*(4–6), 339–343. https://doi.org/10.1016/j.cplett.2004.07.035

Tong, Y., Lyu, H., Xu, Y., Thapaliya, B. P., Li, P., Sun, X.-G., & Dai, S. (2018). *All-Solid-State Interpenetrating Network Polymer Electrolytes for Long Cycle Life of Lithium Metal Batteries*. https://doi.org/10.1039/C8TA03062F

Ujvári, M., Láng, G. G., Vesztergom, S., Szekeres, K. J., Kovács, N., & Gubicza, J. (2015). *Structural changes during the overoxidation of electro- chemically deposited poly (3 , 4-ethylenedioxythiophene) films*. *6*(1), 77–88. https://doi.org/10.5599/jese.225

Ulbricht, M. (2006). Advanced functional polymer membranes. *Polymer*, *47*(7), 2217–2262. https://doi.org/10.1016/j.polymer.2006.01.084

Ushakova, E. E., Sergeev, A. V., Morzhukhin, A., Napolskiy, F. S., Kristavchuk, O., Chertovich, A. V., Yashina, L. V., & Itkis, D. M. (2020). Free-standing Li+-conductive films based on PEO-PVDF blends. *RSC Advances*, *10*(27), 16118–16124. https://doi.org/10.1039/d0ra02325f

Wang, H., Wei, W., & Hu, Y. H. (2015). *Efficient ZnO-based counter electrodes for dye-sensitized solar cells*. *May 2013*. https://doi.org/10.1039/C3TA10892A

Wang, J., Fan, L., Du, Q., & Jiao, K. (2022). Lithium ion transport in solid polymer electrolyte filled with alumina nanoparticles. *Energy Advances*, *5*, 269–276. https://doi.org/10.1039/d2ya00025c

Witkowski, A., & Brajter, A. T. (1992). Overoxidized Polypyrrole Films: A Model for the Design of Permselective Electrodes. *Analytical Chemistry*, *64*(6), 635–641. https://doi.org/10.1021/ac00030a012

Xia, S., Huang, W., Shen, X., Liu, J., Cheng, F., Liu, J., Yang, X., & Guo, H. (2019). Rearrangement on surface structures by boride to enhanced cycle. *Journal of Energy Chemistry*. https://doi.org/10.1016/j.jechem.2019.09.023

Xia, Y., & Ouyang, J. (2012). *Significant Different Conductivities of the Two Grades of Poly(3,4- ethylenedioxythiophene):Poly(styrenesulfonate), Clevios P and Clevios PH1000, Arising from Different Molecular Weights*.

Xiao, Q., Li, Z., Gao, D., & Zhang, H. (2009). A novel sandwiched membrane as polymer electrolyte for application in lithium-ion battery. *Journal of Membrane Science*, *326*(2), 260–264. https://doi.org/10.1016/j.memsci.2008.10.019

Xu, K. (2022). Navigating the minefield of battery literature. *Communications Materials*, *3*(1), 1–7. https://doi.org/10.1038/s43246-022-00251-5

Xue, Z., He, D., & Xie, X. (2015). Poly(ethylene oxide)-based electrolytes for lithium-ion batteries. *Journal of Materials Chemistry A*, *3*(38), 19218–19253. https://doi.org/10.1039/c5ta03471j

Y.F., L., Deng, S. J., Xia, Y., Wang, X. L., Xia, X. H., Wu, J. B., Gu, C. D., & Tu, J. P. (2018). *A superior composite gel polymer electrolyte of Li7La3Zr2O12-poly(vinylidene fluoride-hexafluoropropylene) (PVDF-HFP) for rechargeable solid-state lithium ion batteries*. https://doi.org/10.1016/j.materresbull.2018.02.051

Yao, P., Yu, H., Ding, Z., Liu, Y., Lu, J., Lavorgna, M., Wu, J., & Liu, X. (2019).

Review on Polymer-Based Composite Electrolytes for Lithium Batteries. *Frontiers in Chemistry*, *7*(August), 1–17. https://doi.org/10.3389/fchem.2019.00522

Yao, Y., Zhu, M., Zhao, Z., Tong, B., Fan, Y., & Hua, Z. (2018). Hydrometallurgical Processes for Recycling Spent Lithium-Ion Batteries: A Critical Review. *ACS Sustainable Chemistry and Engineering*, *6*(11), 13611–13627. https://doi.org/10.1021/acssuschemeng.8b03545

Ye, L., & Feng, Z. (2010). Polymer electrolytes as solid solvents and their applications. *Polymer Electrolytes: Fundamentals and Applications*, 550–582. https://doi.org/10.1533/9781845699772.2.550

Ye, Q., Liang, H., Wang, S., Cui, C., Zeng, C., Zhai, T., & Li, H. (2022). Fabricating a PVDF skin for PEO-based SPE to stabilize the interface both at cathode and anode for Li-ion batteries. *Journal of Energy Chemistry*, *70*, 356–362. https://doi.org/10.1016/j.jechem.2022.02.037

Yongfang, L. (2000). *Electrochemical overoxidation of conducting polypyrrole nitrate film in aqueous solutions*. *45*, 1727–1731.

Zhou, B., Jiang, J., Zhang, F., & Zhang, H. (2020). Crosslinked poly(ethylene oxide)-based membrane electrolyte consisting of polyhedral oligomeric silsesquioxane nanocages for all-solid-state lithium ion batteries. *Journal of Power Sources*, *449*(November). https://doi.org/10.1016/j.jpowsour.2019.227541

Zhou, D., Shanmukaraj, D., Tkacheva, A., Armand, M., & Wang, G. (2019). Polymer Electrolytes for Lithium-Based Batteries: Advances and Prospects. *Chem*, *5*(9), 2326–2352. https://doi.org/10.1016/j.chempr.2019.05.009

Zhu, B., Jiang, X., He, S., Yang, X., Long, J., Zhang, Y., & Shao, L. (2020). Rational design of poly(ethylene oxide) based membranes for sustainable CO2capture. *Journal of Materials Chemistry A*, *8*(46), 24233–24252. https://doi.org/10.1039/d0ta08806d

Zhu, Y., Cui, J., Ma, Y., He, Y., Liu, S., He, J., & Xie, J. (2025). *Tuning the interfacial compatibility of poly (vinylidene difluoride) and poly (ethylene oxide) blends for improved solid-state polymer*. *68*(12), 6669–6681.

Zurita, L. (2024). *Ionic Conductivity, Li+ Transference Number, and Diffusion Coefficient of a Solid-State Electrolyte Composite*. *1*.

APPENDICES

APPENDIX 1

Conference Attended:

1. **Participant** Electronic Packaging Interconnect Technology Symposium (EPITS 2024) by Universiti Malaysia Perlis (UniMAP)
2. **Participant** 35th International Conference of Analytical Sciences 2023 (SKAM35)
3. **Timekeeper** 35th International Conference of Analytical Sciences 2023 (SKAM35)


CEGeoGTech
UNIVERSITI MALAYSIA PERLIS
UniMAP
TSTRG
MALAYSIA
THE UNIVERSITY OF QUEENSLAND
AUSTRALIA
BK
THAI SYNCHROTRON
NATIONAL LAB
CERTIFICATE OF APPRECIATION
is presented to
AWATIF BINTI HASSIM
(PRESENTER)
to the success of
ELECTRONIC PACKAGING INTERCONNECT TECHNOLOGY SYMPOSIUM
(EPITS 2024)
26th August 2024
Hotel Saigon Prince
Ho Chi Minh, Vietnam
ASSOC. PROF. IR. DR. SHAYFULL ZAMREE ABD RAHIM
Leader
Centre of Excellence Geopolymer & Green Technology (CEGeoGTech)
Universiti Malaysia Perlis (UniMAP)


SKAM35
The 35th International Conference of Analytical Sciences 2023
"Exploring the Future and Diversity in Sustainability: Challenges and Opportunities"
CERTIFICATE OF APPRECIATION
Awarded to
AWATIF BINTI HASSIM
for recognition as POSTER PRESENTER at the
35th International Conference of Analytical Sciences 2023
(SKAM35)
Held on 28-30th August 2023, Bayview Hotel Langkawi, MALAYSIA
Jointly organised by Faculty of Applied Sciences, Universiti Teknologi MARA (UiTM)
&
Persatuan Sains Analisis Malaysia (ANALIS)
Prof. ChM Dr. Mohd Basyaruddin Abdul Rahman
President of ANALIS
Assoc. Prof. ChM Dr. Sabiha Sanim Saleh
Chairman of SKAM35
ANALIS


SKAM35
The 35th International Conference of Analytical Sciences 2023
"Exploring the Future and Diversity in Sustainability: Challenges and Opportunities"
CERTIFICATE OF APPRECIATION
Awarded to
AWATIF HASSIM
for recognition as
TIMEKEEPER
in The 35th International Conference of Analytical Sciences 2023
(SKAM35)
Held on 28-30th August 2023, Bayview Hotel Langkawi, MALAYSIA
Jointly organised by Faculty of Applied Sciences, Universiti Teknologi MARA (UiTM)
&
Persatuan Sains Analisis Malaysia (ANALIS)
Prof. ChM Dr. Mohd Basyaruddin Abdul Rahman
President of ANALIS
Assoc. Prof. ChM Dr. Sabiha Sanim Saleh
Chairman of SKAM35
ANALIS
Universiti Teknologi MARA

AUTHOR'S PROFILE

Awatif Binti Hassim was born on May 23, 1998, in Kota Bharu, Kelantan, into a middle-class family. Both of her parents are teachers, fostering an environment that greatly values education. She is the third eldest of seven siblings, comprising five sisters and one brother. Awatif started her primary education at Sekolah Kebangsaan Seri Kota in Kota Bharu while continuing her secondary education at Sekolah Menengah Kebangsaan Kota in Kota Bharu, Kelantan. Through her secondary years, Awatif acquired the skills of articulate communication, logical reasoning, eloquence, and critical analysis. For her higher studies, Awatif pursued a Diploma in Polymer Technology, graduating in 2019. In addition, she obtained a Bachelor of Science (Hons.) in Polymer Technology from UiTM Shah Alam University. Currently, Awatif is studying for her Master of Science in Materials Science and Technology from the aforementioned institution. Materials science and polymer technology are her main research interests, with specific emphasis on exploring the crystallinity, physical properties, and ionic conductivity of the polymer membrane separators for lithium-ion battery recycling. The polymer membrane separators are important components in an electrochemical lithium recovery system. This study aims at promoting sustainable practices through resource conservation and waste minimization, leading to energy efficiency.

LIST OF PUBLICATION

Hassim, A., Abd Maliaman, N. N., Kasri, M. A., Mohd Fauzi, F. N. A., Ratim, S., & Mahat, M. M. (2025). Study of conductivity and morphological properties using different composition of PEDOT:PSS/PEO film as a membrane for lithium-ion batteries recycling. In N. R. Abdul Razak, M. A. A. Mohd Salleh, D. S. Che Halin, K. Abdul Razak, F. Somidin, & M. F. H. Baser (Eds.), Proceedings of the Green Materials and Electronic Packaging Interconnect Technology Symposium. ECOOP 1996 (Vol. 418, pp. [insert page range if available]). Springer. https://doi.org/10.1007/978-981-96-2871-1_24

Abd Maliaman, N. N., Hassim, A., Kasri, M. A., Mohd Halizan, M. Z., Shafiee, S. A., & Mahat, M. M. (2025). Fabrication of an interpenetrating polymer network (IPN) using PANI, PVDF, PEO, and LiTFSI for solid polymer electrolyte (SPE) applications. In N. R. Abdul Razak, M. A. A. Mohd Salleh, D. S. Che Halin, K. Abdul Razak, F. Somidin, & M. F. H. Baser (Eds.), Proceedings of the Green Materials and Electronic Packaging Interconnect Technology Symposium. ECOOP 1996 (Vol. 418, pp. [insert page range]). Springer. https://doi.org/10.1007/978-981-96-2871-1_20

Halizan, M. Z. M., Harun, I., Bahruddin, M. F. I., Daud, N., Kasri, M. A., Hassim, A., Maliaman, N. N., Rahman, N. A., Aizamddin, M. F., Shaffee, S. N. A., & Mahat, M. M. (2024). A Technical Review on the Implementation of Lithium-Ion Batteries Waste Recycling Methods (pp. 21–37). https://doi.org/10.1007/978-3-031-48902-0_2

Mohd Halizan, M. Z., Kasri, M. A., Maliaman, N. N., Hassim, A., Shafiee, S. A., Aizamddin, M. F., Shaffee, S. N. A., & Mahat, M. M. (2025). Integration of solid polymer electrolyte into an efficient and environmentally friendly electrochemical approach in lithium-ion batteries recycling. Journal of Energy Storage, Volume 131, Part A, 117491. https://doi.org/10.1016/j.est.2025.117491

UNIVERSITI TEKNOLOGI MARA

PERPUSTAKAAN TUN ABDUL RAZAK
BAHAGIAN SUMBER RUJUKAN UNIVERSITI (BSRU)

BORANG PENYERAHAN BAHAN HARTA INTELEK UiTM

UiTM's Intellectual Property Submission Form

Nama *(Name)* : AWATIF BINTI HASSIM

No. Telefon(Pejabat/Hp) : *Telephone No.(Office / handphone)* 0139332771

Fakulti/Pusat Akademik/Bahagian : *Faculty / Academic Centres / Department* FAKULTI SAINS GUNAAN

E-mel *(E-mail)* : 2023715523@student.uitm.edu.my

Tarikh *(Date)* : 15-07-2026

Pihak Fakulti / Pusat Akademik / Bahagian / Saya bersetuju bahawa dokumen dan tajuk yang disenaraikan untuk dimasukkan ke dalam Repositori Institusi UiTM.
The Faculty / Academic Centres / Department / I agree that the document and titles listed below to be placed in the UiTM Institutional Repository.

JENIS BAHAN (Sila nyatakan) :
Types of Material (Please specify) THESIS

Types of Material: Article / Book / Theses / Bulletin / Seminar / Image / Entrepreneurship / Student Project / Research Report / Industrial Training / Annual Report / Manual / Oral History / Exam Paper / Speech / Dataset / Audio / Video / Others

MAKLUMAT BAHAN ***(Information of Materials)*:**

Bil. *No*	JUDUL BAHAN *Title*	HARDCOPY (✓)	SOFTCOPY (✓)
1.	Characterization of Post- Overoxidized PEDOT: PSS/PEO/PVDF/LiTFSI Composite As a Solid Polymer Electrolyte		✔

* Sila sediakan lampiran sekiranya ruangan yang disediakan tidak mencukupi *(Please provide attachment if necessary)*

TUJUAN PENYERAHAN BAHAN (Sila tandakan √):

Purpose (Please mark √):

1. **Bahan untuk dimuat naik ke dalam Repositori Institusi UiTM**.
   (Materials for uploading into the UiTM Institutional Repository (UiTM IR)):
   Fakulti / Pusat Akademik / Bahagian / Saya perlu memastikan bahawa setiap dokumen telah dibuat semakan terlebih dahulu dan tidak mengandungi sebarang maklumat sulit sebelum diserahkan kepada pihak PTAR.
   The Faculty / Academic Centres / Department must ensure that each document has been reviewed in advance and does not contain any confidential information before being submitted to PTAR. ✔
2. **Bahan mengandungi maklumat TERHAD yang telah ditentukan oleh organisasi / badan di mana penyelidikan dijalankan:**.
   (Materials consisting of RESTRICTED information which has been determined by the organisation/body where the research was conducted):
   Sila nyatakan tarikh tamat embargo (jika ada):
   (Please indicate the embargo expiry date (if any)):
   Embargo expiry date: Day: Month: Year:
   Nota: Embargo Expiry Date adalah tarikh tamat tempoh yang ditetapkan oleh penulis di mana pada atau selepas tarikh ini, bahan tersebut akan dipaparkan secara langsung di Repositori Institusi UiTM dan ianya boleh diakses.
   Note: Embargo Expiry Date is the date that an author or a publisher imposed embargo expires. On and after this date, this document will be accessible in UiTM Institutional Repository.
3. **Bahan boleh diakses secara teks penuh dan terbuka.**
   (Materials can be accessed in full text via open access). ✔
4. **Bahan dipinjamkan sementara untuk tujuan pendigitalan dan akan dikembalikan semula kepada pemilik.**
   (Materials are on temporary loan for digitization and will be returned to the owner). ✔

Pemberitahuan: Jika Repositori Institusi UiTM menerima bukti pelanggaran hak cipta, bahan yang berkaitan akan dikeluarkan serta-merta.
(Notification: If UiTM Institutional Repository receives proof of copyright violation, the relevant item will be removed immediately).

PERAKUAN :

Declaration:
Saya / kami akan bertanggungjawab ke atas bahan yang diserahkan untuk pendigitalan dan muat naik ke dalam Repositori Institusi UiTM.
I / we will be responsible for the materials submitted for digitization and uploaded into UiTM Institutional Repository.

Tandatangan Pemohon
Applicant Signature
Tarikh *(Date)*: 15/07/2026

Tandatangan dan Cop Ketua Jabatan / Bahagian / Penyelia
Head of Division / Department / Supervisor Signature and stamp
DR. SUZANA BINTI RATIM
Senior Lecturer
Applied Sciences Programme
Faculty of Applied Sciences
Universiti Teknologi MARA
Tarikh *(Date)*: 15/07/206

UNTUK KEGUNAAN PEJABAT *(For office use)*

DITERIMA OLEH / *Received By* :
TANDATANGAN / *Signature* :
TARIKH *(Date)*:

DISAHKAN OLEH / *Certified By* :
TANDATANGAN / *Signature* :
TARIKH *(Date)*: